JOURNAL OF HYDRO - METEOROLOGY

ISSN 2525 - 2208

VIETNAM METEOROLOGICAL AND HYDROLOGICAL ADMINISTRATION

No 15
06-2023

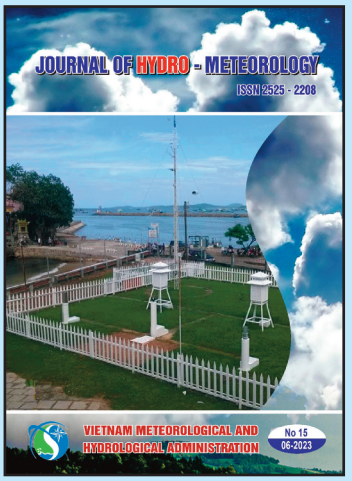

Publishing licence
No: 166/GP-BTTTT - Ministry of Information and Communication dated 17/04/2018

Editorial office
No 8 Phao Dai Lang, Dong Da, Ha Noi
Tel: 024.39364963
Email: tapchikttv@gmail.com

Engraving and printing
Vietnam Agriculture Investment Company Limited
Tel: 0243.5624399

JOURNAL OF HYDRO-METEOROLOGY
Volume 15 - 06/2023

TABLE OF CONTENT

JOURNAL OF
HYDRO-METEOROLOGY

Preface

The Japan International Cooperation Agency (JICA) and the Viet Nam Meteorological and Hydrological Administration (VNMHA) have implemented a 5.5-year bilateral technical cooperation project titled "Project for Strengthening Capacity in Weather Forecasting and Flood Early Warning System" since May 2018. Initially, this project was launched in connection with the use of data from two S-band radars installed in September 2017 at Hai Phong (Phu Lien) and Vinh funded by the Ministry of Foreign Affairs of Japan. The project encompasses four main objectives (output targets): 1) Maintenance and calibration of ground meteorological observation equipment, 2) Quantitative precipitation estimation through observation and radar data analysis, 3) Enhanced weather forecasting, and 4) Effective dissemination of regional weather information. Collaboratively, the JICA project team from Japan and the staff of VNMHA have worked on achieving these objectives. The project is divided into two periods, period 1 (May 2018 to March 2020) and period 2 (April 2020 to December 2023). In August 2020, a special issue of the Journal of Hydro-Meteorology (JHM) was published, featuring six research articles based on the progress reports presented during the 4th meeting of the Joint Coordination Committee (JCC).

This special issue of JHM presents the scientific accomplishments of the JICA project during period 2, highlighting the outcomes shared at the 6th JCC meeting in November 2022. The first article is a comprehensive review paper by Akaeda et al. that provides an overview of the JICA project, while the following articles delve into the specific achievements of the four output activities. Output 1, focused on an attempt to detect reliable rain gauge station, is covered by Kobayashi et al. The achievements in output 2, relating to quality check of rain gauge data and radar data for quantitative precipitation estimates, are described by Tonouchi et al. and Kimpara et al. Output 3, centered on advancements in weather forecasting, is discussed by Sasaki et al. for guidance, and Saito et al. for very short-range forecast of precipitation. Finally, Ichijo et al. elaborate on the achievements in output 4, regarding the mobile services for weather observation information. All seven research articles are collaborative efforts between the JICA team members from Japan and the counterparts from VNMHA. Additionally, a technical report by Akaeda et al. focuses on the various training sessions and seminars conducted throughout the entire duration of the JICA project period.

We express our sincere appreciation to the dedicated members of the JICA project members from Japan and Vietnam. We extend our gratitude to the Headquarters of JICA, VNMHA (including the Aero-Meteorological Observatory, the National Center for Hydro-meteorological Forecasting, the International Cooperation Department, the Hydro-meteorological Network Center, and Hydro-meteorological Data and Information Center), and the Japan Meteorological Business Support Center, and the Japan Weather Association for their unwavering support throughout this endeavor. This volume serves as a valuable review and demonstration of the achievements made during period 2 of the JICA project, and we hope it serves as a useful reference for future technical cooperation between Vietnam and Japan.

June 2023
Kazuo Saito, Editor of JHM
Doan Quang Tri, Acting-Editor-Chief of JHM

JOURNAL OF
HYDRO-METEOROLOGY

Research Article

Achievement of JICA technical cooperation project in period 2

Kenji Akaeda[1]*, Michihiko Tonouchi[2], Nguyen Vinh Thu[3]

[1] Japan International Cooperation Agency, Viet Nam Meteorological and Hydrological Administration, Hanoi, Viet Nam; akaeda191@yahoo.co.jp
[2] Japan Meteorological Business Support Center, Tokyo, 101-0054, Japan; tono@jmbsc.or.jp
[3] Aero-Meteorological Observatory, Viet Nam Meteorological and Hydrological Administration, Hanoi, Viet Nam; nvthu@monre.gov.vn

*Correspondence: akaeda191@yahoo.co.jp; Tel.: +829-761096

Received: 6 May 2023; Accepted: 10 June 2023; Published: 25 June 2023

Abstract: Japan International Cooperation Agency (JICA) and the Viet Nam Meteorological and Hydrological Administration (VNMHA) have implemented a technical cooperation project entitled "Project for Strengthening Capacity in Weather Forecasting and Flood Early Warning System" for more than 5 years from May 2018. In period 2 from April 2020 to the present, the project has achieved some outstanding achievements. Automatic Weather Station (AWS) inspection and calibration method was trained by using the procured traveling standards for temperature, humidity, pressure and precipitation at headquarters, Phu Lien and Vinh. An operational tentative quality control system was introduced to check temperature and precipitation data in near-real time. Quantitative precipitation estimation (QPE) product has been operationally calculated by combining radar and selected rain gauge data. Methods to distinguish qualified rain-gauge data from poor-qualified rain-gauge data were introduced. Precipitation guidance was developed and tested in several heavy rain cases. Short-range precipitation forecasting up to 15 hours has been developed by combining the kinematic extrapolation method and mesoscale numerical forecast. Webpage and mobile application were developed to monitor rainfall situations and related warnings.

Keywords: JICA; Disaster risk reduction; International cooperation; Meteorological observation; Meteorological Forecasting.

1. Introduction

In Vietnam, heavy rainfall brought by typhoons and monsoons causes major disasters such as floods, inundations and landslides every year. To mitigate the damage caused by these disasters, it is necessary to improve the observation, analysis, and forecasting performance of heavy rainfall, as well as to improve the way information on heavy rainfall is presented.

JICA and VNMHA have implemented a technical cooperation project entitled "Project for Strengthening Capacity in Weather Forecasting and Flood Early Warning System" to achieve these objectives. The project was initiated in May 2018 and was originally planned to last until December 2021, but due to the COVID-19 issues that occurred during this period, the project was extended for two years and will continue until December 2023. Figure 1 shows the project implementation timeline. The overall project is largely divided into a first and second period, and the results of the first period, from May 2018 to March 2020, are summarized in [1]. This paper focuses on the results of the second period after April 2020.

Under this project, more accurate weather information will be provided to disaster management agencies and the public by improving (1) maintenance and traceability of meteorological observation equipment, (2) analysis and quality control ability for radar, (3) forecast/warning ability in heavy rain and typhoon, and (4) dissemination ability of meteorological information. The purpose of this project is to contribute to the utilization of the meteorological information provided by VNMHA for disaster risk reduction activities by disaster management agencies and the public. For this purpose, four outputs have been established, (1) maintenance of ground-based observation equipment including rain gauge and radar, (2) development of radar data analysis methods and QPE, (3) advancement of weather forecasting by utilizing observational data and results from numerical weather prediction model, and (4) communication and utilization of weather information. Figure 2 shows the overall project and the relationship among these four outputs. The four outputs are closely related to each other. Technical Working Groups are organized for each output and Working Group (WG) members, several officers from VNMHA and JICA experts, are assigned to implement each of the activities.

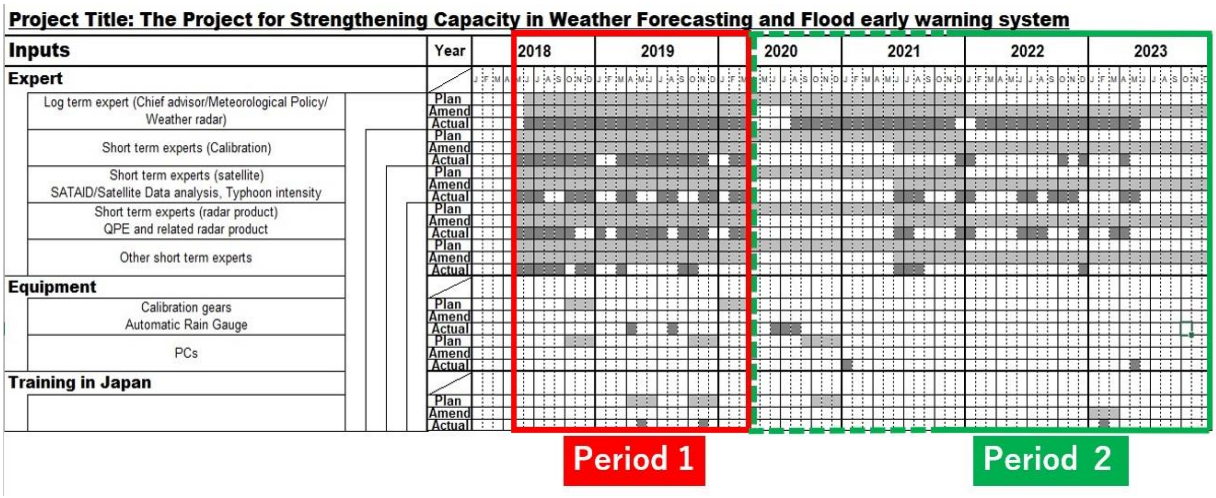

Figure 1. Project operation chart.

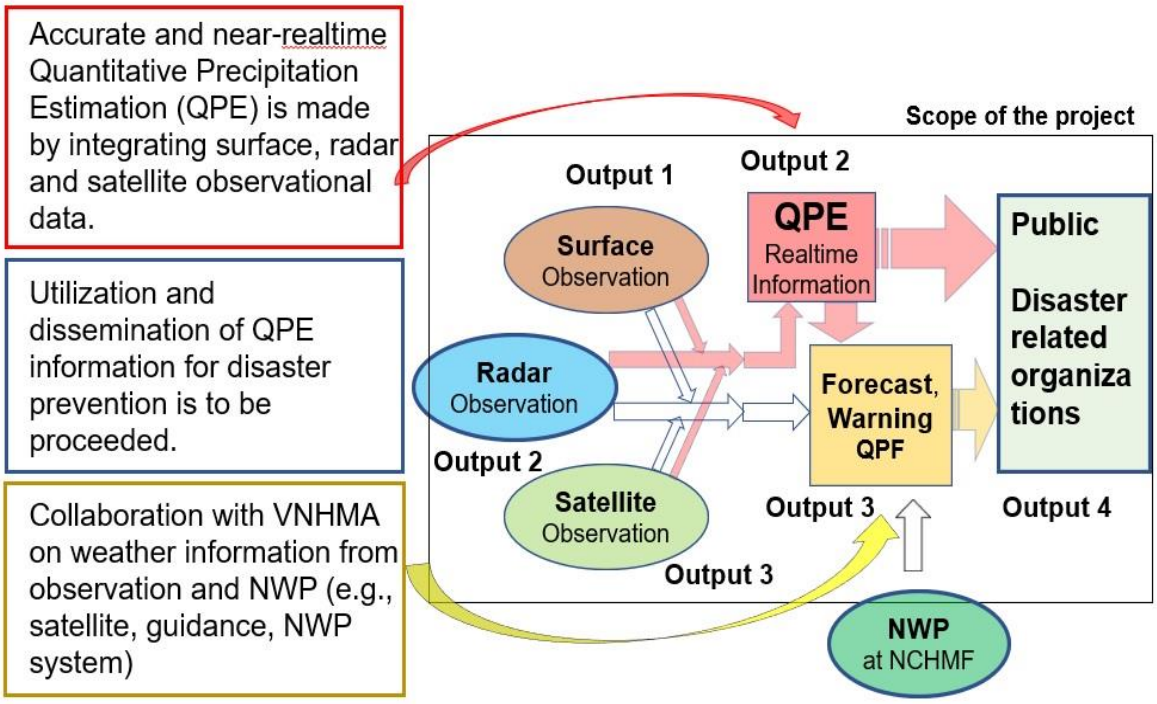

Figure 2. Structure of the project.

The results of the first period of the project are summarized as follows:

(1) Observations are conducted at Synoptic manned stations using common equipment, and the equipment is calibrated regularly. On the other hand, different AWS systems are installed by various providers, and calibration is performed only at the time of installation. Since AWS data will become more important in the future, it is necessary to establish a calibration system for AWS instruments. In addition, quality control of observation data needs to be introduced. Daily inspections of the radar are conducted by site staff and annual inspections are conducted by AMO technical staff, and the equipment is operating stably. Several improvements in radar settings, such as scanning sequences, are future issues.

(2) JMA QC/QPE package was introduced, and a system was built on a trial basis to be applied to 10 radar data and AWS data of about 800 sites. After several improvements in the setting to calculate QPE, this system stably produced QPE products. The selection method to distinguish good-quality rain gauges data from poor-quality rain gauges data should be improved.

(3) Guidance on forecasting maximum and minimum temperatures in 63 cities was developed, and better results were obtained than the numerical weather prediction (NWP) model output itself. In addition, training was conducted on how to analyze numerical forecasts, radar, and satellite data in heavy rainfall cases and how to use them in forecasting work.

(4) Expert surveyed the actual utilization of meteorological information which VNMHA issued. In addition, basement construction work for the installation of new ARGs at 18 sites was conducted to improve the accuracy of QPE, and the installation of ARGs was completed for 15 sites. Real-time data monitoring also started at headquarters.

For details on these activities, please refer to [1].

2. Summary of Activities in Period 2

As mentioned earlier, activities in period 2 stagnated for more than 1 year due to COVID-19. During the COVID-19 restrictions, some lectures and seminars were held online or a combination of online and offline. Activities were resumed as the situation became better. For each output, the results of the second period are summarized as follows.

2.1. Output 1 (observation)

To improve the calibration capability, a thermostatic chamber for temperature calibration was provided to the calibration laboratory in Hanoi, and four sets of mobile standards for atmospheric pressure, temperature, humidity and rainfall were also provided. On the job-training (OJT) was conducted in December 2021 and January 2022 at the headquarters, and in October 2022 at Vinh and Phu Lien regional centers on how to check AWS using these mobile standards. The need to conduct these checks systematically in the future was strongly recommended. In addition, a draft maintenance check sheet was prepared for uniform management and accuracy maintenance of AWS instruments and was tested during the OJT.

The training was given on the importance of metadata, which is the basis of observatory management, and location information was checked for several sites, and it was pointed out that the information currently registered was incorrect. It is also important to record calibration records and differences from standards in metadata as part of instrument management.

To clarify the current situation of rain gauge observation, quality analysis of AWS rain gauge observation was made by comparing with Synoptic observation. The results are given in [2]. A training course by the Japan Meteorological Agency (JMA) lecturers was held in December 2022 to improve the quality control capability of surface observation.

2.2. Output 2 (radar analysis)

A characterization survey of AWS rainfall data at about 1,800 locations is available and classified into levels in terms of reliability. Two-dimensional checks and double-mass analysis were used to check the quality of each AWS data. QPEs using AWS at each level were compared to determine the appropriate level of AWS for use. The results of this analysis are given in [3].

To mitigate the abnormal fluctuations in QPE values that occurred at the beginning of the QPE operation, optimization of the configuration parameters within the QPE algorithm was conducted. As a result of this adjustment, the QPE calculation stabilized and can be used for heavy rainfall monitoring. To further enhance its use for heavy rainfall monitoring, products superimposed with satellite data in SATAID software can also be used.

To improve the accuracy of QPE, training was conducted on how to create clutter maps to deal with ground clutter echoes that can't be removed by the signal processing system, and clutter maps can be introduced in the operational system.

After implementing these various improvements, the calculated QPE was compared with the rain gauge for evaluation, and the characteristics of the QPE were analyzed. As a result, whole accuracy was improved with some low accuracies in areas such as mountainous areas, southern areas, and areas with sparse rain gauge distribution areas.

To improve the accuracy of QPE, the introduction of dual-polarization data was discussed. Quality checks of original data and correction are necessary for the utilization of dual-polarization data. In addition, to make better use of QPE data for disaster prevention, some trials for the superposition of accumulated QPE data with different time intervals and disaster risk maps were made, to specify the estimated area for disaster occurrence.

2.3. Output 3 (forecast)

Improvement of temperature guidance was implemented. The accuracy of guidance was improved by combining the results of multiple NWPs, compared with the result of a single NWP. The guidance that extended the forecast period from 3 to 9 days was also created, and a new PC was prepared in which these products can be monitored in near-real time.

To create precipitation guidance, several cases of heavy rainfall were analyzed and a dataset for creating guidance was developed. Statistical analysis using the dataset was conducted and a prototype guidance based on GSM and IFS results was developed and tested. The results are given in [4].

To improve short-term disaster prevention information, a prototype system of the very short-range forecast of precipitation in Vietnam was developed by merging kinematic extrapolations of composite hourly rainfall analysis and NWP. Verifications showed that the merged rainfalls outperformed both NWP and kinematically extrapolated precipitations for the time range of Forecasting Time (FT) = 3 to 5. Detailed results are described in [5]. To improve short-range NWP, JMA's strategies, including radar data in NWP were introduced in seminars and lectures in training courses [6].

2.4. Output 4 (dissemination)

Three ARGs were installed in mountainous areas and remote island. Together with the 15 ARGs in the first period, we set up 18 ARGs as rain gauge systems for data collection and monitoring and conducted training on how to maintain and manage these systems including the method how to change system settings. In addition, at the 18 ARG installation sites, training was conducted on the maintenance of observation equipment and accuracy confirmation.

Mobile applications and websites for monitoring ARG, radar, and satellite data were developed and put into operation. In addition, weather and disaster prevention information

was also made available for monitoring in the application or website. A detailed explanation for these developments is given in [7].

2.5. Others (training and seminars)

During the project period, a lot of training sessions and seminars related to each of the outputs were held. OJT training was provided at the actual sites for the maintenance and calibration of surface instruments and radar systems. In addition, we invited experts from JMA to conduct training with participants from not only headquarters but regional or local meteorological observatories. We also held training in Japan in which not only lectures or exercises but also site visits to JMA or related organizations were implemented as activities of outputs 1, 2 and 3. A detailed list of these training and seminars is compiled in a separate technical report [6].

3. Additional information on ongoing activities

The project is still ongoing, and some additional information on ongoing activities that are not fully described in section 2 is provided below.

3.1. Near-real time quality control of surface observation data

Since surface observation data are being archived in the Central Data Hub (CDH) in near-real time, we created a tool to read out the data from CDH, perform simple quality control, and display the results. Currently, the target is temperature and rainfall observation data. Each regional center/ local observatory can easily check the condition of instruments within their responsible areas. Figure 3 shows an example of the display. Blue points show normal condition, black points show no data in CDH, and red point shows some possibilities of a problem at the site. You can click this red point and the time variation of the observation data can be displayed in terms of graphic charts, so it is possible to estimate the cause of the problem. In this case, an abrupt change of more than 150 mm in 1 hour is one of the criteria to check the validity of rainfall data.

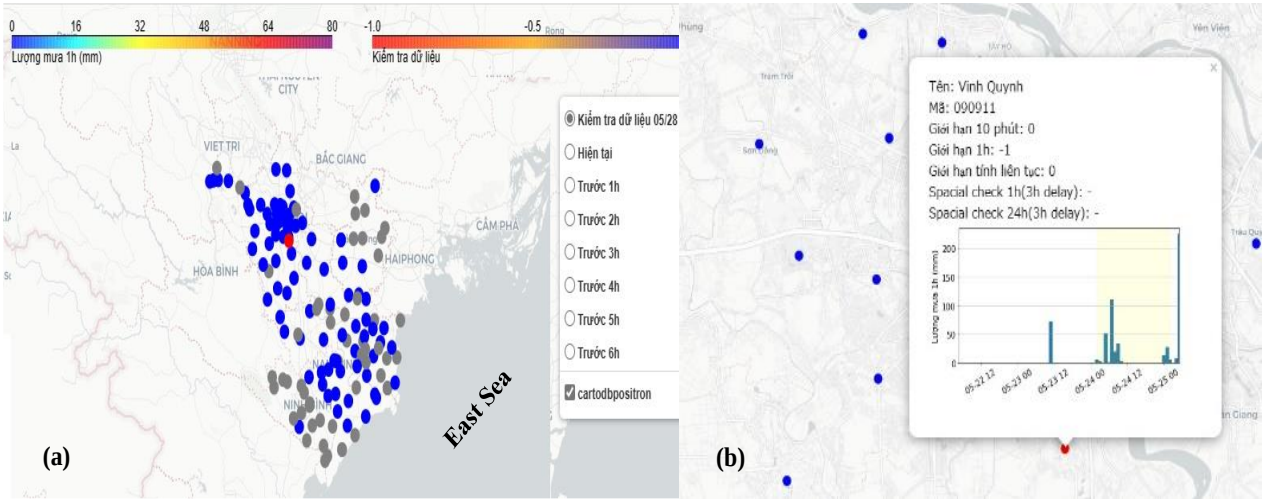

Figure 3. (a) Sample status display of rainfall observation in the Northern Delta region. Blue points show normal, black points show no data and red point shows the possibility of a problem. (b) After magnifying the left display and show the time change of rainfall amount at the red point to check the cause of the problem. (Courtesy of R. Kobayashi - an expert in Output 1).

This display system should be monitored periodically, and on-site investigations and inspections should be conducted for observation points where problems frequently occur.

3.2. Introduction of a disdrometer

Two disdrometers, which can measure the rainfall size distribution on the ground, were installed in December 2022. Currently, a test observation is being conducted in Hanoi with one installed on the roof of the headquarters and the other in the observation field of Ha Dong station. Figure 4 shows the one installed at Ha Dong station.

The observed rainfall size distribution can be used not only to know the characteristics of rainfall in Vietnam but also to calibrate the radar data. Radar reflectivity is highly dependent on rainfall size distribution, the relation between rainfall amount and radar reflectivity can be estimated by using observed rainfall size distribution.

Figure 4. Disdrometer installed at Ha Dong station.

3.3. Utilization of dual polarization data

VNMHA currently operates five dual-polarization radars. By utilizing dual-polarization data, it is possible to analyze rainfall amounts with higher accuracy than with single-polarization radar. Several methods for calculating precipitation from dual-polarization data have been proposed for several different regions. In the future, it will be necessary to determine the optimal method for calculating precipitation in Vietnam by combining the disdrometer data described in 3.2 with dual-polarization observation data.

In addition, since dual-polarization radar analysis depends on subtle differences between horizontally and vertically polarized observations, it is necessary to calibrate radar observations more carefully than single-polarization radar. For this reason, it is necessary to check the dual-polarization data carefully on a daily basis to confirm that the characteristics of the radar have not changed.

4. Future activities and suggestions

This project has made it possible to derive hourly precipitation distribution (QPE) with 1km mesh in near-real time and to conduct quantitative analysis of heavy rainfall that could lead to the estimation of the occurrence of several disasters. In the future, it is necessary to further improve the accuracy. To improve the accuracy of the product, the following points need to be considered. The first point is to improve the accuracy of rain gauge and radar data, which are the basis of the product. To utilize more accurate rainfall data from approximately 2,000 AWS sites nationwide, it is necessary to improve quality control of observation data and develop maintenance management systems, such as calibration and overhaul of rain gauge. Quality control should not be used only to eliminate poor quality data, but should also be used to accelerate an inspection for poor quality stations and encourage calibration and repair of instruments. Regarding the accuracy of QPE, the rain gauges in some areas are so important such as mountainous areas where there are few observation points, areas where multiple radars overlap, area which is important for the QPE calculation algorithm. It is necessary to implement inspection and repair of rain gauges in such areas as a first priority.

For radars, it is necessary to review the scan sequence for optimal observations and to improve the elevation angle table used to calculate PCAPPI. Also, corrections for the radar beam shielding by using high-resolution terrain data will improve accuracy. In the case of dual-polarization radar, correction for rainfall attenuation can be useful and it is easy to utilize this product in the system.

The second point is the improvement of the product calculation algorithm. The current QPE algorithm does not use the beam height information of the observation data when handling PCAPPI data. The improvement of this point is expected to improve the calculated

rainfall values. In addition, the current algorithm is based on the correction with rain gauges, if a rainfall area exists only over the ocean, the correction by rain gauges may not be effective and the correction may be insufficient. When using current QPE products, it is necessary to know the characteristics of such products.

There are two major directions in which QPE products can be applied. One is to calculate a disaster risk index which is more closely related to the disaster from the rainfall itself. Early warning information for the disaster is issued based on this kind of index. Landslides, floods, and inundations are three major disasters caused by heavy rainfall. These disasters are caused by a combination of several factors including soil moisture or total precipitation in the basin, in addition to the amount of precipitation at the disaster location. Therefore, it is necessary to calculate the soil moisture index, runoff index, and inundation index that are closely related to the occurrence of each disaster when these indexes are combined with rainfall amount. In addition, since the conditions for the occurrence of disasters vary from region to region, it is necessary to decide the criteria to estimate the occurrence for each region. To decide the criteria in each region, past records of rainfall and disaster in that region are necessary. By using these past records, the index can be calculated and compared the index with past disasters for each region and establish criteria such as which value of the index should prompt early warning of the occurrence of a disaster in that region. For this purpose, it is necessary to compile data on the occurrence of past disasters for each region, and such a database needs to be developed along with data on past rainfall amounts.

The second way to utilize QPE products is to use them for precipitation forecasting. For precipitation forecasting, there are two major methods depending on the forecast time. For forecast less than 1 hour, the kinematic extrapolation method is useful and forecast longer than 6 hours the utilization of numerical weather prediction is useful. For forecast times between 1 and 6 hours, it is effective to combine the results of both kinematic extrapolation and numerical weather prediction. QPE products are used as initial conditions for kinematic extrapolation. In the future, it will be important to utilize these methods according to the forecast time.

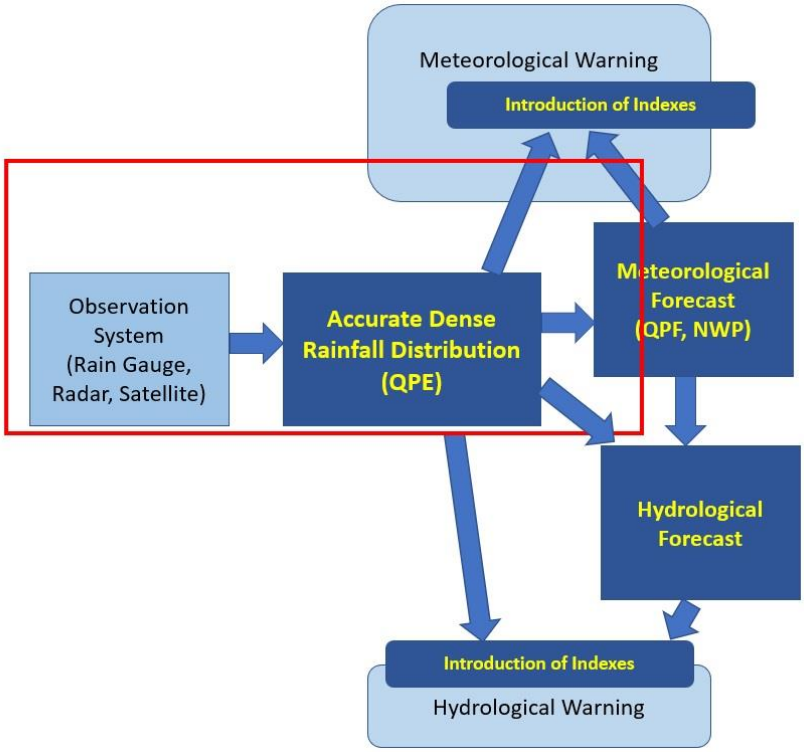

Figure 5. The schematic chart creates early warnings from observation through forecasting to final warnings. This technical cooperation project covers the field showing the red box.

While there are various methods to improve the accuracy of precipitation forecasting in NWP, it is also important to assimilate observed information on wind and water vapor into NWP. From meteorological radar, it is possible to set up a wet (100% humidity) area by considering the radar echo area as a cloud area and it is possible to assimilate wind information from Doppler data. In addition, it will be useful to introduce new observation systems for deriving wind and water vapor information and to assimilate these data into the NWP model.

Figure 5 shows a simple schematic diagram from observation to information dissemination for disaster risk reduction due to heavy rainfall. In this project, we have mainly conducted the part where precipitation distributions are created from observation data and partly conducted their utilization on the forecast and information dissemination. In the future, it is necessary to contribute to disaster risk reduction in Vietnam by enhancing the areas of meteorological and hydrological forecasting and developing indexes and regional criteria to improve the accuracy of warnings.

5. Conclusion

This project established a technical basis to derive QPE by combining rain gauges and radars. This product covers the whole area of Vietnam hourly with a resolution of 1km. There are several factors to keep its quality or improve its quality. Maintenance and calibration of observational systems, including rain gauges and radars, keep the accuracy of observation data and lead to achieving the quality of QPE. Some evaluation and adjustments of the settings of QPE algorithm are also necessary to improve its quality.

Temperature and precipitation guidelines were developed in this project, which showed better results than the model output. A prototype system of the very short-range forecast of precipitation was also developed by merging kinematic extrapolations of composite hourly rainfall analysis and NWP and QPE product will be used as initial state of the kinematic extrapolations. Further strategies of NWP development are necessary to improve the performance of short-range forecasting.

The project aims to disseminate weather information based on the developed product in this project. New risk maps are tentatively developed based on QPE and new mobile application and web pages are developed. Further development of information for disaster risk reduction based on new indexes is future issues. For developing more accurate and timely meteorological information, VNMHA and JICA continuously challenge to clear matters step by step steadily.

Author Contributions: This article is written by K.A., M.T. and is partly based on the progress report of the project [8]. The article was commented on by N.V.T.

Funding: This research was performed under the JICA Project for “Strengthening Capacity in Weather Forecasting and Flood Early Warning System” in the Social Republic of Vietnam.

Acknowledgments: This JICA technical cooperation project was supported by the people of Japan as JICA projects and technical assistance by JMA as DRR technical cooperation of WMO international cooperation frame for Southeast Asian countries. We express our special thanks to JICA Tokyo and JICA Vietnam experts who supported the project and staff members of the VNMHA, JMBSC and JWA who have joined the JICA Project.

Conflicts of Interest: The authors declare no conflict of interest.

References

1. Tonouchi, M.; Kasuya, Y.; Tanaka, Y.; Akatsu, K.; Akaeda, K.; Thu, N.V. Activities of JICA on disaster prevention and achievement of JICA project in Period 1. *VN J. Hydrometeorol.* **2020**, *5*, 1–12.

2. Kobayashi, R.; Duc, L.X.; Tien, P.M. Attempt to detect maintenance-need rain gauge station by double-mass analysis. *J. Hydro-Meteorol*. **2023**, *15*, 10–20.
3. Tonouchi, M.; Hoa, B.T.K.; Hung, N.V.; Cuong, N.M. Quality check of rain gauge data for Quantitative Precipitation Estimate. *J. Hydro-Meteorol*. **2023**, *15*, 21–27.
4. Sasaki, K.; Anh, V.T. Development of precipitation guidance for 36 regions in Vietnam up to 5 days ahead. *J. Hydro-Meteorol*. **2023**, *15*, 40–58.
5. Saito, K.; Hung M.K.; Tien D.D. Development of a prototype system of the very short-range forecast of precipitation in Vietnam. *J. Hydro-Meteorol*. **2023**, *15*, 59–79.
6. Akaeda, K.; Saito, K.; Sasaki, K.; Ichijo, H. Training and seminars at the JICA project in Viet Nam. *J. Hydro-Meteorol*. **2023**, *15*, 91–105.
7. Ichijo, H.; Manh, N.V.; Phuong, V.M.; Huy, N.V.; Nhan, P.V.T. Development of Mobile Services for Weather Observation Information. *J. Hydro-Meteorol*. **2023**, *15*, 80–90.
8. JICA and JMBSC. The project for strengthening capacity in weather forecasting and flood early warning system in Vietnam. Progress Report 4 (Second period), 2023, pp. 75.

JOURNAL OF
HYDRO-METEOROLOGY

Research Article

Attempt to detect maintenance need rain gauge station by double-mass analysis

Ryohei Kobayashi[1]*, Le Xuan Duc[2], Pham Minh Tien[3]

[1] International Affairs Department, Japan Meteorological Business Support Center, Tokyo, 101–0054, Japan; kobayashi@jmbsc.or.jp
[2] Hydrometeorological Observation Center, Viet Nam Meteorological and Hydrological Administration, Hanoi, Vietnam; lxduc@monre.gov.vn
[3] Ha Noi University of Natural Resources and Environment, Hanoi, Vietnam; pmtien@hunre.edu.vn

*Correspondence: kobayashi@jmbsc.or.jp; Tel.: +81–352810440

Received: 5 March 2023; Accepted: 26 April 2023; Published: 25 June 2023

Abstract: Currently, 112 Automatic Weather Stations (AWS) and over 1,000 Automatic Rain Gauges (ARG), approximately 2,000 AWS in total including stations outside the national hydrometeorological network are installed in the nationwide country of Vietnam so that they can be used for Quantitative Precipitation Estimation of weather radars, etc. Meanwhile, it takes a vast amount of time and cost to properly operate and maintain the large number of AWS. Besides, rain gauges cannot be checked whether it has properly operated without a certain amount of rain. This research attempted to detect maintenance-need rain gauges of the AWS by the slope and R^2 values obtained by double-mass analysis against the distance between the stations. Evaluated distances were used for the classification of AWS. As "Class 1 AWS" is the distance within 5 km and "Class 2 AWS" is the distance within 20 km and the criteria were obtained by AMeDAS data of the Japan Meteorological Agency. Additionally, the process is cycled several times to expand the candidate AWS. The result says that stations except 125 Class 1 AWSs and 710 Class 2 AWSs need to be checked. It is suggested that this assessment can be used to detect maintenance-need stations; however, periodical maintenance is still needed for proper observation because this assessment also needs reliable AWSs.

Keywords: Automatic Weather Station; Automatic Rain Gauge; Maintenance; Double-mass Analysis.

1. Introduction

[1] surveyed the status of Automatic Weather Stations (AWS) and Automatic Rain Gauges (ARG) operated by the Viet Nam Meteorological and Hydrological Administration (VNMHA) in 2019 and the VNMHA currently operates 186 Synoptic stations, 112 AWS, and over 1,000 ARG. In total, around 2,000 AWS are operated including stations outside the national hydrometeorological network, according to the data retrieved from the Central Data Hub (CDH). All data observed by the stations have been sent and stored in CDH at the VNMHA headquarters and used for monitoring and forecasting operations, especially Quantitative Precipitation Estimation (QPE) of weather radars [2]. However, because of the large number of stations, it is not easy to maintain the AWS periodically. In fact, it is easy to find some ARG stations that keep 0 mm of precipitation even if the surroundings of the station are observing rainfall. These stations should be detected and maintained as soon as possible, but the detection method exampled above needs to wait for massive rainfall around the station.

In this paper, we proposed an alternate method for the Quality Check of rain gauge data to find AWS/ARG sites that need to be maintained by using the double-mass analysis method as a data assessment. The double-mass analysis is normally used for checking the transformation of the environment of the station [3], but this method analyzes the relationship between other near stations assuming that well-maintained stations have a constant relationship. For this reason, maintenance-need stations can be detected without waiting for massive rainfalls.

2. Used data

2.1. Data period

We used Synoptic station data, AWS data, and JICA-ARG data. All data were provided by Aero-Meteorological Observation (AMO) of VNMHA. Each data period is shown in Table 1. The date and time are stamped with Vietnamese local time (GMT+7:00). As AWS data are not sufficient until 31 December 2020, this assessment is conducted with data from January to December 2021.

Table 1. Data period.

Station type (data storing interval)	From	To
Synoptic (6 hours)	2019/01/01 01:00	2022/01/05 19:00
AWS (10 minutes)	2020/03/05 00:00	2021/12/30 23:50
ARG (st1 – st15) (10 minutes) *	2019/09/25 15:20	2022/01/13 14:20
ARG (st16 – st18) (10 minutes)	2021/07/14 11:20	2022/01/13 14:20

*The beginning time of observation is different at each ARG station.

2.2. Synoptic station

Synoptic data used in the assessment were provided by the AMO (not CDH or forecast division) in a DAT file (kind of a text file of which the extension is ".dat"). The total number of stations in the file is 174. The station's geo-coordinate information was provided by the AMO as well. As Synoptic data are stored all observation data such as temperature, precipitation, etc. into a 6-hourly DAT file with a space-separated method. Only assessment data (precipitation) were extracted and realigned.

2.3. AWS

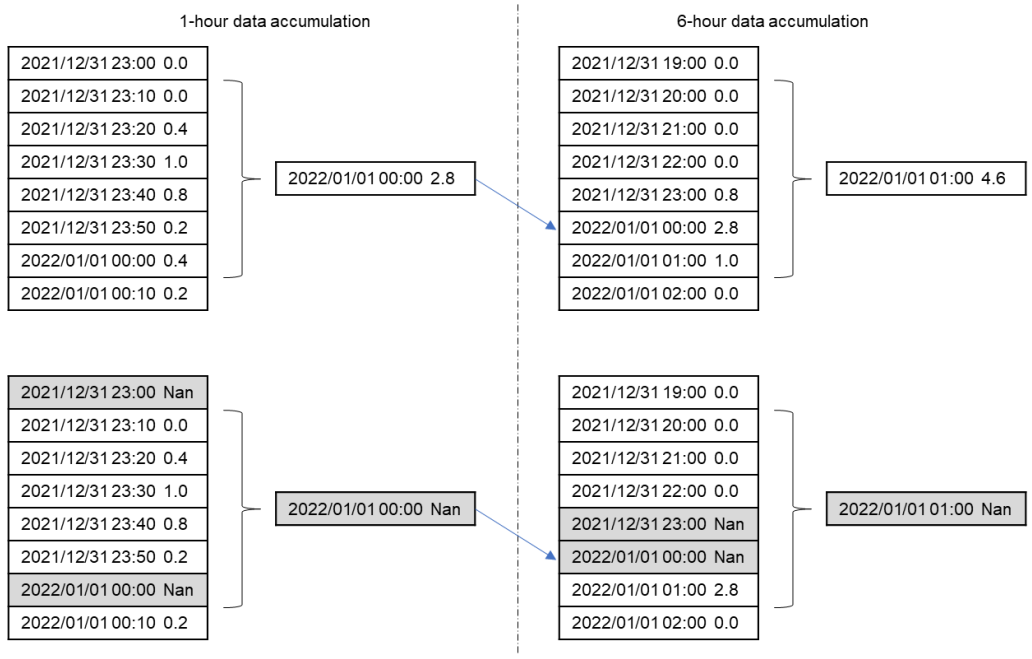

Figure 1. An example of data error (left: 1- hour data, right: 6- hour data).

AWS data used in the assessment were obtained via JICA Linux PC. The total number of data is 2,332 stations as far as JICA Linux PC could obtain after June 2021.

AWS data are separated into 10-minute data. Therefore, AWS data were accumulated into 1-hour and 6-hour data were used for the assessment. 1-hour accumulation data are calculated from 10, 20, 30, 40, 50, and 00 minutes of data. If one of the 10-minute data is lost, the accumulation data of the time is regarded as NaN (Not a number, or blank). 6-hour data processing is calculated in the same manner. An example is shown in Figure 1.

2.4. JICA–ARG

ARG data used in the assessment were obtained from the ARG server directly. The total number of ARGs is 18 stations. These stations were installed in 2019 and 2021, therefore, the beginning time of observation is different for each data. Geo-coordinated data were provided by Mr. Ichijo who oversees these ARGs.

ARG data is saved every 10-minute data into one DAT file for one station with a comma-separated method. ARG data were accumulated into 1-hour and 6-hour data used for the assessment. The accumulation manner is the same as the manner used for AWS.

3. Assessment method

3.1. Classification of AWS

In the assessment, AWS and ARG were classified into two classes. The Class 1 AWS is to be located around the Synoptic station and compared with Synoptic data. The Class 2 AWS is categorized as the site whose distance from the reference site is within a few kilometers and compared with the Class 1 or 2 AWS so that candidates for Class 2 AWS can be sampled as much as possible even in remote areas. Both classes have their criteria.

3.2. Assessment method

The assessment was conducted by an evaluation of a slope of the regression line whose intercept is set to be 0.0 and the R^2 value (square of Pearson's correlation coefficient) of the double-mass analysis curve between each candidate station and a reference. The slope and the R^2 value were computed every month by using the past three-month observation data.

If the candidate station is located at the same place as the reference, although there is an uneven catching rate of rain, the candidate will observe almost the same value. Therefore, in the double-mass analysis, the slope will be nearly 1.0, and the R^2 value will also be nearly 1.0. However, the slope and the R^2 value will enlarge a gap from 1.0 if the station is located farther and farther away from a reference.

Slope calculation: The slope in the result of the double-mass analysis is obtained by single regression analysis by the least-squares method. In the regression analysis, the intercept is set as 0.0 because the initial precipitation is 0.0 mm for both rain gauge stations.

R^2 calculation: Although there are a lot of methods to obtain the R^2 value, the R^2 value in this assessment is calculated as the square of Pearson's correlation coefficient. The R^2 value is obtained from the result of the double-mass analysis because the scatter plot of hourly precipitation cannot find any relativeness, but the result of the double-mass analysis showed relativeness.

Distance calculation: Distance between reference and candidate stations was calculated with Hubeny's distance formula (by Geodetic Reference System 1980, Pole radius 6,356,752.314 m, Equator radius: 6,378,137 m).

These calculations were computed with Python 3x. After computing the slope and R^2 value, Class 1 and 2 AWSs were retrieved as per the criteria. These program flowcharts are shown in Figure 2.

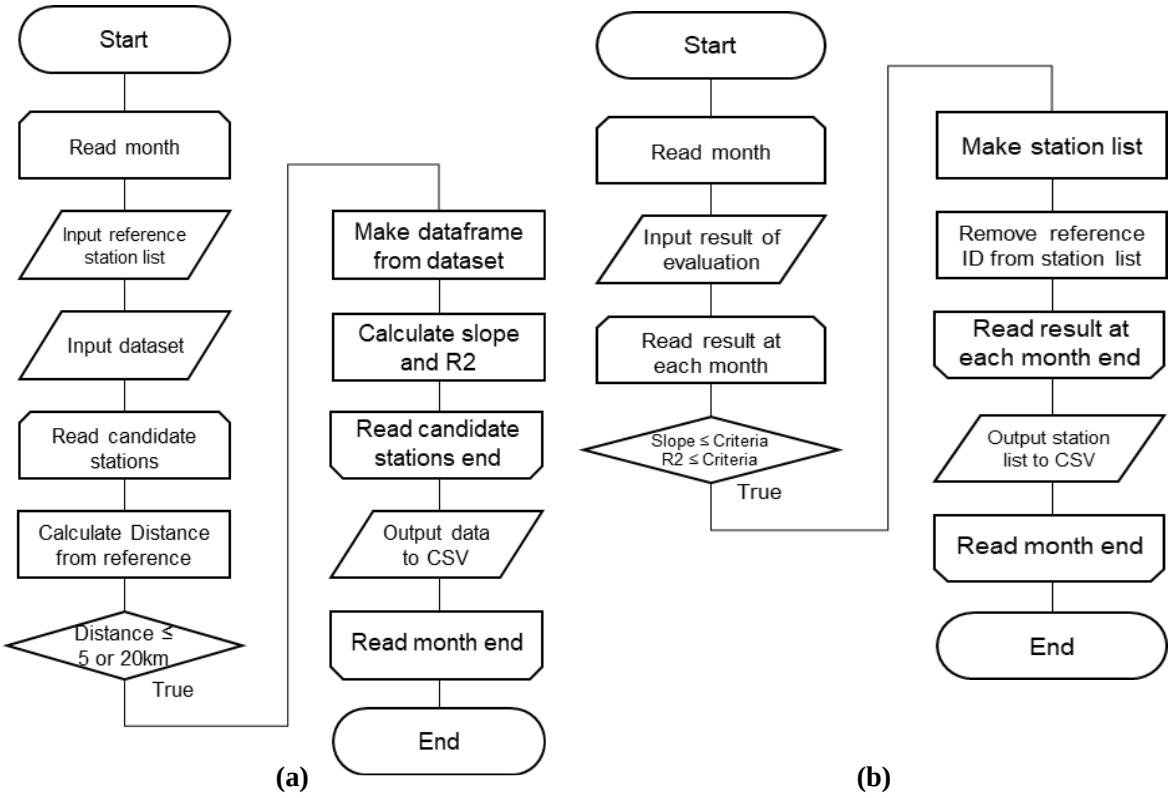

Figure 2. Program flowcharts: (a) Calculation of the slope and the R^2 value; (b) Screen the stations.

3.3. Criteria of the assessment

Used data for the criteria: To provide criteria of the slope and the R^2 value for the assessment, AMeDAS (Automated Meteorological Data Acquisition System: the AWSs in Japan operated by Japan Meteorological Agency (JMA)) data in Okinawa prefecture of Japan located in a tropical zone was evaluated. AMeDAS is well maintained every year and its rain gauge is calibrated every five years by JMA. Evaluated stations are listed in Table 2. Data used for this examination was 30-year data from May 1992 to April 2022 (some stations are from the 2000s).

Table 2. Reference stations and evaluated stations.

Name	Data available	Distance from the reference
Naha	**01/05/1992**	**Reference**
Naha Ashimine	01/01/2003	5.0 km (Naha)
Itokazu	01/05/1992	9.8 km (Naha)
Goya	01/05/1992	17.8 km (Naha)
Yomitan	01/05/1992	22.7 km (Naha)
Tokashiki	01/05/1992	32.3 km (Naha)
Miyagijima	19/12/2007	33.3 km (Naha)
Nago	**01/05/1992**	**Reference**
Motobe	01/05/1992	12.2 km (Nago)
Higashi	01/05/1992	19.2 km (Nago)
Miyagijima	19/12/2007	25.6 km (Nago)
Kunigami	20/12/2005	26.0 km (Nago)
Yomitan	01/05/1992	31.0 km (Nago)
Goya	01/05/1992	33.7 km (Nago)
Miyakojima	**01/05/1992**	**Reference**
Kagamihara	01/01/2003	2.1 km (Miyako)
Shimojijima	01/01/2003	14.1 km (Miyako)

Name	Data available	Distance from the reference
Gusukube	01/05/1992	14.4 km (Miyako)
Ishigakijima	**01/05/1992**	**Reference**
Moriyama	07/03/2013	10.5 km (Ishigaki)
Kabira	01/05/1992	14.6 km (Ishigaki)
Ibaruma	01/05/1992	22.3 km (Ishigaki)
Oohara	01/05/1992	30.6 km (Ishigaki)
Kumejima	**01/05/1992**	**Reference**
Kitahara	01/01/2003	9.4 km (Kumejima)
Tonaki	26/08/2014	34.0 km (Kumejima)

Method to define the criteria of the slope

The slope is computed with three-month data for each month. 95 percentiles of the slope at respective distances are to be evaluated as the criteria.

Method to define the criteria of the R^2

The R^2 value is also computed with three-month data and output per month too. 95 percentiles of the R^2 value at respective distances are to be evaluated as the criteria.

Method to define the distance

Representativeness of localized rainfall can be around 2.5 km in hourly precipitation and around 5 km in 24-hourly precipitation [4]. Therefore, the range of Class 1 AWS is to be 5 km from a reference. Whereas it is difficult to find AWS located within 5 km, especially in remote areas, another range for the remote stations is temporarily defined by using the results of the slope and the R^2 value.

Result of the criteria for the assessment

AMeDAS evaluation results are shown in Table 3. The slope values show differences as absolute values of calculated slope value minus one. The slope values were rounding up by five-tenth units and the R^2 values were rounding down by one-tenth unit.

Table 3. Result of the slope and the R^2 values at a respective distance.

Reference	Compared station	Total number of results (month)	Distance (km)	Slope	R^2
				95 percentiles	95 percentiles
Miyakojima	Kagamihara	230	2.1	1.0 ± 0.25	0.99
Naha	Naha Ashimine	230	5.0	1.0 ± 0.35	0.98
Kumejima	Kitahara	230	9.4	1.0 ± 0.40	0.97
Naha	Itokazu	355	9.8	1.0 ± 0.45	0.94
Ishigakijima	Moriyama	107	10.5	1.0 ± 0.35	0.96
Nago	Motobe	355	12.2	1.0 ± 0.35	0.95
Miyakojima	Shimojijima	230	14.1	1.0 ± 0.45	0.94
Miyakojima	Gusukube	355	14.4	1.0 ± 0.40	0.95
Ishigakijima	Kabira	355	14.6	1.0 ± 0.65	0.93
Naha	Goya	355	17.8	1.0 ± 0.40	0.95
Nago	Higashi	355	19.2	1.0 ± 0.45	0.93
Ishigakijima	Ibaruma	355	22.3	1.0 ± 0.70	0.91
Naha	Yomitan	355	22.7	1.0 ± 0.45	0.93
Nago	Miyagijima	170	25.6	1.0 ± 0.55	0.90
Nago	Kunigami	194	26.0	1.0 ± 0.60	0.94
Ishigakijima	Oohara	355	30.6	1.0 ± 0.50	0.93
Nago	Yomitan	355	31.0	1.0 ± 0.45	0.93
Naha	Tokashiki	355	32.3	1.0 ± 0.50	0.90
Naha	Miyagijima	170	33.3	1.0 ± 0.50	0.89
Nago	Goya	355	33.7	1.0 ± 0.50	0.92
Kumejima	Tonaki	90	34	1.0 ± 0.45	0.97

It can be found a tendency that the slope and the R^2 values will be widened farther in the Table above. However, as it is difficult to set a range of the assessment with only this result, the distance is temporarily set as 20 km, in which the AMeDAS network is installed on average.

According to thresholds of distance, the criteria of the slope will be between 1.0 ± 0.35, and the R^2 value will be under 0.98 for Class 1 AWS. For Class 2 AWS, the criteria of the slope will be between 1.0 ± 0.65, and the R^2 value will be under 0.93. A summary of the results is in Table 4.

Table 4. Criteria for the assessment.

	Slope	**R^2**	**Remarks**
Class 1 AWS	1.0 ±0.35 (Including)	0.98 (Including)	Within 5 km from a reference
Class 2 AWS	1.0 ±0.65 (Including)	0.93 (Including)	Within 20 km from a reference

4. Definition of Class 1 AWS

4.1. Dataset

Referring provided 191 Synoptic station names, IDs, and geo-coordinates, 179 AWSs were extracted as Class 1 AWS candidates.

4.2. Result of Class 1 AWS

As per the criteria for Class 1 AWS, evaluation was done each month by using the past three-month data from the evaluation month. The result of the Class 1 AWSs from March to December 2021 (the data set is from 1st January to 31st December 2021) is listed in Table 5.

Table 5. Class 1 AWS (March to December 2021).

	Station ID of Class 1 AWS as of evaluation month/year									
	3/2021	**4/2021**	**5/2021**	**6/2021**	**7/2021**	**8/2021**	**9/2021**	**10/2021**	**11/2021**	**12/2021**
1	004811	004811	004811	004811	004811	004811	004811	090889	090889	091052
2	090018	090018	090660	091052	090660	092203	090904	091052	091052	1010404003
3	090660	090660	1010404003	092101	091052	1010404003	090912	1010404003	091920	1010404301
4	090889	1010404003	1010404301	092203	091920	1010404301	1010404003	1010404301	1010404003	1010404702
5	091052	1010404301	1010404702	1010404003	092203	1010404702	1010404301	1010404702	1010404301	1010405204
6	1010404003	1010404702	1010405204	1010404301	1010404003	1010405204	1010404702	1010405204	1010404702	1012017804
7	1010404301	1012018001	1012018001	1010404702	1010404301	1012017804	1010405204	1012017804	1010405204	1012018001
8	1010404702	1012219307	1012018502	1010405204	1010404702	1012018001	1012017804	1012018001	1012017804	1012018502
9	1012017804	1012219504	1012219307	1012018001	1010405204	1012018502	1012018001	1012018905	1012018001	1012018905
10	1012018001	1012219605	1012219504	1012018502	1012017804	1012219401	1012219401	1012219401	1012018502	1012219401
11	1012018502	1012219903	1012219605	1012219307	1012018001	1012219504	1012219903	1012219903	1012018905	1012219504
12	1012219307	1012220706	1012219903	1012219401	1012018502	1012219903	1012220102	1012220102	1012219401	1012219903
13	1012219504	1012422002	1012220706	1012219605	1012219903	1012220706	1012220706	1012422002	1012219903	1012220102
14	1012219605	1013130701	1012422002	1012219903	1012220706	1012422002	1012422002	1012422303	1012220102	1012421304
15	1012219903	1013130802	1012422303	1012220706	1012422002	1012422303	1012422303	1012725601	1012422303	1012421901
16	1012220102	1013131803	1013130701	1012422002	1012422303	1012725601	1012725601	1013130802	1012725601	1012422303
17	1012220706	129145	1013130802	1012422303	1012725601	1013130701	1013130701	129145	1013130802	1012725601
18	1012422002	351435	129145	1013130701	1013130701	1013130802	1013130802	219512	129145	1013130802
19	1012422303	48/25	232043	1013130802	129145	129145	129145	232043	219512	129145
20	1013130701	48/61	351435	129145	197706	197706	219512	351435	232043	219512
21	1013130802	48/63	48/25	197706	232043	351435	232043	48/25	351435	232043
22	1013131803	48800	48/26	232043	351435	48/26	351435	48/26	48/25	351435
23	129145	48802	48/61	351435	48/25	48/61	48/26	48/61	48/26	48/25
24	232043	48810	48/63	48/25	48/26	48/63	48/61	48/63	48/61	48/26
25	351435	48811	48800	48/26	48/61	48800	48/63	48800	48/63	48/61
26	48/25	48812	48802	48/61	48/63	48806	48800	48802	48800	48/63
27	48/26	48815	48806	48/63	48800	48811	48811	48811	48811	48800
28	48/51	48821	48810	48800	48806	48812	48812	48812	48812	48806
29	48/61	48831	48811	48806	48811	48814	48814	48814	48814	48811
30	48800	48835	48812	48811	48812	48815	48815	48815	48815	48812
31	48802	48870	48815	48812	48814	48818	48818	48818	48818	48814
32	48810	48887	48818	48815	48815	48821	48821	48821	48821	48815
33	48811	48890	48821	48818	48818	48823	48823	48827	48827	48821
34	48812	493521	48823	48821	48821	48827	48827	48894	48873	48827
35	48815	552000	48827	48823	48823	48870	48873	48896	48875	48870
36	48818	553800	48831	48831	48870	48873	48894	48898	48894	48873
37	48821	555600	48835	48835	48873	48886	48896	493521	48896	48875

	Station ID of Class 1 AWS as of evaluation month/year									
	3/2021	**4/2021**	**5/2021**	**6/2021**	**7/2021**	**8/2021**	**9/2021**	**10/2021**	**11/2021**	**12/2021**
38	48827	556300	48870	48870	48886	501508	48898	501508	48898	48886
39	48831	556400	48873	48873	48890	555300	493521	552000	493521	48894
40	48835	556500	48887	48886	493521	555600	501508	553400	501508	48896
41	493521	556600	48890	48890	501508	556300	552000	553500	552000	48898
42	501508	556700	493521	493521	553400	556400	553400	553800	553400	493521
43	552000	556800	553800	501508	553800	556500	553500	554700	553500	501508
44	553500	557000	555600	552000	555300	556600	553800	555300	553800	552000
45	553800	557100	556300	555600	555600	556700	554700	555600	554700	553400
46	555300	557200	556400	556300	556300	556800	555300	556300	555300	553500
47	555600	557300	556500	556400	556400	557000	555600	556400	555600	553800
48	556400	557400	556600	556500	556500	557100	556300	556500	556300	554700
49	556500	557500	556700	556600	556600	557200	556400	556600	556400	555300
50	556600	557700	556800	556700	556700	557300	556500	556700	556500	555600
51	556700	561800	557000	556800	556800	557400	556600	556800	556600	556300
52	556800	603900	557100	557000	557000	557500	556700	557000	556700	556400
53	557000	604000	557200	557100	557100	557600	556800	557100	556800	556500
54	557100	604100	557300	557200	557200	557700	557000	557200	557000	556600
55	557200	604200	557400	557300	557300	561800	557100	557300	557100	556700
56	557300	604300	557500	557400	557400	603900	557200	557400	557200	556800
57	557400	604400	557600	557500	557500	604000	557300	557500	557300	557000
58	557500	604600	557700	557600	557600	604100	557400	557600	557400	557100
59	557700	625960	561800	557700	557700	604200	557500	557700	557500	557200
60	561800	653845	603900	561800	561800	604300	557600	561800	557600	557300
61	604000	986042	604000	603900	603900	604600	557700	603900	557700	557400
62	604200	ARG0000045	604100	604000	604000	604700	561800	604000	561800	557500
63	604400	AWS0000009	604200	604100	604100	604800	603900	604200	603900	557600
64	604600	AWS0000011	604300	604200	604200	609600	604000	604300	604000	557700
65	604800	AWS0000012	604600	604300	604300	625960	604200	604400	604200	561800
66	625960	AWS0000013	604700	604400	604600	653200	604300	604600	604300	603900
67	653845	AWS0000015	625960	604600	604700	653845	604600	604700	604400	604000
68	838293	AWS0000016	626493	604700	604800	838293	604700	604800	604600	604200
69	904892	AWS0000018	653200	604800	609600	869500	604800	609600	604700	604300
70	968206	ST001	653845	609600	653200	870000	609600	625960	604800	604400
71	986042	st1	968206	625960	653845	904892	653200	653200	609600	604600
72	ST001	st11	986042	653200	838293	968206	653845	653845	653200	604700
73	st1	st12	ARG0000045	653845	870000	986042	838293	838293	653845	604800
74	st11	st14	AWS0000006	904892	904892	ARG0000045	863700	863700	863700	625960
75	st14	st15	AWS0000007	968206	968206	AWS0000001	863800	863800	863800	653200
76	st15	st2	AWS0000010	ARG0000045	ARG0000045	AWS0000002	869500	865700	865700	653845
77	st2	st3	AWS0000012	AWS0000002	AWS0000002	AWS0000004	904892	869500	869500	838293
78	st3	st4	AWS0000013	AWS0000004	AWS0000004	AWS0000005	968206	904892	904892	863700
79	st4	st5	AWS0000015	AWS0000006	AWS0000005	AWS0000006	986042	968206	968206	863800
80	st5	st6	AWS0000016	AWS0000007	AWS0000006	AWS0000007	ARG0000041	986042	986042	865700
81	st6	st7	AWS0000017	AWS0000008	AWS0000007	AWS0000008	ARG0000045	ARG0000041	ARG0000041	869500
82	st7	st8	AWS0000020	AWS0000010	AWS0000008	AWS0000009	AWS0000001	ARG0000045	ARG0000045	870000
83	st8	st9	ST001	AWS0000012	AWS0000010	AWS0000010	AWS0000002	AWS0000001	AWS0000001	904892
84	st9		st1	AWS0000013	AWS0000012	AWS0000012	AWS0000005	AWS0000002	AWS0000002	968206
85			st11	AWS0000015	AWS0000013	AWS0000013	AWS0000006	AWS0000004	AWS0000005	986042
86			st12	AWS0000016	AWS0000015	AWS0000015	AWS0000007	AWS0000005	AWS0000006	ARG0000041
87			st14	AWS0000017	AWS0000016	AWS0000016	AWS0000008	AWS0000006	AWS0000007	ARG0000045
88			st15	AWS0000020	AWS0000017	AWS0000017	AWS0000009	AWS0000007	AWS0000008	AWS0000001
89			st2	ST001	AWS0000018	AWS0000018	AWS0000010	AWS0000008	AWS0000009	AWS0000002
90			st3	ST002	AWS0000020	AWS0000020	AWS0000011	AWS0000009	AWS0000010	AWS0000004
91			st4	st1	AWS0000022	AWS0000022	AWS0000015	AWS0000010	AWS0000013	AWS0000005
92			st5	st11	ST001	ST001	AWS0000016	AWS0000013	AWS0000015	AWS0000006
93			st6	st12	ST002	ST002	AWS0000017	AWS0000015	AWS0000016	AWS0000007
94			st7	st13	ST013	ST013	AWS0000020	AWS0000016	AWS0000017	AWS0000008
95			st8	st14	ST021	ST021	AWS0000022	AWS0000017	AWS0000019	AWS0000009
96			st9	st15	ST023	ST023	ST001	AWS0000020	AWS0000020	AWS0000010
97				st2	st1	st1	ST002	AWS0000022	AWS0000022	AWS0000015
98				st3	st11	st11	ST013	ST001	ST001	AWS0000016
99				st4	st12	st12	ST021	ST002	ST013	AWS0000017
100				st5	st13	st13	ST023	ST013	ST021	AWS0000020
101				st6	st14	st14	st1	ST021	ST023	AWS0000022
102				st7	st15	st15	st11	ST023	st1	ST001
103				st8	st16	st16	st12	st1	st11	ST002
104				st9	st17	st17	st13	st11	st12	ST013
105					st18	st18	st14	st12	st13	ST021
106					st2	st2	st15	st13	st14	ST023
107					st3	st3	st16	st14	st15	st1
108					st4	st4	st17	st15	st17	st11
109					st5	st5	st18	st16	st18	st12
110					st6	st6	st2	st17	st2	st13
111					st7	st7	st3	st18	st3	st14
112					st8	st8	st4	st2	st4	st15
113					st9	st9	st5	st3	st5	st16
114							st6	st4	st6	st17
115							st7	st5	st7	st18
116							st8	st6	st8	st2

	Station ID of Class 1 AWS as of evaluation month/year									
	3/2021	**4/2021**	**5/2021**	**6/2021**	**7/2021**	**8/2021**	**9/2021**	**10/2021**	**11/2021**	**12/2021**
117							st9	st7	st9	st3
118								st8		st4
119								st9		st5
120										st6
121										st7
122										st8
123										st9

4.3. Details of the result

This assessment method can detect stations well related to observation value at respective Synoptic stations. An example of good relativeness is shown in Figure 3. The left figure shows a double–mass analysis curve, and the right figure shows a scatter plot of observation data.

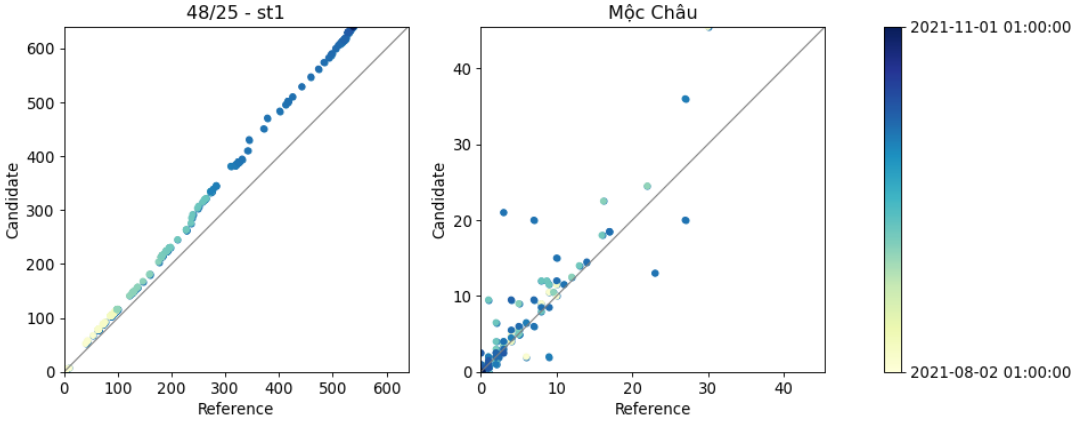

Figure 3. An example of AWS highly correlated to the Synoptic station as of October 2021. [Left: double-mass analysis curve, right: scatter plot of observation data.] ID: st1, Slope: 1.19275, R^2: 0.99962.

4.3.1. Poor example

On the other hand, an example of a station poorly correlated to the Synoptic station is shown in Figure 4. As only the SYNOP axis plot data in the right figure, this station (48810) had not observed precipitation, although the Synoptic station observed.

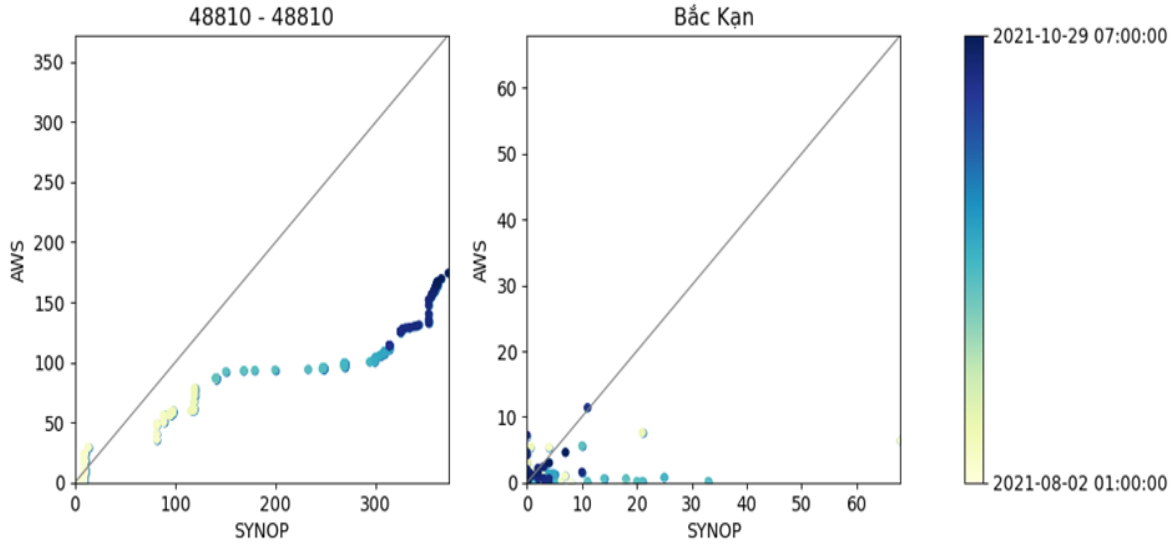

Figure 4. An example of AWS poorly correlated to the Synoptic station as of October 2021. [Left: double-mass analysis curve, right: scatter plot of observation data.] ID: 48810, Slope: 0.40968, R^2: 0.92028.

4.3.2. Slope of the regression line, which does not meet the criteria

If the slope of the regression line of the double-mass analysis curve is steep or too low, the station will be eliminated in the month. The example shown in Figure 5 might have overestimated precipitation compared to Synoptic station values. Some problems might have happened in October because September's slope is 1.18043.

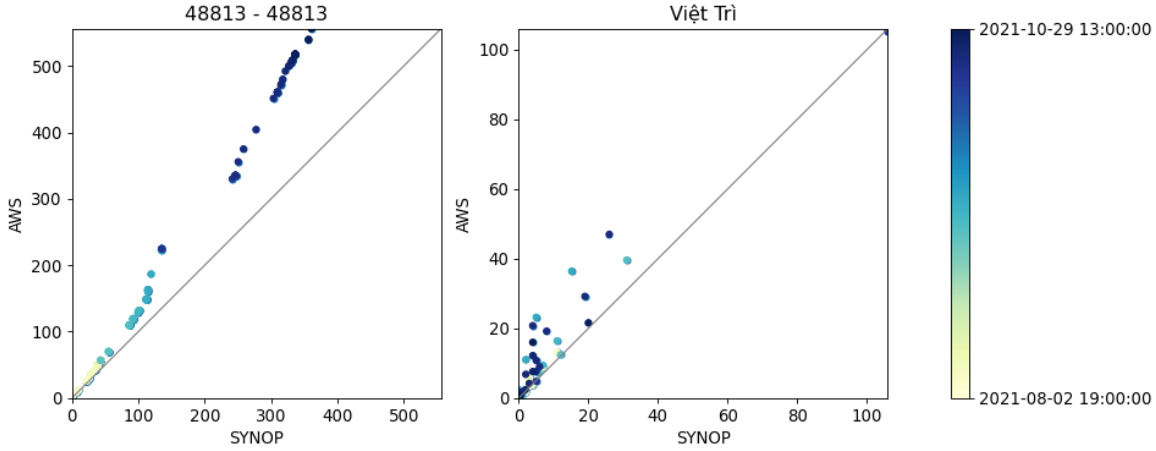

Figure 5. An example of AWS with a steep slope as of October 2021. [Left: double-mass analysis curve, right: scatter plot of observation data.] ID: 48813, Slope: 1.48437, R^2: 0.99363.

4.3.3. Check with time series

Since evaluation was done every month, it is possible to detect when an observation error occurred. An example of the results aligned with periods is shown in Figure 6. AWS 604100 had been observed properly until August 2021, but the data observed from September might have been wrong and its slope and R^2 value had not met the criteria since then.

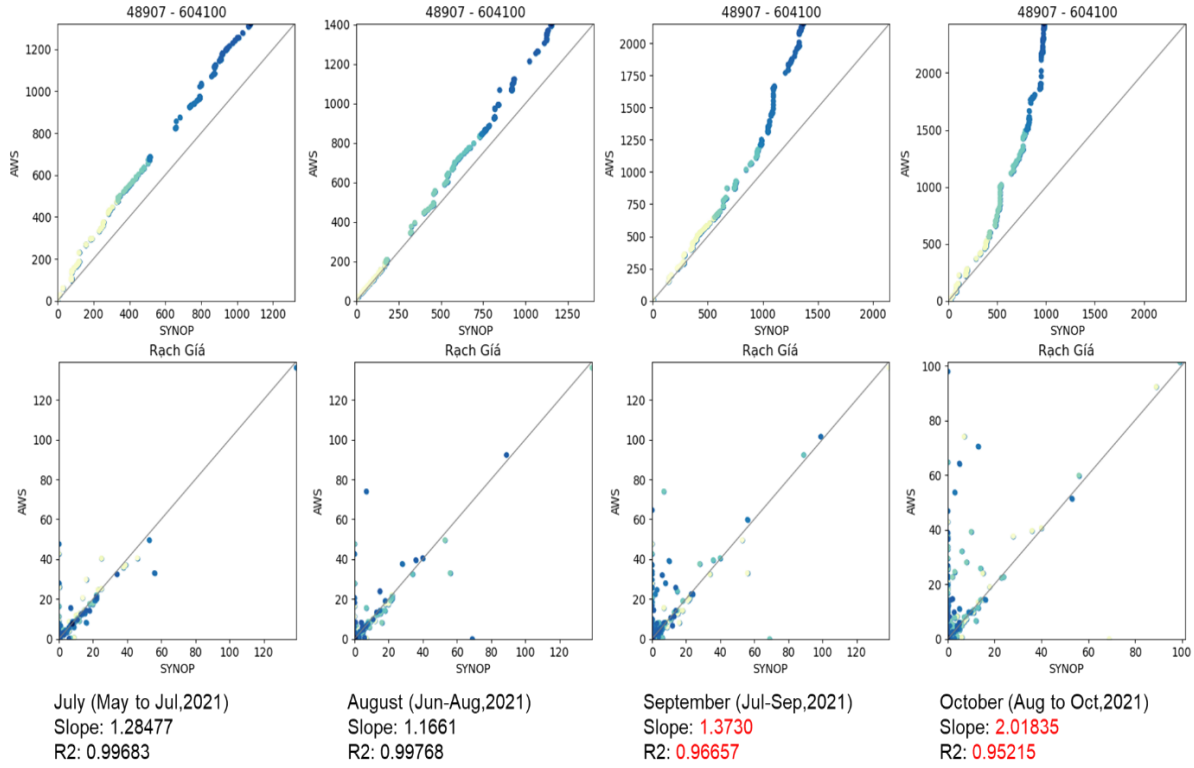

Figure 6. Comparison of before and after an error occurred (ID: 604100). [Upper: double-mass analysis curve, lower: scatter plot of observation data.] *Values written in red do not meet the criteria for Class 1 AWS.

5. Definition of Class 2 AWS

5.1. Dataset

Referring to Class 1 AWS defined in the above monthly, AWSs located around the other AWSs of both Class 1 and Class 2 within 20 km away were extracted as Class 2 AWS candidates.

5.2 Result of Class 2 AWS

As per the criteria for Class 2 AWS, evaluation was done each month by using the past 3-month data from the evaluation month. The result of the Class 2 AWSs in December 2021 (the dataset is from 1st October to 31st December 2021) is 710 stations in total. As reference stations are changed every month, candidates will also be changed according to the reference. Therefore, non-listed Class 2 AWSs have two reasons; observation data had not met the criteria or there was no reference corresponding to the candidate.

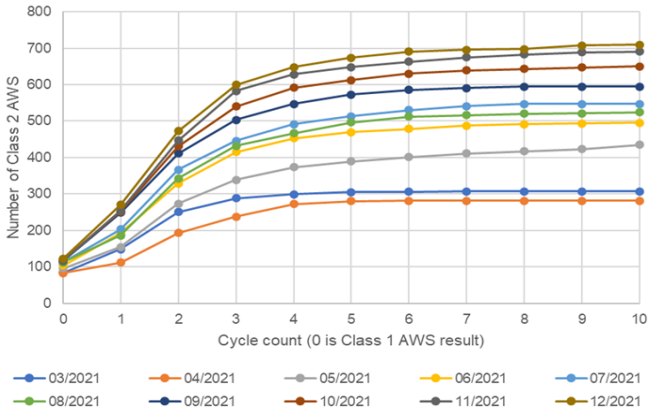

Figure 7. Relativeness between the number of stations and cycle count.

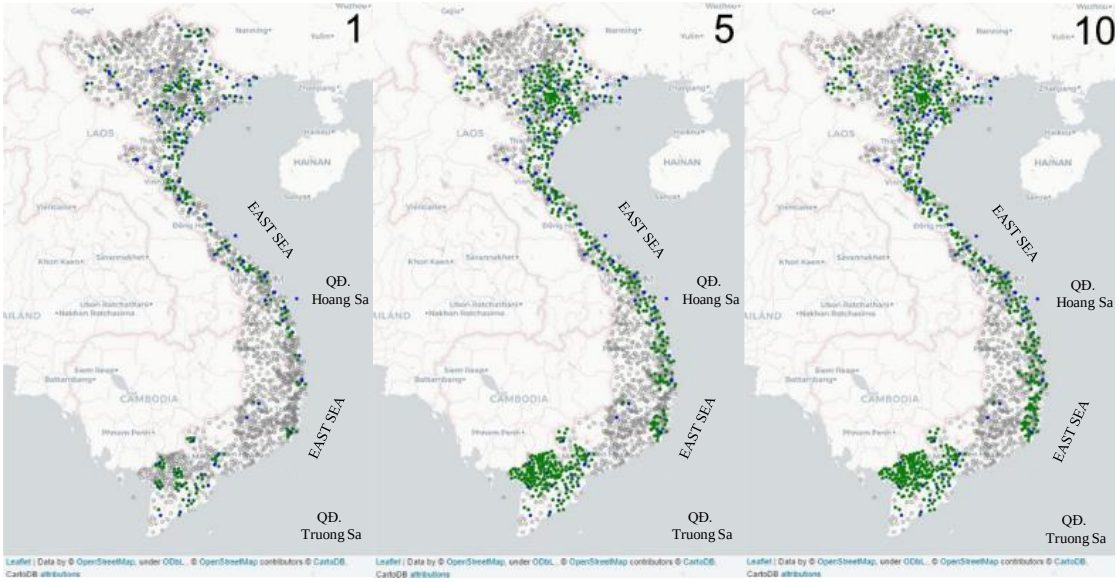

Figure 8. The first assessment, five and ten-cycled-assessment results (October to December 2021). [Blue: Class 1 AWS, Green: Class 1 AWS, Gray: candidate AWS.]. *This map plots the station where data were provided from the AMO in 2022 and the locations of Hoang Sa Islands, Truong Sa Islands, and East Sea are not shown on the map.

Figure 7 shows a relativeness between the number of Class 2 AWS and cycle count, and Figure 8 shows a transition of evaluated AWSs as Class 2 in 10-cycle processing. Since this

assessment refers to the latest Class 2 AWS (initial reference is Class 1 AWS) to retrieve candidate stations, repeated assessment cycles can enlarge the number of evaluated stations and the result will converge to a number. Additionally, this result also indicates that the number of Class 1 AWS (initial number of references) is key to obtaining a large number of evaluated stations.

6. Summary and Conclusions

This assessment method proposed in this study gives more capability to assess AWS located nearby another station. However, some areas, especially the northwest mountain area (Tây Bắc) and mid-south highland area (Tây nguyên Trung Bộ) cannot have been assessed. It is difficult to locate the reason. One of the reasons may be supposed to be the criteria obtained from AMeDAS. Because the AMeDAS used for the criteria are installed in some small islands in the southern part of Japan where no steep mountains, therefore, a difference in geographical precipitation pattern could not have been covered by this method and the criteria. Additionally, the assessment distance between the reference and candidates had been 20 km temporarily. There remains for discussion.

This assessment method was based on the data of the JMA, but the data of the VNMHA/AMO are surely required for obtaining the proper criteria for this assessment method. Therefore, continuous maintenance on some reference AWSs is yet required for the proper criteria even if this assessment will be conducted ever since.

Supplementary Materials: The JMA observation data used in the assessment are available online at https://www.data.jma.go.jp/gmd/risk/obsdl/index.php. Station data of the JMA are available online at https://www.jma.go.jp/jma/kishou/know/amedas/ame_master.pdf.

Author Contributions: This article drafting, by Mr. R. Kobayashi; writing–review and editing, by Mr. R Kobayashi, Mr. Le Xuan Duc and Mr. Pham Minh Tien; All authors have read and agreed to the publish.

Acknowledgments: This JICA technical cooperation project was supported by the people of Japan as the JICA projects and technical assistance by the JMA as DRR technical cooperation of WMO international cooperation frame for Southeast Asian counties. We express our special thanks to JICA experts and all staff members of the VNMHA who joined and supported the project.

References

1. Mikami, M.; Ichijo, H.; Matsubara, K.; Duc, L.X.; Nguyen, H.A. A proposal of AWS maintenance and periodic calibration tools and installation of AWGs for Radar QPE calibration. *VN J. Hydrometeorol.* **2020**, *05*, 13–35.
2. Makihara, Y. A method for improving radar estimates of precipitation by comparing data from radars and rain gauges. *J. Meteor. Soc. Japan* **1996**, *74*, 459–480. doi:10.2151/jmsj1965.74.4_459.
3. Searcy, J.K.; Hardison, C.H. Double–Mass Curves. *Geol. Surv. Water Supply Paper* **1960**, *1541–B*, 34–40.
4. Suzuki, H.; Nakakita, E.; Takahashi, H. Spatial representativeness of rainfall: Analysis using data observed at railway stations and meteorological stations. *Annu. J. Hydraul. Eng.* **2008**, *52*, 187–192.

JOURNAL OF
HYDRO-METEOROLOGY

Research Article

Quality check of rain gauge data for quantitative precipitation estimate

Michihiko Tonouchi[1]*, Bui Thi Khanh Hoa[2], Nguyen Viet Hung[2], Nguyen Minh Cuong[2]

[1] International Affairs Department, Japan Meteorological Business Support Center, Tokyo, 101-0054, Japan; tono@jmbsc.or.jp

[2] Aero-Meteorological Observatory, The Viet Nam Meteorological and Hydrological Administration, Hanoi, Vietnam; khanhhoa303@gmail.com; nguyenviethungb115@gmail.com; nguyenminhcuong30596@ gmail.com

*****Correspondence: tono@jmbsc.or.jp; Tel.: +81-3-5281-0440

Received: 4 May 2023; Accepted: 15 June 2023; Published: 25 June 2023

Abstract: The Quantitative Precipitation Estimation (QPE) method of the Japan Meteorological Agency (JMA) using radar and rain gauge data has been started to be deployed at the Viet Nam Meteorological and Hydrological Administration (VNMHA) since 2019 through a technical cooperation project of the Japan International Cooperation Agency (JICA). Quality control of radar and rain gauge data is a vital issue in keeping the accuracy of QPE. Especially rain gauge data is essential because QPE processes regard rain gauge data as exact values in calibration processes. VNMHA had yet to develop a quality control system and regular maintenance scheme for Automatic Weather Stations (AWS) and Automatic Rain Gauges (ARG). In order to make a reliable QPE product, a quality check for rain gauge data comparing mutual rain gauge data experimented and 1) missing data ratio, 2) proportion to mean of nearly ten stations, and 3) double sum curve check was selected as thresholds to select relatively reliable rain gauge stations. As a result of the quality check for rain gauge data in May 2023, 1,299 stations were chosen, and QPE with rain gauges selected showed stable precipitation distribution.

Keywords: QPE; Quality check; Rain gauge; Precipitation map; Radar data calibration.

1. Introduction

The bilateral cooperation project between the JICA and the VNMHA named "Strengthening Capacity in Weather Forecasting and Flood Early Warning System" has been conducted since June 2018. The project targets developing weather products for Disaster Risk Reduction [1]. As an indicator for precipitation monitoring, QPE was introduced during the 1st period of the project. QPE regards rain gauge data as teacher signals (exact values), calibrates radar observation data with it, and converts it to precipitation amount by using a simple Z-R relationship [2].

The algorism of QPE are: 1) quality control and one-hour accumulation of rain gauge data; 2) conversion from radar volume scan intensity data to lowest level distribution and one-hour accumulation; 3) 1st calibration by rain gauge data (comparison of precipitation at each radar area using converted precipitation from radar scans and rain gauge data); 4) 2nd calibration by rain gauge data (variational calculus methods, harmonizing both converted radar precipitation data in overlap area); 5) produce a national composite map [2–4].

VNMHA manages ten radars and around 2,000 AWS and ARG (hereafter described as "ARG"), and rain gauge data is collected to the Central Data Hub (CDH). VNMHA

additionally manages 186 synoptic stations, and equipment at synoptic stations is compared with standard equipment regularly [4]. Synoptic station data is the most reliable data in Viet Nam; however, synoptic observation is implemented three- or six-hourly, and QPE requires at least one hourly precipitation data for its calibration processes. VNMHA calibrates/checks the accuracy of rain gauges at ARG before installing them; however, after installations, the accuracy of ARG is not checked frequently [5].

Ideally, the rain gauge of ARG should be quality checked with re-analysis data of Numerical Weather Prediction, for example, the WIGOS Data Quality Monitoring System (WDQMS) web tool [6], and equipment at doubtful observation should be checked and repaired promptly. However, VNMHA had yet to introduce a quality check system and maintenance on ARG stations. In order to evaluate the reliability of ARG data, the Radar Product Team (working group 2) conducted a quality check of rain gauge data for QPE in 2021 and 2022.

2. Indexes for quality check

For the operation of QPE, a collection of stable and steady rain gauge data is required, and VNMHA has a relatively dense observation network compared to nearby countries. In the quality check process, each station's data was compared with a mean of the nearest ten station's data (hereafter described as "area precipitation"), and the following indexes for the quality check were calculated.

1. Reporting ratio of ARG (more than 80 percent);
2. Reporting ratio of missing value and abnormal data (0-byte data) (less than 20 percent);
3. Abnormal data ratio (negative value or immense value, more than 500 mm/hour);
4. Small value data ratio 1 (no precipitation at the station when area precipitation is more than 5mm/hour);
5. Small value data ratio 2 (precipitation at the station is smaller than 1/10 of area precipitation);
6. Big value data ratio 1 (precipitation at the station is three times bigger than area precipitation when area precipitation is more than 5mm/hour);
7. Big value data ratio 2 (precipitation at the station is more than 15 mm, and area precipitation is smaller than 5mm/hour);
8. Proportion compared to area precipitation.

The trial was done for October 2021 data, and index-1 and index-8 were selected as thresholds. After excluding stations trapped by two thresholds, 3rd check was implemented by a double sum curve. A double sum curve (Figure 1) consisted of a time sequence of accumulated precipitation ($= \sum_{h=1}^{24\times[number\ of\ day\ in\ a\ month]}(R_h)$) at the station, nearest three stations and mean of area precipitation in a month in an upper figure and accumulated precipitation at nearest three stations and area precipitation (vertical axis) were plotted in a lower figure with accumulated precipitation at the exact station (horizontal axis). A good example is shown in Figure 1, lines smoothly changed in the same manner in an upper figure, and the angle of the plotted line was near the 45-degree line (y = x) in a lower figure.

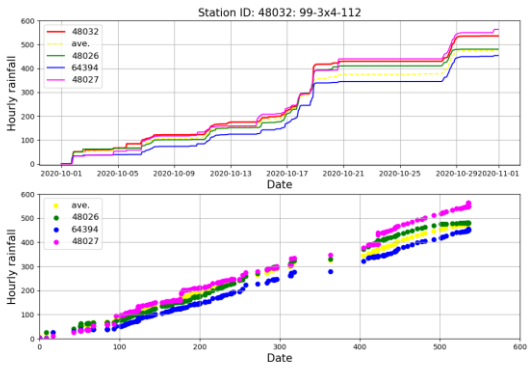

Figure 1. Double sum curve.

Examples excluded by the "double sum curve" are shown in Figure 2. In the case of a), in the 2nd half of the month, the lowest line (accumulated precipitation marked with ☆) did not increase because of failures on a rain gauge or a communication line. In the case of b), the shape of the curve on the lowest line (marked with ☆) is similar to others, but total precipitation is almost 40 percent of others. In the case of c), there were two gaps (surrounded by □) in an upper figure, and a few steps appeared in a lower figure.

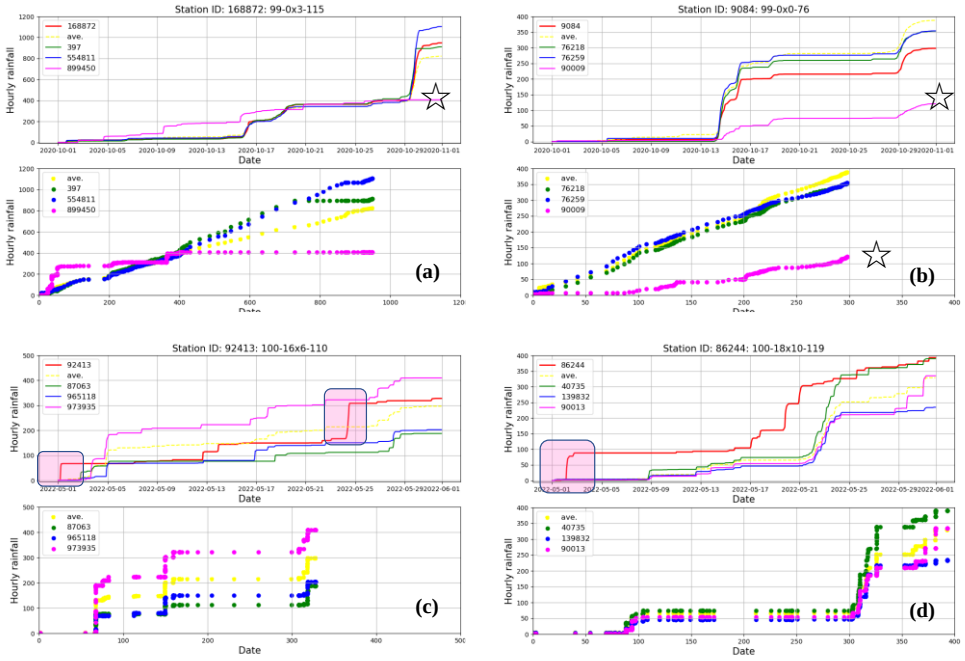

Figure 2. Double sum curves at stations excluded.

Observation failure seemed to happen at the station or isolated rain only nearby the station, or observation time was incorrect. In the case of showers brought by convective clouds, such isolated rains might happen; however, if such gaps are frequently observed, the data seems not to be reliable. In the dry season, the frequency and total amount of precipitation become smaller, and double sum curves tend to be scattered. Quality checks by double sum curves should be adopted for rainy season data.

The same evaluation was adopted for May 2022 data, and the review of ARGs is plotted in Figure 3. (Screening threshold was the same as in October 2021). In Figure 3, stations are categorized into three levels (Level 3: precipitation at the station is within 20 percent of area precipitation, Level 2: within 50%, and Level 3: within 100% of area precipitation). Level 3 stations (83 to 120 percent precipitation compared to area precipitation) are plotted as a circle (●), Level 2 stations (75-83 percent or

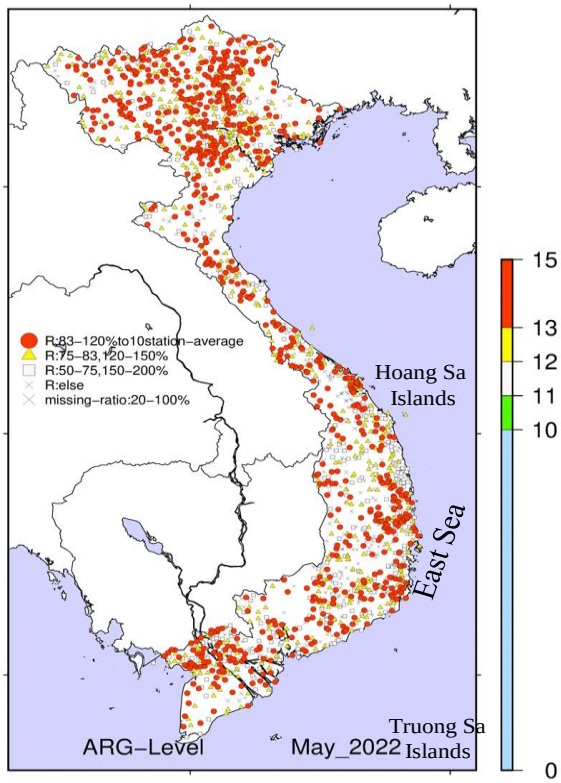

Figure 3. Evaluation of ARG.

150-200 percent to area precipitation) are plotted as a triangle (△), Level 1 stations (50-75 percent or 150-200 percent) are plotted as a square (□). Additionally, stations bigger than 200 percent or smaller than 50 percent value to area precipitation are plotted as a smaller cross (x), and stations with a missing report ratio of more than 20 percent are plotted as a bigger cross (×). The number of ARG stations in May 2022 was 1,913; Level 3 stations were 774; Level 2 stations were 525 (Level 2+3 were 1,299), and Level 1 stations were 408 (Level 1+2+3 were 1,607).

As shown in Figure 3, the density of ARG is thicker in northern Viet Nam, and in these areas, the number of Level 3 stations is more; on the other hand, in a mountainous area, northwest area, coarse ARG area, for example, North-central area or in central, the number of Level 3 stations are smaller. As mentioned above, QPE treats rain gauge data as exact signals for calibration, so if VNMHA has a plan for new installation of AWS/ARG or quality check activities (AQC, maintenance activities at ARG stations), VNMHA could start activities from these mountainous areas or coarse ARG area.

3. Comparison of QPE results with the synoptic station

To evaluate QPE results, comparisons between 6 hourly precipitation at synoptic stations and QPE values at the nearest grid point were implemented. Monthly accumulated precipitation of QPE (1 hourly × 24 hours/day × 31 days) is plotted in the right figure, and monthly total precipitation at synoptic stations is plotted in the left figure of Figure 4. The QPE monthly precipitation map well-described distribution of spacial precipitation features in the month. In remote areas from radar sites, for example, northwest mountain areas, QPE precipitation tends to become smaller than synoptic observation data because radar cannot scan lower dense rain layers, radar locates far from areas, and/or geographical barriers block lower radar beams.

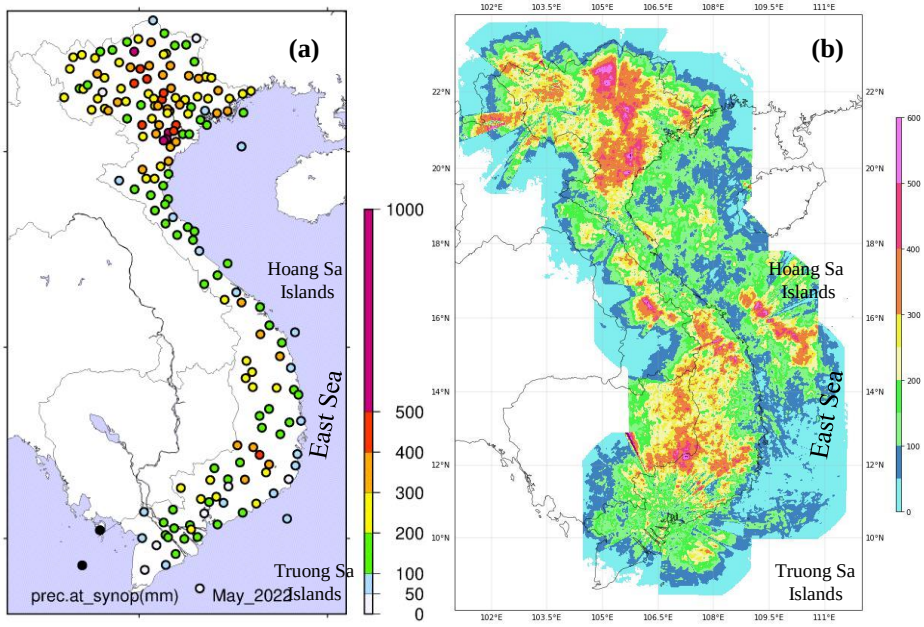

Figure 4. Precipitation at synoptic stations (a) and QPE (b).

Generally, the number of rain gauge data used for QPE becomes bigger, and the results of QPE become more stable. However, when big or small values were observed, especially in 2 radar-overlapped areas, sometimes over-calibration occurred, and then QPE results became unstable. An example of over-correction is shown in the upper figure of Figure 5. In this case, heavy rain was observed in 2 radar overlapped areas, and 2nd calibration factor

became pretty big, and as a result, extreme rain areas were analyzed (surrounded by boxes). In the below figure of Figure 5, the results with ARG station table quality checked are shown. At 22UTC, there is a heavy precipitation area in the northern area, and at 24UTC, another strong rain area was estimated in the Lao PDR area (Figure 5). However, after removing abnormal data at 22UTC and 24UTC, QPE was adjusted and became more stable. In operational QPE, limitations of 1st and 2nd calibration factors are set to avoid over-correction caused by coarse rain gauge density in the overlap area in QPE processes, additionally.

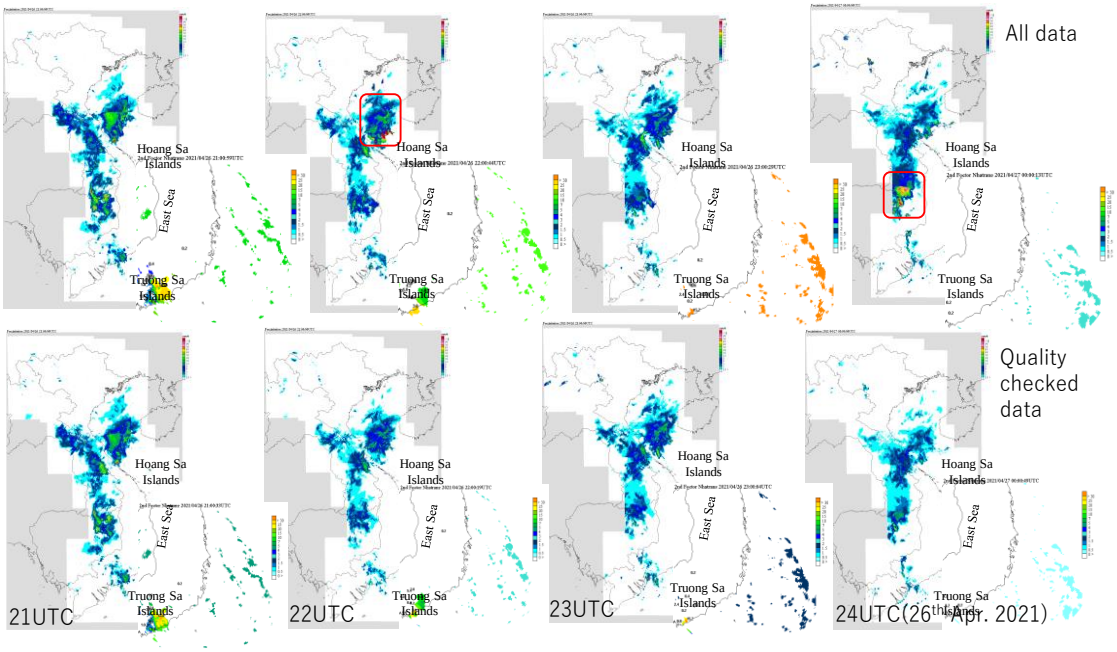

Figure 5. QPE results with quality checked data: upper: All data, lower: quality checked data, at 21 to 24UTC 26 April 2021, each figure shows QPE result and 2nd calibration factor.

Figure 6 and Table 1, comparison results between synoptic observation data and QPE 6 hourly accumulated data were shown. Comparisons were evaluated by the "slope" and "correlation coefficient" of simple regression equations. "Slope" is calculated as the slope in the regression analysis when the intercept is set as 0.0. The left figure is the correlation coefficient distribution, the middle figure is a slope of a simple regression equation (QPE precipitation to synoptic observation), and the right figure is the monthly total precipitation in May 2021 (accumulated 1-month precipitation by QPE).

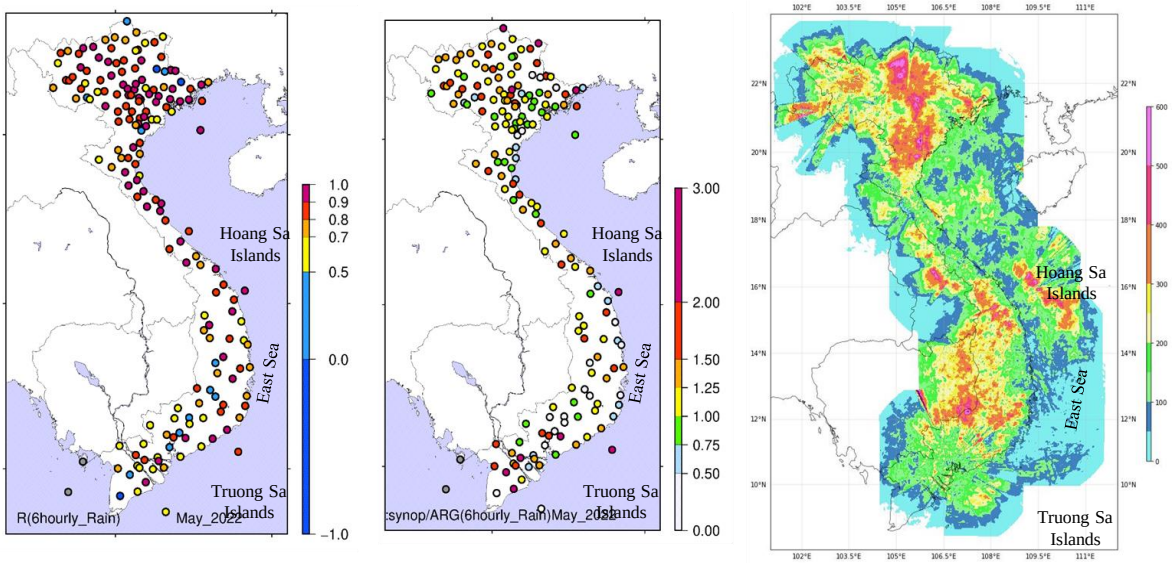

Figure 6. Evaluation of QPE with synoptic observation data (May 2021).

In the northern and north-central areas, the "correlation coefficient" is higher, but it is relatively small in the southern region. And "slope" of each station is mostly smaller than 1.0. It means QPE at the station is generally smaller than synoptic observation data. In mountainous areas or remote areas, the slope is bigger than 3.0 or smaller than 0.5. Stations with relatively smaller correlation coefficients and/or bigger/smaller slope factors should be checked first by comparison with a rain gauge checker through on-site maintenance activities.

If the number of stations becomes smaller, QPE becomes unstable, mainly when pretty heavy rain is observed. On the other hand, if the number of stations becomes bigger, risks which include not reliable stations, become bigger. Considering both demerits, the Level 2 station is recommended for QPE as a result of quality checks.

Table 1. Number of stations in evaluations of QPE and synoptic data in accordance with ARG-Levels.

	Correlation coefficient	**Number of station**	**Slope**	**Number of station**
Level 2	0.9 ≤	50	0.83~1.20	57
~1,300	0.8 ≤	104	0.63~1.50	113
	0.5 ≤	165	0.50~2.00	151
Station table in October 2020	0.9 ≤	42	0.83~1.20	52
~800	0.8 ≤	92	0.63~1.50	102
	0.5 ≤	162	0.50~2.00	142
Level 1+ 2+3	0.9 ≤	50	0.83~1.20	55
~1,700	0.8 ≤	107	0.63~1.50	114
	0.5 ≤	165	0.50~2.00	151

(*) The total number of synoptic stations used for comparisons is 165.

Quality check processes for ARGs are summarized in Figure 7, and these comparisons were automatically implemented in the QPE server on a monthly basis. For stable QPE, quality checks on ARGs should be continued, and an ARG station list for QPE should be regularly updated based on Quality checks.

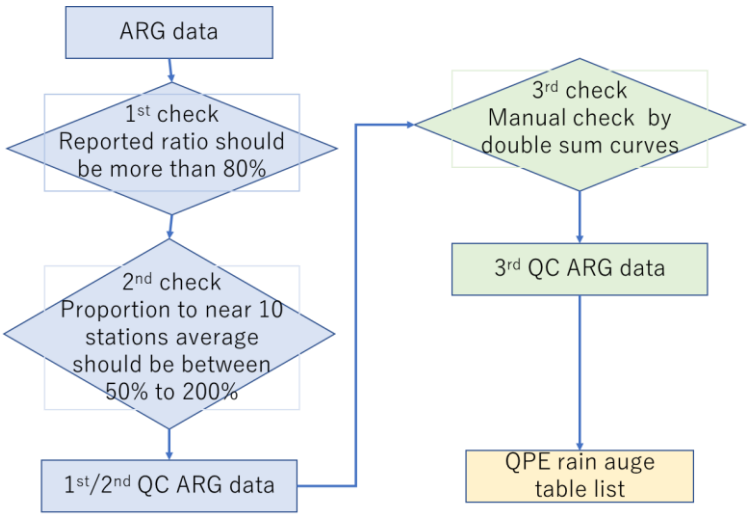

Figure 7. A flow for quality check of rain gauge for QPE.

3. Conclusions

The study results are: 1) a method for evaluating ARG data not considering other data (synoptic stations data) was reported; 2) QPE reliability was evaluated with synoptic data. To keep the accuracy of ARG observation, automatic quality checks and maintenance at ARG stations based on a guideline on maintenance are recommended.

In Japan, QPE data is used for soil water index, risk index for landslides, and flood risk index for flood (https://www.jma.go.jp/bosai/en_risk). And VNMHA operates QPE and shares its results on the website (http://amo.gov.vn/rain/) as 1-, 3-, 6-, 12-, 24-, 48-, and 72-hours accumulated precipitation maps. To develop risk indexes used in Japan, VNMHA needs to collect disaster events records with date, time, and location (latitude and longitude) to analyze with QPE data.

A table of rain gauge stations (Level 2) for QPE was proposed and temporarily used for its operation. For future research and developments of products, VNMHA needs to re-analyze QPE with quality-checked radar and ARG data. Raw observation data is indispensable for these purposes, and storage of raw observation data is strongly recommended.

Author Contributions: This article drafting: M.T.; Writing review and editing: B.T.K.H., N.V.H., N.M.C.

Acknowledgments: This JICA technical cooperation project was supported by the people of Japan as the JICA projects and technical assistance by the JMA as DRR technical cooperation of WMO international cooperation frame for Southeast Asian counties. We express our special thanks to JICA experts and all staff members of the VNMHA who joined and supported the project.

Disclaimer: The authors declare that this article is the work of the authors, has not been published anywhere, and has not been copied from previous studies; there is no conflict of interest in the author group.

References

1. Tonouchi, M.; Kasuya, Y.; Tanaka, Y.; Akatsu, K.; Akaeda, K.; Nguyen, V.T. Activities of JICA on disaster prevention and achievement of JICA project in Period 1. *VN J. Hydrometeorol.* **2020**, *5*, 1–12.
2. Kimpara, C.; Tonouchi, M.; Hoa, B.T.K.; Hung, N.V.; Cuong, N.M.; Akaeda, K.; Quantitative precipitation estimation by combining rain gauge and meteorological radar network in Vietnam. *VN J. Hydrometeorol.* **2020**, *5*, 36–50.
3. Makihara, Y. A method for improving radar estimates of precipitation by comparing data from radars and rain gauges. *J. Meteor. Soc. Japan* **1996**, *74*, 459–480. Doi:10.2151/jmsj1965.74.4_459.
4. Makihara, Y. Algorithms for precipitation nowcasting focused on detailed analysis using radar and rain gauge data. Technical Reports of the MRI, **2000**, *39*, 63–111. doi:10.11483/mritechrepo.39.
5. Kobayashi, R.; Duc, L.X.; Tien, P.M. Attempt to detect maintenance-need rain gauge station by double-mass analysis. *J. Hydro-Meteorol*. **2023**, *15*, 10–20.
6. World Meteorological Organization. WIGOS Data Quality Monitoring System, https://wdqms.wmo.int/about, monitored on 5 June 2023.

JOURNAL OF
HYDRO-METEOROLOGY

Research Article

Evaluation of the radar-based quantitative precipitation estimation composite in Viet Nam

Chiho Kimpara[1], Michihiko Tonouchi[2], Bui Thi Khanh Hoa[3], Nguyen Viet Hung[3], Nguyen Minh Cuong[3], Kenji Akaeda[4]*

[1] Japan Weather Association, Tokyo170-6055, Japan; kimpara.chiho@jwa.or.jp
[2] Japan Meteorological Business Support Center, Tokyo101-0054, Japan; tono@jmbsc.or.jp
[3] Aero Meteorological Observatory, Hanoi 10000, Vietnam; khanhhoa303@gmail.com; nguyenviethungb115@gmail.com; nguyenminhcuong30596@ gmail.com
[4] Japan International Cooperation Agency, Tokyo102-0084, Japan; akaeda191@yahoo.co.jp

*Correspondence: akaeda191@yahoo.co.jp; Tel.: +84–829761096

Received: 12 May 2023; Accepted: 23 June 2023; Published: 25 June 2023

Abstract: Real-time monitoring of quantitative precipitation distribution is essential to prevent natural disasters caused by heavy rainfall. Precipitation distribution by rain gauge network or combined with radar/satellite data is operationally used in Viet Nam. Previously, meteorological radar data was simply converted to precipitation amount using a simple Z-R relationship. To get accurate quantitative precipitation estimation (QPE) data, converted precipitation amounts from radar should be corrected by rain gauge data. In the ongoing JICA technical cooperation project, preliminary development of the QPE product has been conducted by utilizing the data from the automatic rain gauge network and meteorological radar network in Viet Nam. The fundamental part of this QPE algorithm has been used and updated by Japan Meteorological Agency (JMA) for more than 25 years. This is the first attempt to get quantitative precipitation distribution with a precise resolution by combining radar and rain gauge data in Viet Nam. This paper describes each process to introduce this QPE method to Viet Nam and indicates the results through the project. Future issues to improve its accuracy are also mentioned.

Keywords: Radar; Rain gauge; QPE; Quality Control, JICA.

1. Introduction

Weather radar is an effective system for monitoring precipitation, but various methods are needed for its quantitative use. Japan Meteorological Agency (JMA) has developed a system to calculate quantitative precipitation estimation (QPE) by combining radar and rain gauges [1–2]. Based on this QPE, JMA uses it for short-time precipitation forecasts and for calculating landslides, inundation, and flood indices that are directly related to the occurrence of these disasters. JICA initiated a technical cooperation project with the Viet Nam Meteorological and Hydrological Administration (VNMHA) to introduce these JMA methods to Viet Nam. Since June 2018, a bilateral cooperative project (hereinafter described as "Project") between JICA and the VNMHA named "Strengthening capacity in weather forecasting and flood early warning system in Viet Nam" has been conducted [3–4]. A basic QPE system was introduced in the first period of the Project, and an outline of the QPE in Viet Nam was reported [5].

For improvement of QPE, various kinds of issues should be considered. The priority is to improve the quality of the rain gauge and radar observation data used in the analysis. Second, the QPE algorithm needs to be improved to fit the situation in Vietnam. In the future, the utilization of dual-polarization radar is also an important theme. However, further efforts should be made to calibrate and maintain radar for the utilization of dual-polarization radar. Several improvements for QPE have been conducted in the second half of the Project from 2020 to 2023, and these trials are reported in section 2, and some evaluation results are summarized in section 3.

2. Materials and methods

2.1. Observation Data

In VNMHA, two types of rain gauge stations are under operation. One is manual rain gauge stations which are located at 186 locations. The staff on duty at the station measures the accumulated rain amount every six hours. The other is automatic rain gauge (ARG) stations located at around 500 points. In these ARG stations, 10-minutes of rainfall amount is recorded and transferred to the data center at the VNMHA headquarters. VNMHA also receives more than 1500 ARG data operating outside VNMHA and a total of more than 2000 ARG data is available.

There are many ARG sites, but the quality of some sites is problematic. The problems of some sites are as follows; poor data transmission rate, continuation of non-zero constant value, and significant differences from surrounding sites. In this QPE algorithm, rain gauge values are treated as true values, so any errors in the rain gauge cannot be corrected. Quality control is essential to identify poor-quality rain gauge data [6].

Currently, ten meteorological radars of VNMHA are operated by the Aero Meteorological Observatory (AMO). Their locations and maximum detection range are shown in Figure 1, and their characteristics are shown in Table 1. Several different generations and types of radars are under operation. The radar network consists of two S-band radars and eight C-band radars, which consist of five Doppler radars and five dual-polarized Doppler radars. These radars have been newly replaced since 2017 (including a minor upgrade of the signal/data processing unit). This radar network covers almost the whole country and surrounding sea except for some areas where the lower layer is difficult to detect in the mountainous region.

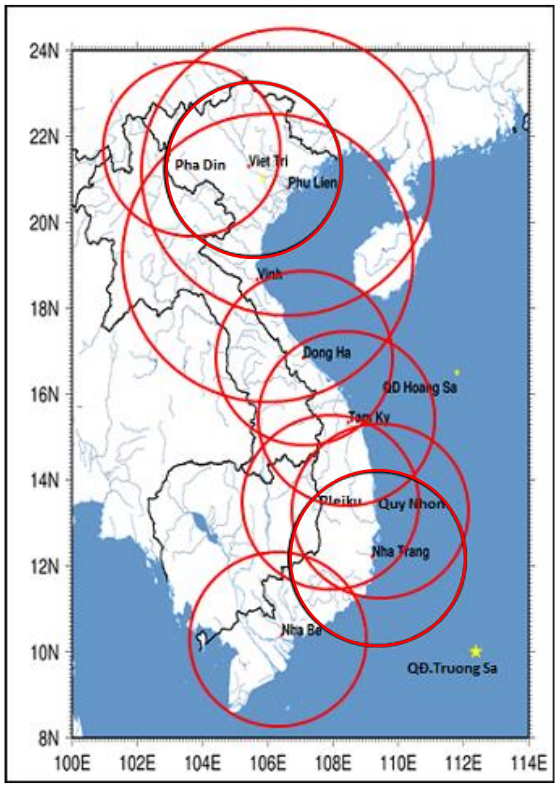

Figure 1. Meteorological radar network in March 2023. Larger circles represent Japan Radio Company (JRC) radars and other circles represent Vaisala radars.

Table 1. Characteristics of radars. D and S in the third column indicate dual-polarized radar and single-polarized radar, correspondingly. The first and second values in the detection range column show maximum detection range in intensity mode and Doppler mode respectively.

Radar Site	Height (m)	Type	Band	Detection Range (km)	Beam Width (deg)	Manufacturer
Phadin	1470	D	C	300/120	1.0	Vaisala
Viettri	154	D	C	300/120	1.0	Vaisala
Phulien	146	S	S	450/200	1.7	JRC
Vinh	92	S	S	450/200	1.7	JRC
Dongha	40	S	C	300/120	1.2	Vaisala
Tamky	52	S	C	300/120	1.2	Vaisala
Pleiku	842	D	C	300/120	1.0	Vaisala
Quynhon	582	D	C	300/120	1.0	Vaisala
Nhatrang	467	D	C	300/120	1.0	Vaisala
Nhabe	35	S	C	300/120	1.0	Vaisala

2.2. Method of QPE Calculation and its Improvements

The QPE value is obtained by combining the one-hour integrated radar value and the rain gauge value and applying a two-step correction process (primary correction and secondary correction). The basic algorithm is explained in [5]. A simplified version of the software made by JMA was installed. The essential calculation part is almost the same, but the part of the effect of beam altitude is not included.

After the software was implemented, various adjustments were made to fit the Vietnamese situation. In Vietnam, stable calculation of QPE required not only adjustment, but also improvement of the algorithm, optimization of the settings used in the calculation, and selection of rain gauges to be used. We comment on several important points below.

2.2.1. QPE algorithm

In the early stage of operation, QPE results were sometimes unstable. Especially when most of the echoes were at sea and only a few were on land, unstable results were often evident. Since the current algorithm uses a method of determining the primary correction factor for each radar in an area where multiple radars overlap by comparing each radar with the rain gauges in that area, it was found that the calculation results may vary over time if the number of valid rain gauges in this area is small.

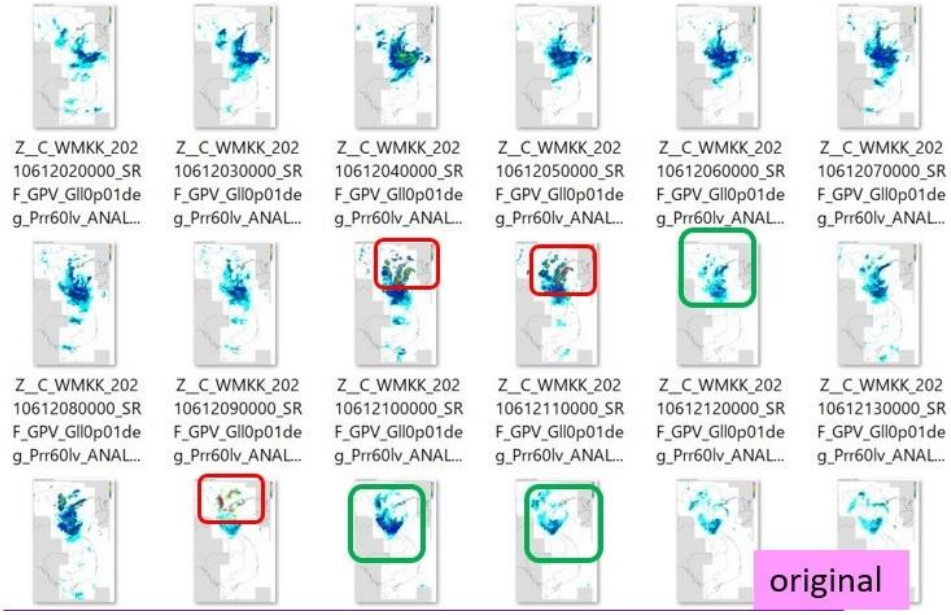

Figure 2. QPE results are based on the original algorithm.

The following changes were made to solve this problem.

- During the primary correction, if the average rainfall in the overlapping area is 10 mm or more, no correction is made, and the primary correction factor is set to 1.

- If there are less than 4 rain gauges of 5 to 10 mm in the overlapping area during the primary correction, no correction is made, and the primary correction factor is set to 1.

These modifications were made in March 2020.

These improvements suppressed overcorrections in the overlap region and stabilized the QPE calculation results. A comparison of Figures 2 and 3 shows the effect of this improvement. When focusing on the red square regions, the values are excessive in Figure 2 but not in Figure 3. On the other hand, this change has a side effect, which tends to suppress the area of intense rainfall. The green square regions in Figures 2 and 3 illustrate this characteristic.

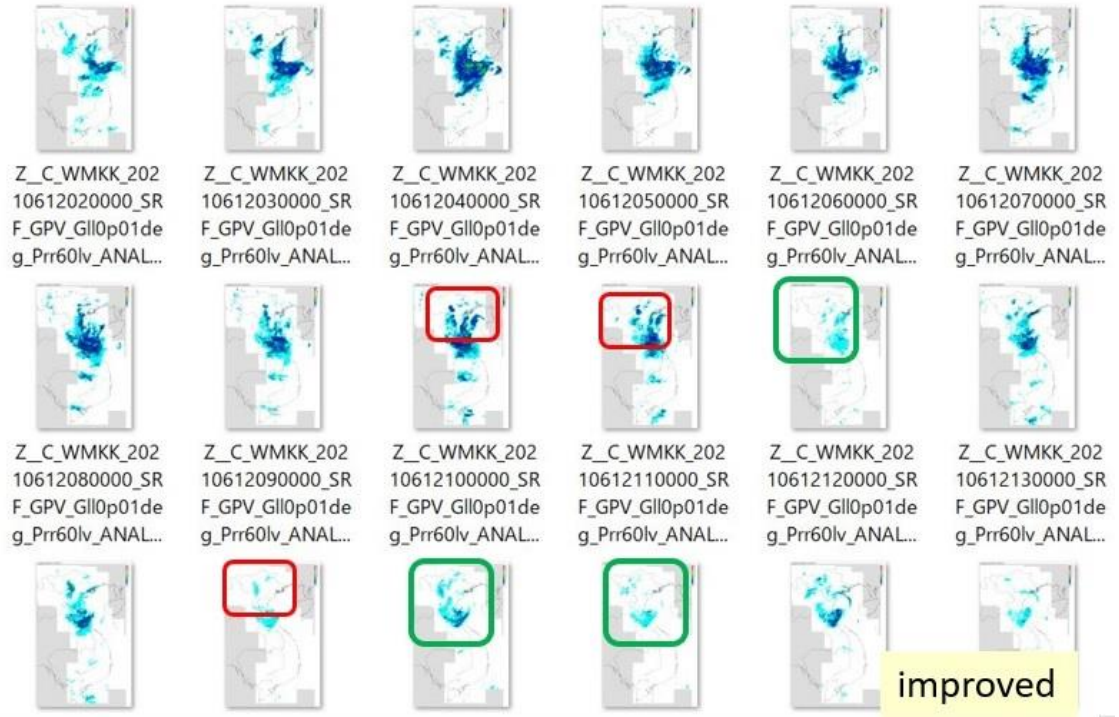

Figure 3. QPE results are based on the improved algorithm. Data are the same as in Figure 2.

2.2.2. Rain gauge list

Which rain gauge data to use is a critical issue in determining the accuracy of the QPE. Basically, the more rain gauge data, the more accurate the QPE. However, if the rain gauge contains abnormal observations, the accuracy of the QPE will drop dramatically.

Although there are more than 2000 ARG data in Vietnam, they include points with low data acquisition rates or problematic observations. A comparison of ARGs and human observations has been reported to verify the accuracy of ARGs [7]. There is also an attempt to combine several QC factors to validate and categorize the accuracy of ARGs [6]. This paper also evaluated the impact on QPE produced by each category.

In this paper, 805 sites were selected from 2000 sites that were determined to be normal based on their data acquisition rates and comparison with surrounding sites and used to calculate QPE.

2.2.3. PCAPPI table

The settings in the PCAPPI table also play an important role in the accuracy of the QPE. To calculate the QPE accurately, it is necessary to use radar observation data of good quality at as low altitude as possible. In mountainous areas, the radar beam is shielded or

partially shielded, which reduces observation accuracy. Utilizing topographic data, the elevation angle to be used by azimuth is determined in relation to the altitude at which the radar is installed.

If the elevation angle to be used is calculated mechanically from topographic data, the angle may change within a narrow azimuth range. Figure 4a shows an example of the QPE distribution in the initial setup, but the distribution is discontinuous in the area circled in red. Such discontinuous distribution is due to the PCAPPI table being set with a fine azimuthal width. Figure 5 shows the PCAPPI table settings before and after the modification. By changing the settings in this way, discontinuity areas can be avoided as shown in Figure 4b.

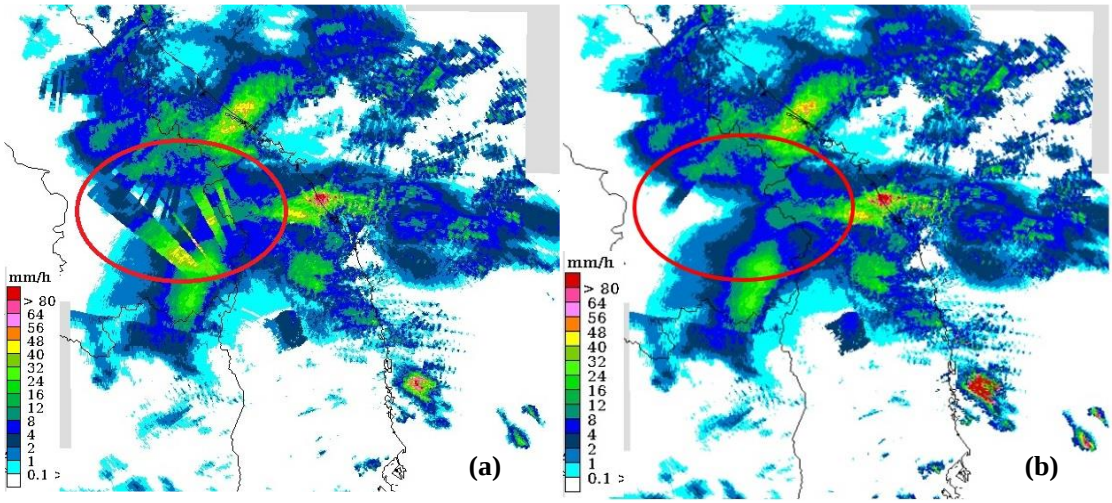

Figure 4. QPE distribution: (a) with initial PCAPPI settings; (b) with modified settings in the central region at 15LST 7 October 2020.

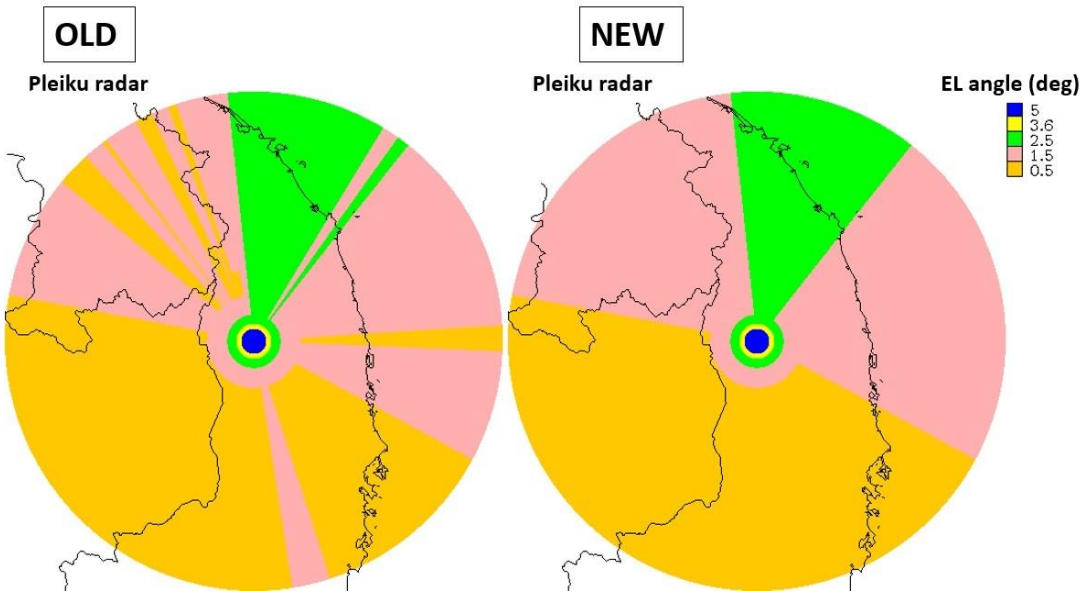

Figure 5. Initial (left) and modified (right) PCAPPI table of Pleiku radar.

When using the PCAPPI table, it is necessary to introduce smoothing processes such as interpolation between elevation angles in regions where the elevation angle changes. This method is used to avoid discontinuous distributions while taking advantage of lower altitude observation data will be possible. Figure 6 shows the difference between before and after introducing the smoothing processes when the PCAPPI table is updated. It shows that the wedge-shaped echoes in the previous image (a) changed to a more natural shape in the new image (b) due to the revised elevation angle and the use of smoothing.

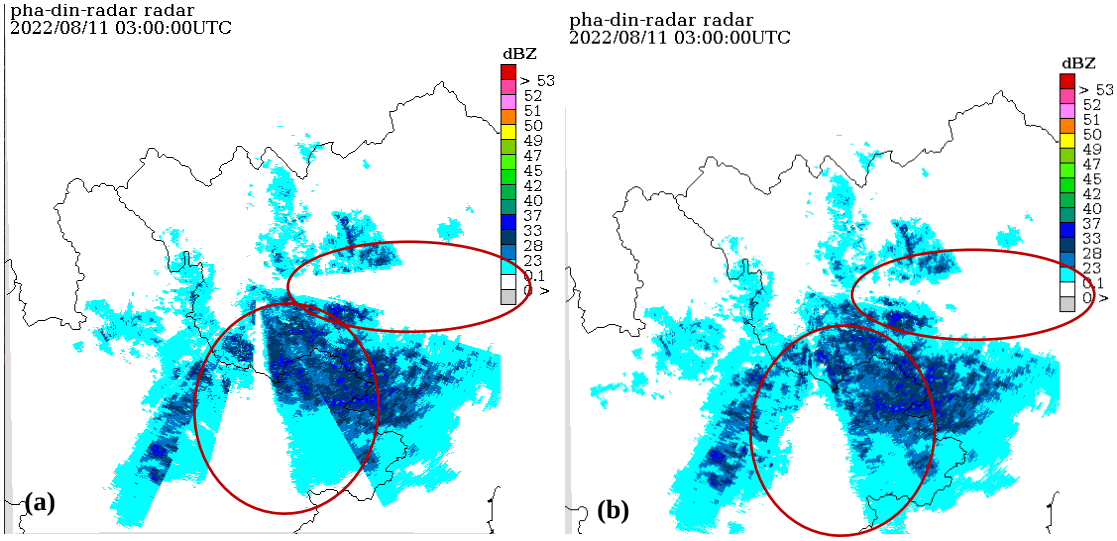

Figure 6. QPE distribution with initial PCAPPI settings in the Northwest region at 10LST 11 August 2022: (a) Old table with no smoothing; (b) New table with smoothing.

3. Results

3.1. Evaluation of QPE results and tendency of QPE products

Results of QPE products are evaluated from the whole country on around 800 rain gauge stations data with the exact grid points of QPE precipitation maps at each station. For this evaluation process, rain gauges not used for calibration are chosen. Scattergrams (Figure 7), statistical indicators, and time-series graphs evaluated the accuracy of QPE. The comparison was made for three statistical indicators, and the characteristics of QPE results are as follows. In Figure 7, the slanted solid line shows the most accurate result. From these four figures, the plot concentration, and the red slope of the regression line show that the accuracy of stations (b) and (d) is high.

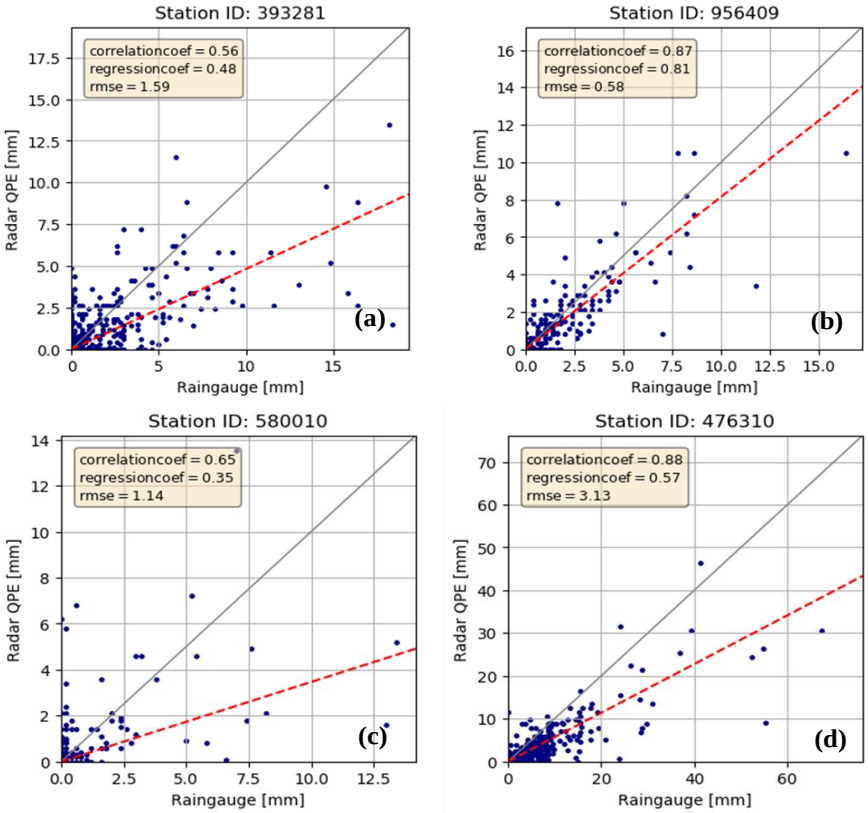

Figure 7. Hourly QPE vs rain gauge scatterplots of (a) Đạ Chais, (b) Phượng Mao, (c) Mường Mùn, and (d) Ba Điền stations.

- Correlation coefficient (CC): Correlation Coefficient (CC) is a statistical measure of the strength of the relationship between the two data sets, Radar QPE, and ground-based rain gauge. If the CC is closer to 1.0, the better the correlation between QPE and rain gauge.

- Root Mean Square Error (RMSE): RMSE shows differences between the model and the observation. The RMSE value is always non-negative and tends to be larger in the region with more rain. Therefore, using it for comparison in the same region is better.

The distribution of CC and RMSE are plotted on maps (Figure 8). The high CC are located in the Central coast area and Near Hanoi, while low CC is in the mountain area and Southern area. Most of the radar in Viet Nam is located near major cities along with the eastern coast and the altitudes are quite low. The beam angles are set higher to monitor the mountain area or to avoid ground clutters, and then the beam height is too high to catch the low clouds, especially in the western (mountain) side of the country. Some stations with low CC in the red areas are the stations with low data receiving since many of the AWS with high receive rate is used for the calibration.

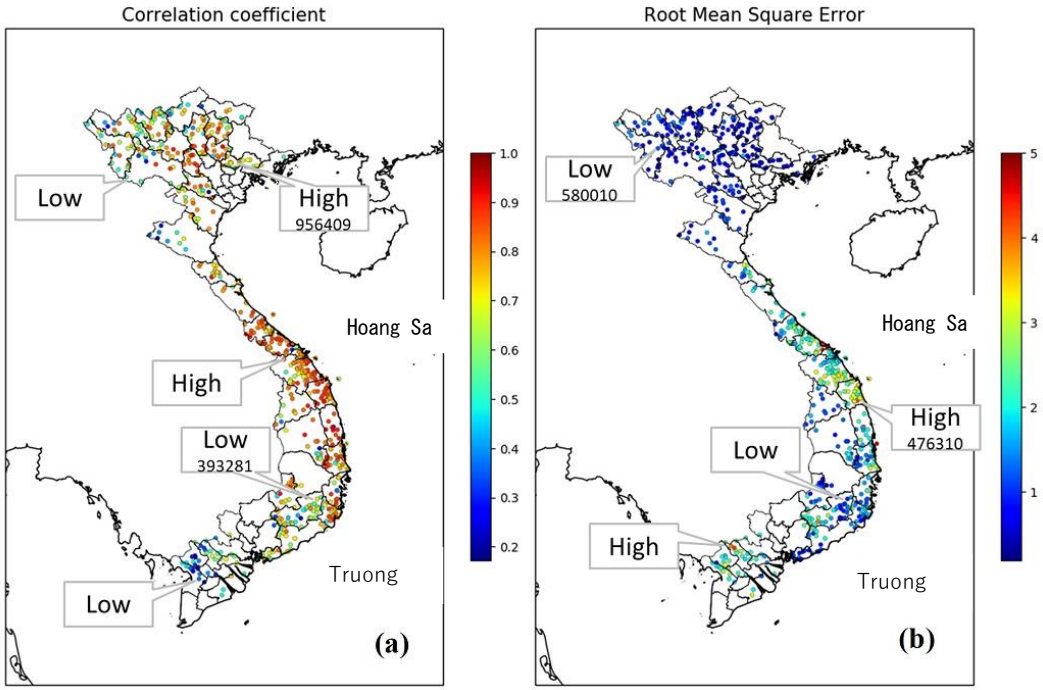

Figure 8. The distribution plot of statistical indicators: (a) correlation coefficient; (b) root mean square error.

There were some updates on the evaluation method between radar and rain gauge. In the first validation, the value from the grid right above the rain gauge was used, but now it is using the maximum value among the surrounding nine grids over the rain gauge (3km × 3km). This method takes into consideration the observation height and the rain carried away by the wind and is the same method as the Verification in the JMA-QPE package.

Figure 9 is the time-series graph from August 10 to August 13, 2022. The blue bar is rain gauge data, the red line is from radar QPE. The bottom time series graph Since wind advection is considered, the lower graph is more consistent with the rain gauge values since it uses the maximum value among the surrounding nine grids over the rain gauge.

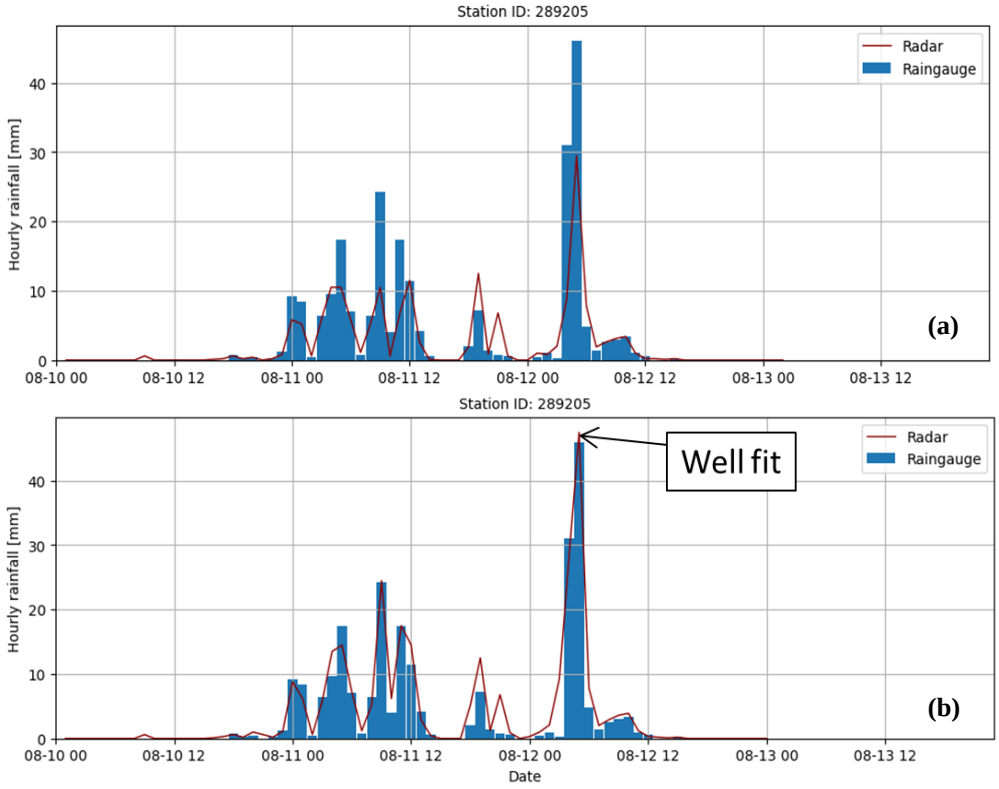

Figure 9. The time-series graph of statistical indicators at An Khánh station, Hà Nội: (a) using a single grid; (b) Using the maximum value among the surrounding nine grids over the rain gauge.

3.2. Further improvement of QPE product

3.2.1. Clutter map introduction and its calculation

A single polarization radar has functions to remove clutters, for example, reflectivity, velocity, and velocity width calculated by Fast Fourier Transform (FFT) based on spectral analysis of the orthogonal detection signal from receiving unit outputs. However, a single polarization radar cannot remove clutters, clear air echoes, chaffs, and so on (dual-polarization radar can discriminate and remove non-precipitation echoes using dual-polarization techniques). In JMA QPE software package has a function for clutter maps, and in 2021, clutter map calculation methods were developed.

Clutter map functions consist of "decrease" and "cut," and values of "decrease" and "cut" (Figure 10) would be calculated from observed echoes on non-precipitation examples at each radar site. Noises that clutter maps can effectively eliminate are removed through clutter maps, such as stationary ground clutters from static ground objects such as buildings and topography, stationary sea clutters (Sea clutters in strong wind conditions can be avoided by changing the PCAPPI table to use a higher elevation or by

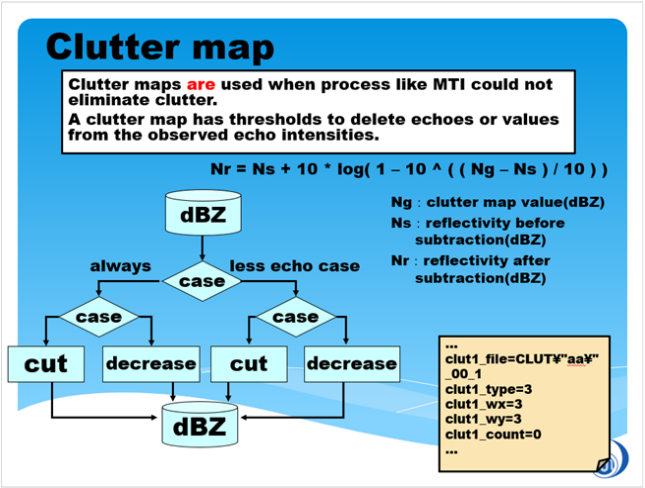

Figure 10. The process flow diagram of the clutter map.

changing the elevation itself.), and point clutters from wind turbines. In Figure 11, clutter due to topography shown inside the red circle in the left figure around Vinh's radar has been reduced in the right figure after the clutter map process.

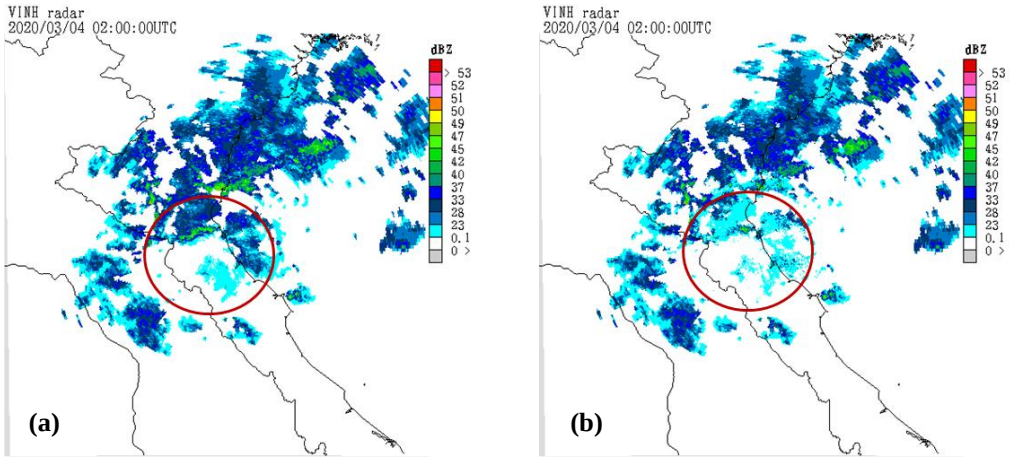

Figure 11. Before (a) and after (b) the clutter map is applied.

Recently, many wind farms have been planned and installed in Viet Nam to shift to clean energy sources. To remove reflections of wind farms, the 'pseudo-masking' method shown in Figure 12 is proposed. The method is PPI elevation in directions and distances where wind farms exist should shift to a higher elevation, not affected by wind farms.

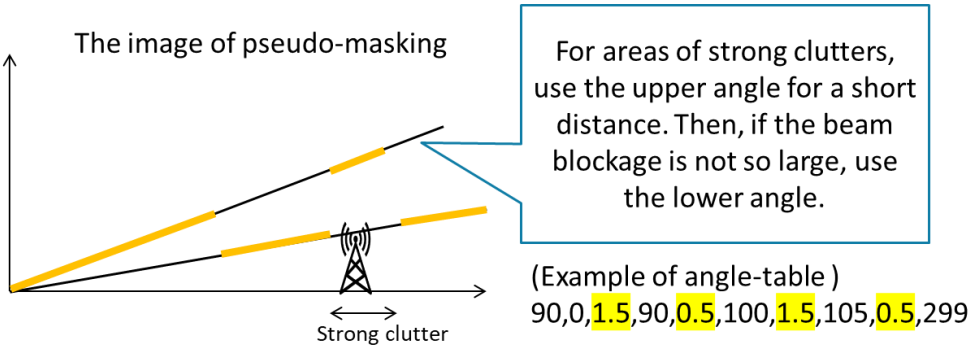

Figure 12. The time-series graph of statistical indicators at An Khánh station.

3.2.2. 10-minute interval QPE

QPE calculations are done initially once an hour using hourly rainfalls for both radar and rain gauges. But now, QPE can be updated at 10-minute intervals using the API's 10-minute rain gauge data. The main advantages of updating at 10-minute intervals are that it facilitates monitoring of short-duration heavy rainfall that dissipates in an hour or so. In addition, QPE can be updated at 10-minute intervals.

The short-interval version of the QPE uses 10-minute rain gauge observations from the API, so the quality of the rain gauge needs to be verified separately since there is a lack of data due to data transfer. Considering these circumstances, the conventional hourly QPE, which uses rain gauges that pass QC, is calculated in parallel.

3.2.3. Utilization of dual-polarized data

Usage of dual-polarization radar data is firstly quality check and removal of non-precipitation echoes. Dual-polarization radar has various products; for example, Differential Reflectivity (ZDR [dB]) calculated by the following formula attenuates precipitations in the background area of heavy rains shown in Figure 13.

$$Z_{DR}\,[\mathrm{dB}] = 10\log_{10}\frac{Z_{HH}}{Z_{VV}} \quad (1)$$

When the particles are raindrops, Z_{DR} generally has a positive value or close to zero. Z_{DR} is effective but sensitive since it is the ratio between Z_h and Z_v, therefore the accuracy of Z_{DR} depends on the adjustment between Z_h and Z_v (Figure 14). Only a few people pay attention to Zv, but periodical calibration is essential to maintain the accuracy of dual-pol radar.

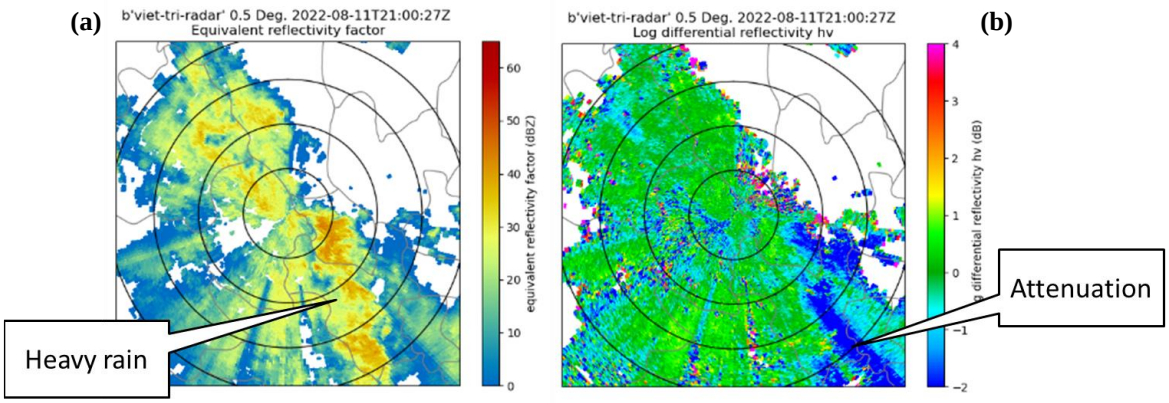

Figure 13. The PPI image of Z_h (a) and Z_{DR} (b) at 04 LST 12 August 2022.

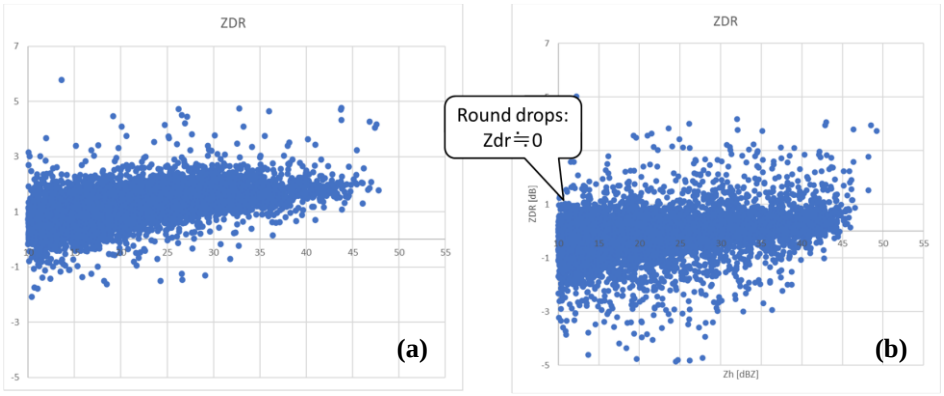

Figure 14. The scattergram of Z_h vs Z_{DR} of before (a) and after (b) the calibration.

4. Future issues

Various improvements have been made to QPE products to ensure stable operation and improve accuracy. However, the following actions are needed in each category to improve accuracy further.

4.1. Improve the quality of rain gauge data

- Necessary to introduce systematic checks, calibration, and maintenance for ARG to increase the reliability of ARG data.
- Necessary to introduce an improved QC method for ARG data to increase the availability of ARG data.
- Rain gauge network is not uniform: necessary to move or add some rain gauges to sparse areas, especially in the radar overlapping area and mountainous area.

4.2. Improve the quality of radar data

- Improve scan strategy and thereby the quality of radar;
- Improve calibration by using disdrometer;

- Combined utilization of Intensity mode with Doppler mode;
- Improve observation quality for mountainous areas;
- Utilization of dual-polarized data.

4.3. Improve the algorithm of the QPE product

- Introduce smoothing between adjacent ELs to calculate PCAPPI;
- Introduce beam height effect to calculate QPE;
- Improve algorithm to calculate primary correction factor when echo approaches from the sea.

5. Conclusions

Currently, ten meteorological radars and about 800 ARG data are combined to make hourly QPE products covering the whole Viet Nam. In the early stages of operation, QPE values sometimes became unstable, and abnormally large values were displayed. Enhanced quality control of ARG and radar data and improved calculation algorithms have made it possible to suppress such anomalous values. With these series of modifications, the QPE product is now stable and operational.

These QPE products can be easily checked on the website and are available to forecasters and other users, as well as to disaster management officials outside the VNMHA. The AMO also provides a system on its website that displays the risk of landslides in real time by accumulating these QPE values and combining them with information on the risk of landslide occurrence. This system is still experimental, but it is essential to continue improvements as an application of QPE.

Author Contributions: Conceptualization: C.K., M.T.; Methodology: C.K., N.V.H., N.M.C.; Software: C.K., B.T.K.H.; Validation: C.K., M.T., B.T.K.H.; Formal analysis: K.A.; Writing–original draft preparation: C.K., B.T.K.H.; Writing–review and editing: All authors have read and agreed to the published version of the manuscript.

Funding: This study is supported by the JICA project for strengthening capacity in weather forecasting and flood early warning systems in Viet Nam.

Acknowledgments: The authors thank the Japan Meteorological Agency for providing the package for calculating QPE products and for their support for the installation. Also, the authors thank Nguyen Vinh Thu, Director of the Aero Meteorological Observatory for his support and suggestions for this project. Thanks are extended to Nguyen Quang Vinh of the Aero Meteorological Observatory for his technical support to various radar analyses.

Conflicts of Interest: The authors declare no conflict of interest.

References

1. Makihara, Y. A method for improving radar estimates of precipitation by comparing data from radars and rain gauges. *J. Meteor. Soc. Japan* **1996**, *74*, 459–480. doi: 10.2151/jmsj1965.74.4.
2. Makihara, Y. Algorithms for precipitation nowcasting focused on detailed analysis using radar and rain gauge data. Technical Reports of the MRI, 2000, 39, 63–111. doi:10.11483/mritechrepo.39.
3. Tonouchi, M.; Kasuya, Y.; Tanaka, Y.; Akatsu, K.; Akaeda, K.; Nguyen, V.T. Activities of JICA on disaster prevention and achievement of JICA project in Period 1. *VN J. Hydrometeorol.* **2020**, *5*, 1–12.
4. Akaeda, K.; Tonouchi, M.; Thu, N.V. Achievement of JICA Technical Cooperation Project in Period 2. *J. Hydro-Meteorol.* **2023**, *15*, 1–9.

5. Kimpara, C.; Tonouchi, M.; Hoa, B.T.K.; Hung, N.V.; Cuong, N.M.; Akaeda, K. Quantitative Precipitation Estimation by combining rain gauge and meteorological radar network in Viet Nam. *J. Hydrometeorol.* **2020**, *5*, 36–50.
6. Tonouchi, M.; Hoa, B.T.K.; Hung, N.V.; Cuong, N.M. Quality check of rain gauge data for quantitative precipitation estimate. *J. Hydro-Meteorol.* **2023**, *15*, 21–27.
7. Kobayashi, R.; Duc, L.X.; Tien, P.M. Attempt to detect maintenance-need rain gauge station by double-mass analysis. *J. Hydro-Meteorol.* **2023**, *15*, 10–20.

JOURNAL OF
HYDRO-METEOROLOGY

Research Article

Development of precipitation guidance for 36 regions in Vietnam up to 5 days ahead

Kiichi Sasaki[1]*, Vu Tuan Anh[2]

[1] Japan Meteorological Business Support Center, Tokyo101-0054 Japan; k-sasaki@jmbsc.or.jp
[2] National Center for Hydro-Meteorological Forecasting, Hanoi 10000, Vietnam; lamhoaanh@gmail.com

*Corresponding author: k–sasaki@jmbsc.or.jp; Tel.: +81–352810440

Received: 10 February 2023; Accepted: 21 March 2023; Published: 25 June 2023

Abstract: Development of forecast guidance is one of main activities of Output 3 of the JICA Project to improve forecasting services of VNMHA. Maximum and minimum temperature guidance was developed for 63 cities up to 10 days ahead in the first phase of the Project. Development of precipitation guidance was the primary activity of Output 3 in the second phase of the Project. Statistical analysis on 24-hour rainfall observations and predictions by JMA GSM and ECWMF IFS showed that the correlation between them was low for each station but relatively high for each region. Preliminary investigation of POP trial guidance calculated with logistic regression and multiple linear regression for 4 stations and 4 regions showed the verifications scores (BSS: Brier Skill Score) for regional POP were considerably higher than those for station POP. IFS-GSM-integrated precipitation guidance was developed to improve regional mean/max rainfall guidance and had slightly better verification results than IFS and GSM precipitation guidance. Based on these verification results, precipitation guidance on regional POP and regional mean and max for 12-hour rainfall (tonight and tomorrow daytime) and for 24-hour rainfall (after that) was developed for 36 regions in Vietnam up to 5-days ahead. Precipitation guidance was generally able to predict a reasonable amount of rainfall for heavy rain events caused by tropical cyclones in 2022, however there were several heavy rain events where IFS and GSM rainfall predictions were quite low, and rainfall guidance was also quite low.

Keywords: Precipitation guidance; Station POP; Regional POP; Regional mean and max rainfall.

1. Introduction

The JICA Project for Strengthening Capacity in Weather Forecasting and Flood Early Warning System started in April 2018 [1]. In the first phase of the project, maximum and minimum temperature guidance for 63 cities up to 10 days ahead was developed by the working group 3 (WG3) of the Project [2]. WG3 worked on precipitation guidance for POP and daily rainfall etc. in the second phase of the project. The National Center for Hydro-Meteorological Forecasting (NCHMF) issues city forecasts such as maximum and minimum temperatures for 63 cities in Vietnam but does not issue quantitative forecasts on precipitation such as probability of precipitation (POP). The main objective of WG3 activities in the second phase is to provide guidance materials to forecasters to assist them in issuing quantitative forecast information on precipitation.

MOS guidance is widely used as an objective forecast material to support the issuance of quantitative forecasts. MOS guidance has been used in the United States since around 1970

as an objective forecasting material using numerical predictions [3–4]. In Japan, the guidance operation started in the late 1970s. At JMA, all guidance was prepared using multiple linear regression until around 1996. Multiple linear regression is still widely used in the United States, Canada, and many other countries because it is easy to grasp the characteristics of the guidance and can be used effectively [5–9]. In this work, we used multiple linear regression and logistic regression based on training materials on guidance in the JICA group training course in meteorology implemented by JMA from the perspective of creating guidance that is easy for forecasters to understand.

A statistical analysis on 24-hour rainfall observations and Numerical Weather Prediction (NWP) rainfall predictions by JMA GSM Grid Point Values (GPVs) and ECMWF IFS GPVs was first performed to understand the accuracy of precipitation predictions by NWP models in Vietnam, and then preliminary investigation for POP guidance and for regional mean and max 24-hour rainfall was conducted. The statistical analysis and preliminary investigation showed that the correlation between rainfall observations and NWP predictions and verification results of rainfall guidance were not exceptionally good at each station but were relatively good in each reason. With respect to POP guidance, past research has shown that POP guidance by logistic regression has better verification scores than that by multiple linear regression [10]. In this study, the POP guidance by logistic regression scored better with respect to station POPs, but the regional POP guidance by multiple linear regression scored considerably better than the station POP guidance by logistic regression. Based on the results, experimental precipitation guidance for regional 12-hour/24-hour POP, regional mean and max 12-hour/24-hour rainfall was developed for 63 provinces up to 5 days ahead. This technical note reports on activities of WG3 related to the development of precipitation guidance during the second phase of the Project.

2. Materials and Methods

Guidance is one of the applied products of NWP. Guidance is produced by post-processing NWP output to improve the accuracy of the predictions of temperature and precipitation calculated by the NWP model by correcting them statistically. To create guidance, one must first use NWP data and observation data of the weather element to be forecasted to create a forecast equation using statistical methods. For this purpose, pairs of past NWP data and observation data are prepared. From these data, a forecast equation is created using the observation data of the weather element to be forecasted as the objective variable and the elements of the NWP data that have strong causal relationships with the observation data as explanatory variables. Statistical methods for guidance include linear multiple regression, logistic regression, Kalman filter, and neural network. Kalman filter was used for temperature guidance, while multiple linear regression and logistic regression were used to develop precipitation guidance. Multiple linear regression is a lump-sum statistical method, and the characteristics of the guidance can be easily understood and effectively applied. Logistic regression is one of the statistical methods used for the problem of classifying phenomena into two classes, such as the presence or absence of lightning, for example, and is often used for probability-type guidance.

2.1. NWP GPV and rainfall observation data set

2.1.1. Dataset with surface GPVs for the first statistical analysis

In developing precipitation guidance, it is necessary to know the meteorological characteristics of rainfall in Vietnam and the error characteristics of NWP rainfall predictions. We first created a two-year dataset of 24-hour rainfall observations and GSM surface predictions for 186 stations and conducted statistical analysis with the data set to obtain relations between rainfall observations and NWP predictions. The dataset was created

using observation data files (186smMMyYY.xls) prepared by NCHMF, GSM GPVs obtained from JMA High-Resolution GSM Data Service (https://www.wis-jma.go.jp/cms/gsm/download.html), and IFS GPVs prepared by NCHMF's NWP division. In addition, we divided Vietnam into 21 regions based on its administrative division and created a regional dataset for each region. A sample of regional data set for Hanoi region Day1 for Jan 2018 to Dec 2019 is shown in Figure 1. For the IFS, datasets like those for the GSM were created, but the data period was different depending on data availability.

Date	Rain0_1	Robs_mean	Robs_max	Rgpv_mean	Rgpv_max	Hgpv_mean	Cgpv_mean	Ugpv_max	Vgpv_max	Fgpv_max
20180102	0	0.34	2.7	0.95	1.44	88.34	71.17	-4.12	-1.69	4.45
20180103	0	0.63	3.2	1.15	1.88	89.19	79.02	-3.93	-2.75	4.8
20180104	1	1.27	2.8	1.34	2.62	90.99	88.64	-3.34	-3.05	4.47
20180105	0	0.82	3.6	1.05	1.56	91.06	90.82	-3.48	1.67	3.67
20180106	0	0.24	0.9	1.14	1.56	90.72	84.32	-3.56	1.78	3.97
20180107	0	0.36	1.8	2.82	6.12	91.19	82.67	-3.31	-2.24	4
20180108	1	1.79	5.9	6.63	12.72	93.26	89.08	-7.77	-5.16	9.33
20180109	1	3.32	8.8	2.25	3.38	68.51	80.89	-2.84	-5.97	6.61
20180110	0	0.01	0.1	0	0.03	34.2	80.16	-0.57	-5.07	5.07

regional mean/max 24h-rain obs regional mean/max GSM 24h-rain GPV

Figure 1. GSM GPV and regional mean and max observation data set for Hanoi region for the period of Jan 2018 - Dec 2019. Surface GPVs (Rgpv_mean: regional mean 24-hour rainfall, Rgpv_max: regional max 24-hour rainfall, Hgpv_mean: regional mean relative humidity, Cgpv_mean: regional mean total cloud amount, Ugpv_max: regional max wind u-component, Vgpv_max: regional max wind v-component, Fgpv_max: regional max wind speed).

2.1.2. Dataset with surface and upper GPVs for preliminary investigation and experimental precipitation guidance

Datasets for four representative stations and regions from northern to southern Vietnam were created for the period from Jun 2018 to Sep 2021 using GSM surface and upper GPVs to conduct a preliminary investigation of precipitation guidance. As for the upper level GPVs, each wind component and relative humidity at 950 hPa, 850 hPa and 700 hPa were used, and additional predictors such as KI (K index), SSI (Showalter stability index), PW (Possible Water) and PCWV were calculated and added to the dataset. PCWV is one of the predictors in the JMA precipitation guidance and expressed by the following equation 1:

$$\text{PCWV} = -\text{PW} \times (\text{wind–speed at 850hPa}) \times (\text{P–velocity at 850hPa}) \quad (1)$$

If P-velocity at 850hPa > 0 then PCWV = 0.

For trial operation of precipitation guidance, regional datasets were created by subdividing Vietnam into 36 regions to make each region as close as possible to the 63 city forecast districts (5 municipalities and 58 provinces). In addition, 12-hour rainfall observations and GPV datasets corresponding to the 12-hour forecast for tonight (7:00 pm today to 7:00 am tomorrow) and tomorrow daytime (7:00 am to 7:00 pm tomorrow) were created in accordance with NCHMF's city forecasts. 24-hour rainfall observations and GPV datasets were created for Day 2, Day 3, Day 4 and Day 5. These datasets were created using GSM GPVs for GSM precipitation guidance, IFS GPVs for IFS precipitation guidance and both IFS and GSM GPVs for IFS-GSM integrated precipitation guidance.

2.1.3. Selection of predictors for POP guidance

Since there are so many predictors in the datasets, we subjectively selected about 10 potential predictors by making a correlation analysis between 24-hour POP observations and each predictor. Figure 2 shows correlation coefficients between station POP observations and

predictors at the four stations and those between regional POP observations and predictors in the four regions. Correlations were not extremely high for either the stations or the regions, but in general correlation coefficients between regional POP observations and regional mean predictors were higher than those for station POP.

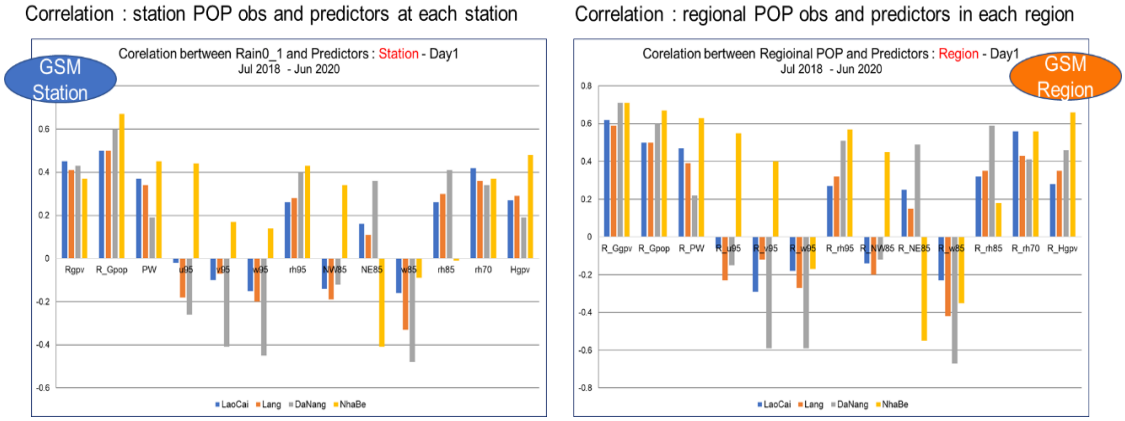

Figure 2. Correlation coefficients between station POP observations and GSM predictors for Day1 (left) and those between regional POP observations and GSM predictors for Day1 (right). Predictors (Rgpv: 24-hour rainfall, R_Gpop: regional mean POP, PW: possible water, u95: wind u-component at 950hPa, v95: wind v-component at 950hPa, w95: p-velocity at 950hPa, rh95: relative humidity at 950hPa, NW85: wind NW-component at 850hPa, NE85: wind NE-component at 850hPa, w85: p-velocity at 850hPa, rh85: relative humidity at 850hPa, rh70: relative humidity at 700hPa, Hgpv: surface relative humidity; prefix R_: regional mean).

For the calculation of station POPs, we subjectively selected potential predictors which had relatively high correlations with POP observations and calculated with logistic regression using all selected predictors at each station, and then objectively selected final predictors for each station using stepwise method. Selection of predictors for regional POPs was done in the same way as for station POPs, using multiple linear regression and stepwise methods. Selected potential predictors for station POP guidance and regional POP guidance are shown in table 1.

Table 1. Selected potential predictors for station POP, regional POP, regional mean rainfall, and regional max rainfall guidance. The prefix R_ stands for regional.

Station POP	Regional POP	regional mean rainfall	regional max rainfall
R_mean 24h rainfall	R_mean 24h rainfall	R_mean 24h rainfall	R_max 24h rainfall
R_mean POP	R_mean POP	R_mean POP	R_mean POP
Possible Water	R_mean Possible Water	R_mean Possible Water	R_mean Possible Water
NE wind at 850hPa	R_mean total cloud amount	R_mean PCWV	R_mean PCWV
NW wind at 850hPa	R_mean surface humidity	R_mean total cloud amount	R_mean total cloud amount
P-velocity at 850hPa	R_mean_u_wind at 850hPa	R_mean surface humidity	R_mean surface humidity
Humidity at 700hPa	R_mean_v_wind at 850hPa	R_mean_NE_wind at 850hPa	R_mean_NE_wind at 850hPa
	R_mean_P-velocity at 850hPa	R_mean_NW_wind at 850hPa	R_mean_NW_wind at 850hPa
	R_mean_Humidity at 850hPa	R_mean_P-velocity at 850hPa	R_mean_P-velocity at 850hPa
		R_mean_Humidity at 850hPa	R_mean_Humidity at 850hPa

2.1.4. Calculation procedure of station POP and regional POP

The predictand of station POP24 is 1 if more than 1mm of rainfall is observed at each station in 24 hours and 0 if less than 1 mm, and the predictand of regional POP24 is the mean of the station POPs in each region. In addition, we calculated regional POHP24 using the predictand, which is 1 if more than 30 mm of rainfall is observed at least 1 station in each

region in 24 hours and 0 if less than 30mm. Since the predictand of station POP is 0 or 1 (binominal), station POP was calculated by logistic regression. On the other hand, the predictand of regional POP is 0 to 1, and the regional POP was calculated by multiple linear regression. The predictand of regional POHP is 0 or 1, and regional POHP was calculated by logistic regression. Each regression equation is as follows [11]:

Logistic regression:

$$\text{forecast equation: } \ln(p/(1-p)) = a_0 + a_1x_1 + a_2x_2 + \dots , \quad (2)$$

$$p = \exp(a_0 + a_1x_1 + a_2x_2 + \dots) /(1+\exp(a_0 + a_1x_1 + a_2x_2 + \dots) \quad (3)$$

where p is the probability (supplied with 0 or 1 for response variable); x_i the predictor and a_i the coefficient of the predictor.

Multiple linear regression:

$$\text{forecast equation: } p = a_0 + a_1x_1 + a_2x_2 + \dots , \quad (4)$$

where p is the probability (supplied with 0 to 1 for response variable), x_i the predictor and a_i the coefficient of the predictor.

The calculation procedure of station POP and regional POP is as follows: 1) select potential predictors subjectively for station POP and reginal POP based on correlation analysis, 2) calculate logistic regression for station POP and multiple liner regression for regional POP with the selected potential predictors, and then select final predictors for each station and region using stepwise method, 3) apply the obtained forecast equations to verification period datasets for verification. R's glm() and lm() functions were used to calculate logistic regression and multiple liner regression, and stepwise function was used for selecting predictors objectively [11].

2.1.5. Verification of POP and POHP

POP24 is the probability that more than 1 mm of precipitation will fall on any random point of the forecast area during 24-hours from 7:00 pm yesterday to 7:00 pm today. POHP24 is the probability that more than 30mm of precipitation will fall on at least one point of the forecast area during the 24-hours. Brier Score (BS) and Brier Skill Score (BSS) are used for the verification of probability forecasts [12–13]. The BS and BSS formulas are given below. As for BS, the smaller the better and perfect score is 0. As for BSS, the larger the better. If BSS ≤ 0 ($BS_{clm} \leq BS$), probability forecasts are no improvement; If BSS > 0 ($BS_{clm} > BS$), probability forecasts are improvement; If BSS = 1 (BS = 0), probability forecasts are perfect (no error). BSS represents the rate of improvement from climatic probability.

$$BS = \Sigma (Fi - O_i)^2/n \quad (5)$$

where n is the number of data; F_i the probability forecast (0 to 1) and the O_i observation (0 or 1).

$$BSS = (BSclm - BS)/BS_{clm} \quad (6)$$

where BS_{clm} is the BS of climatic probability (use climate value (mean of observed POP) as Forecast).

2.1.6. Calculation procedure of regional mean/max rainfall guidance

Since the accuracy of precipitation predictions at each station was not exactly accurate, we decided to develop 12-hour and 24-hour regional mean and max rainfall guidance as the first experimental precipitation guidance. The rainfall guidance was calculated using multiple linear regression, which is easy to operate and to understand forecast equations and results. The calculation procedures of rainfall guidance are almost the same as the POP guidance: 1) select potential predictors subjectively for regional mean and max rainfall guidance based on correlation analysis; 2) Calculate multiple liner regression for regional mean and max rainfall with the selected potential predictors, and then select final predictors for each region using

stepwise method; 3) Apply the obtained forecast equations to verification period data for verification.

2.1.7. Daily calculation procedure of precipitation guidance

The procedure for calculating daily guidance is illustrated in Figure 3: 1) download 6-hourly GSM surface and upper GPVs and collect IFS GPV data from NWP section of NCHMF, and calculate additional predictors; 2) create station-region datasets for 36 regions using the latest GSM and IFS GPVs for IFS, GSM, and IFS-GSM precipitation guidance; 3) apply the forecast equations obtained in each region with development period data to the latest daily dataset.

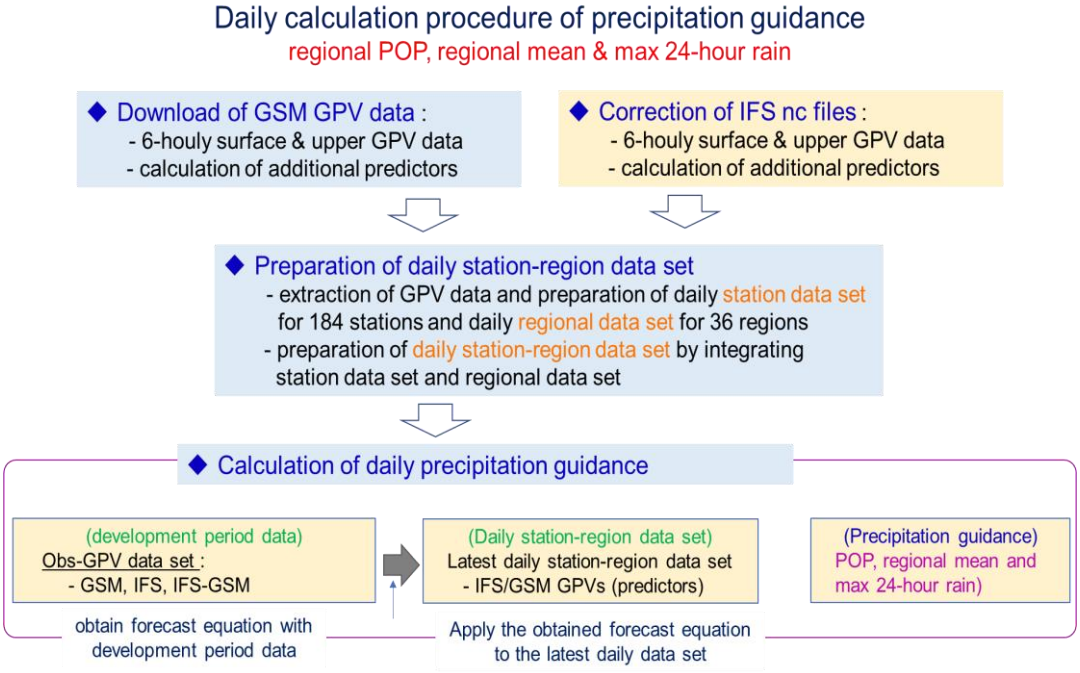

Figure 3. Illustration of daily calculation procedure of precipitation guidance.

3. Result and discussion

3.1. Statistical analysis using rainfall observation-GPV dataset

Rain is very localized and the accuracy of rainfall predictions by NWP model is not yet sufficient for quantitative forecasting. As a first step toward developing precipitation guidance, we conducted various statistical analyses using the rainfall observation-GPV dataset to understand the status of the accuracy of rainfall predictions by NWP models in Vietnam.

3.1.1. Scatter diagram of 24-hour rainfall at stations

First, we created scatter diagrams of observations and GSM predictions for 24-hour rainfall at 186 SYNOP stations using 2-years of rainfall observation-GPV datasets from Jan 2018 to Dec 2019. Figure 4 shows scatter diagrams, regression equations and correlation coefficients for 24-hour rainfall observations and predictions by GSM at Dien Bien, Ha Noi (Lang), Hue and Ho Chi Minh (Nha Be). The scatter diagrams all showed large variations, and heavy rainfalls were often observed even if the predicted rainfalls were low, especially in Hue. The correlation coefficients ranged from 0.45 to 0.62. Looking at the 186 stations, the correlation was generally low in the northern and southern regions, and relatively high in the central region.

3.1.2. Scatter diagram of 24-hour rainfall in regions

Since the correlations were not very high at each station, we next divided Vietnam into 21 regions so that each region would contain more than several SYNOP stations and examined the correlations in each region. The regions were divided based on administrative districts, and if there were only a few SYNOP stations in each province, two or three provinces were merged into one region. Figure 5 shows scatter diagrams for 24-hour regional mean rainfall observations and predictions by GSM in region 1 (Dien Bien), region 8 (Ha Noi), region 12 (Hue) and region 19 (Ho Chi Minh). The variation of scatter diagrams in each region was smaller than that at each station, and the correlation coefficients ranged from 0.65 to 0.74, considerably higher than the correlations at the stations.

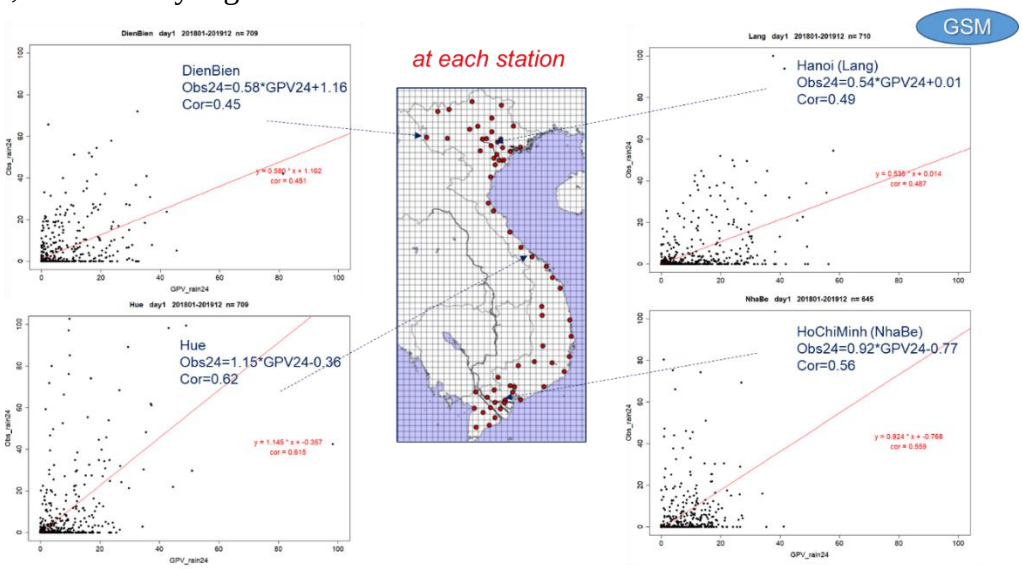

Figure 4. Scatter diagram of 24-hour rainfall observations and predictions for Day1 by GSM at 4 stations.

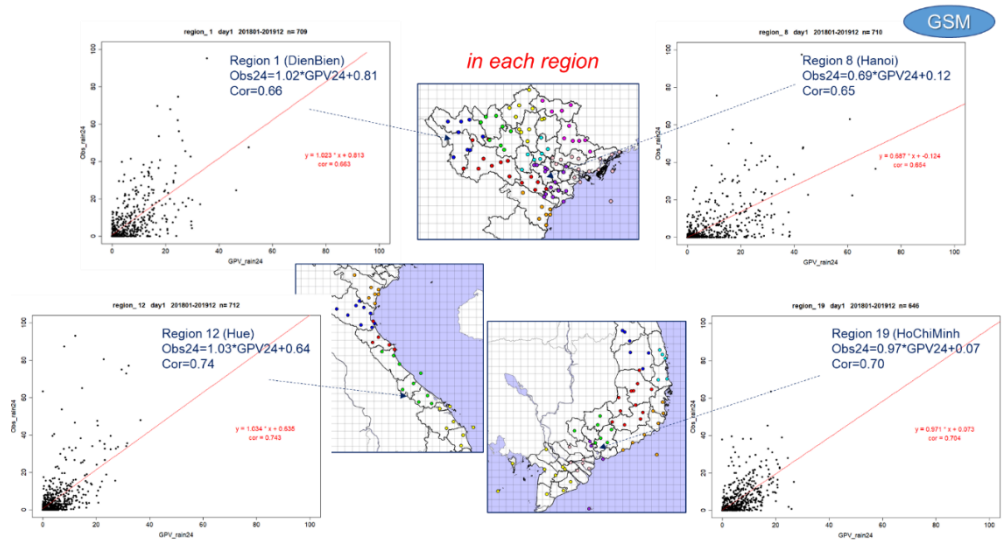

Figure 5. Scatter diagram of 24-hour rainfall observations and predictions for Day1 by GSM in 4 regions. Data period is from Jan 2018 to Dec 2019.

Then, we created similar scatter diagrams with IFS predictions using rainfall observation-GPV datasets from Jun 2019 to Dec 2020. The variation of the IFS regional scatter diagrams was much smaller compared to the GSM station scatter diagrams, and the correlation coefficients were also quite high, ranging from 0.62 to 0.84 (Figure not shown).

3.1.3. Correlation between 24-hour rainfall observations and IFS/GSM predictions

Figure 6 shows the distribution of correlation coefficients between 24-hour rainfall observations and IFS predictions (left side), GSM predictions (right side) for 186 stations and 21 regions. Correlation coefficients for each station were higher in the central region and lower in the northern mountainous region and the south region in both IFS and GSM. In the central region, many stations had correlation coefficients above 0.7, while in the northern mountainous region and the south region, many stations had correlation coefficients below 0.5, and several stations had correlation coefficients below 0.4.

The correlation coefficients of regional mean 24-hour rainfall were considerably higher than those of the stations in each region concerned in both IFS and GSM, especially in the northern mountainous regions and the southern region, where the station correlations were relatively low. IFS regional correlation coefficients were higher than 0.7 in many regions, and they were slightly higher than GSM correlation coefficients for both station and regional correlations in many stations and regions.

The correlation coefficients for regional max 24-hour rainfall were lower than those for regional mean 24-hour rainfall but were greater than 0.6 in many regions. There were a few regions with a correlation coefficient of less than 0.5 in the south.

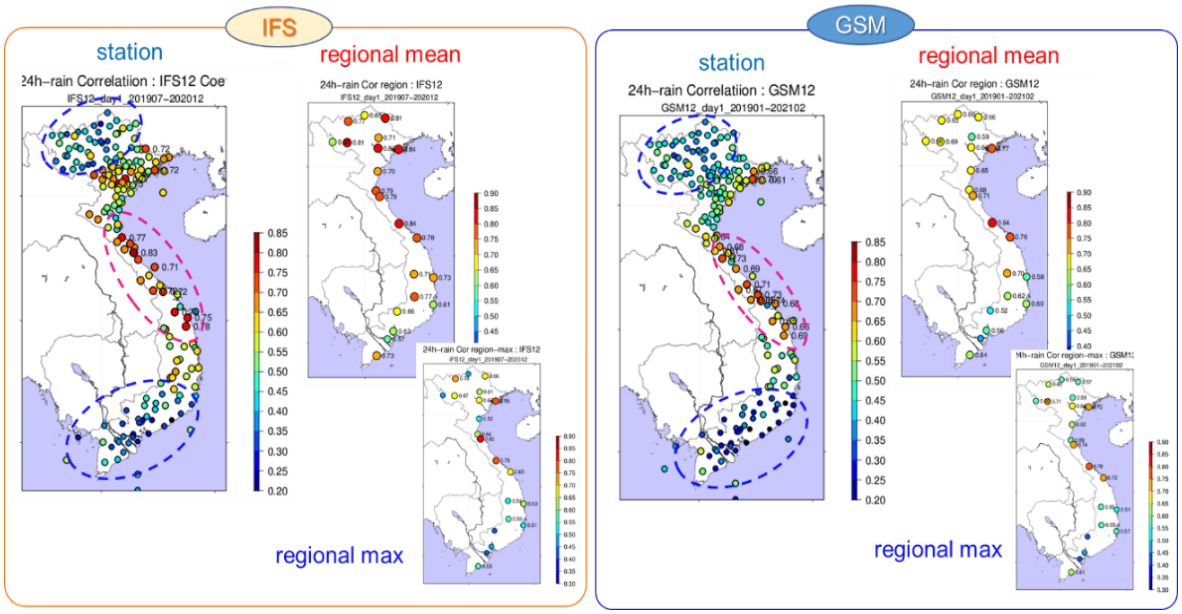

Figure 6. Distribution of correlation coefficients between 24-hour rainfall observations and IFS/GSM predictions at 186 SYNOP stations and in 21 regions.

3.2. Preliminary investigation for POP guidance

3.2.1. Monthly days with 24-hour rainfall of 1mm or more and 30 mm or more

Toward the development of POP guidance, we created two-year datasets of 24-hour rainfall observations and GSM predictions from Mar 2020 to Mar 2022 for 186 stations, and calculated the number of monthly rainy days with daily rainfall of 1 mm or more and the number of monthly heavy rainy days with daily rainfall of 30 mm or more. Figure 7 shows monthly days with 24-hour rainfall of 1mm or more and 30 mm or more in Lao Cai, Hanoi, Da Nang and Ho Chi Minh. Rainy days were more frequent from August to October in Hanoi and Ho Chi Minh, in August in Lao Cai, and from October to December in Da Nang at least once every two days. Heavy rainfall was most common from August to October in Lao Cai, Hanoi and Ho Chi Minh, about once every several days. In Da Nang, heavy rainfall was especially frequent in October, about once every three days.

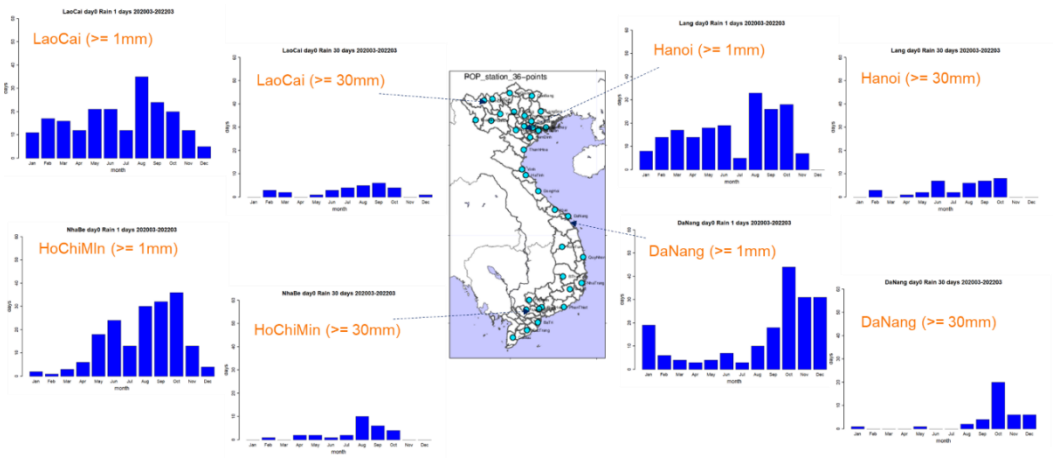

Figure 7. Monthly days with 24-hour rainfall of 1mm or more and 30mm or more in the two–year period from March 2020 to March 2022.

3.2.2. Verification of POP trial guidance for 4 stations and 4 regions

We created 24-hour rainfall observations and GSM predictions datasets for 4 stations and 4 regions (Lao Cai, Ha Noi, Da Nang and Ho Chi Minh) for POP trial guidance and its verification. Development period is from Mar 2020 to Sep 2021 and verification period is Jul 2018 to Jun 2020. One major station in each relevant region was used to calculate the station POP and several stations in each relevant region were used to calculate the regional POP.

Figure 8 shows reliability diagrams of POPs at 4 stations of Lao Cai, Lang (Ha Noi), Da Nang and Nha Be (Ho Chi Minh) for Day 1 (tomorrow). Daily calculated POPs (0 to 1) were subtotaled every 0.1, and the average of them and the average of the corresponding POP observations were plotted on the diagram. It's ideal if the plot rides on a yellow straight line. Brier Skill Score (BSS) and correlation coefficient between POP observations and calculated POPs are also shown on the top of each diagram. The plots for Lao Cai and Lang (Ha Noi) were generally on the yellow line, while those for Da Nang and Nha Be (Ho Chi Minh) were a bit more scattered. BSSs ranged from 0.26 to 0.29. Figure 9 shows reliability diagrams of POPs in 4 regions of Lao Cai, Ha Noi, Da Nang and Ho Chi Minh for Day 1. The plots for the 4 regions were generally on the yellow line and BSSs were considerably higher than those of the POPs at 4stations, ranging from 0.39 to 0.58.

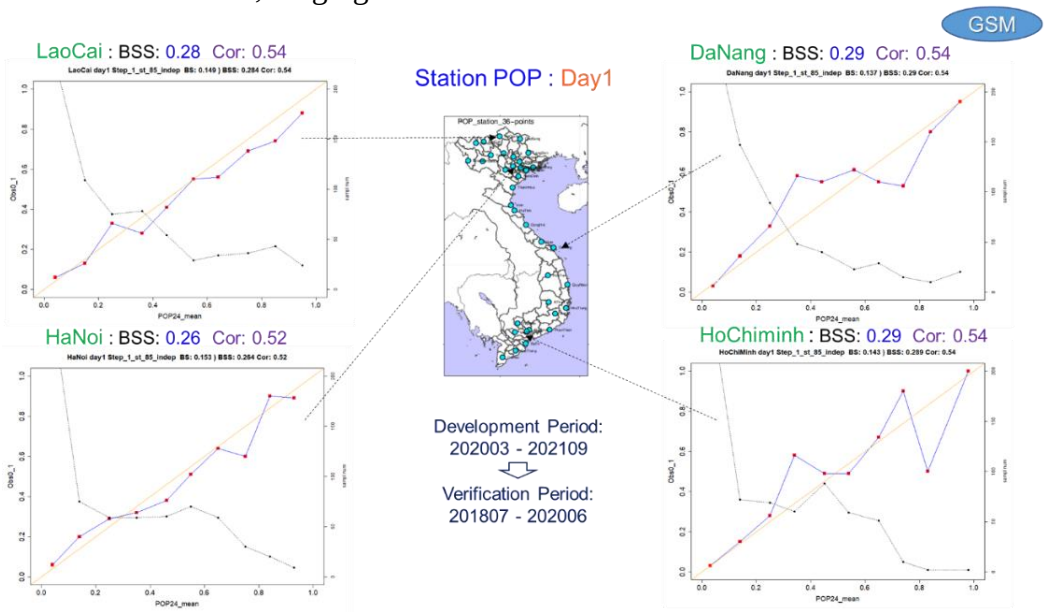

Figure 8. Reliability diagrams of station POPs at 4 stations for Day1.

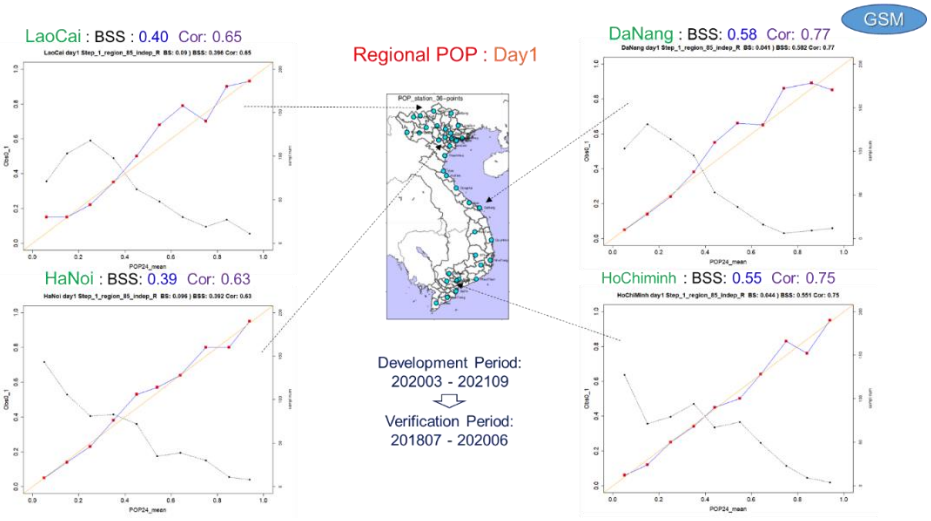

Figure 9. Reliability diagrams of regional POPs in 4 regions for Day1.

Looking at reliability diagrams at the 4 stations and in the 4 regions for Day 5 (5-days ahead), the variation in the diagrams increased than those for Day 1, and BSSs of station POPs were much lower ranging from 0.12 to 0.24, while BSSs of regional POPs were ranging from 0.19 to 0.42. BSSs of regional POPs were considerably lower than those for Day 1, but considerably higher than BSSs of station POPs for Day 5 (Figure not shown).

3.3. Preliminary investigation for regional mean and max 24-hour rainfall guidance

Following the verification of trial POP guidance in 4 regions, we calculated regional mean and max 24-hour rainfall guidance and conducted verification with the same datasets used for POP trial guidance. Figure 10 shows scatter diagrams of regional mean 24-hour rainfall observations and regional mean 24-hour rainfall guidance for Lao Cai, Ha Noi, Da Nang and Ho Chi Minh. Scatter diagrams for Lao Cai and Ho Chi Minh City showed relatively little variation, while those for Hanoi and Da Nang showed a large variation. Correlation coefficients between regional mean 24-hour rainfall observations and guidance for Hanoi and Danang were relatively low (0.5 and 0.56 respectively), while those for Lao Cai and Ho Chi Minh were relatively high (0.7 and 0.71 respectively). Scatter diagrams of regional max 24-hour rainfall observations and regional max 24-hour rainfall guidance for the 4 regions showed a large variation in all regions, with correlation coefficients ranging from 0.52 to 0.68 (Figure not shown).

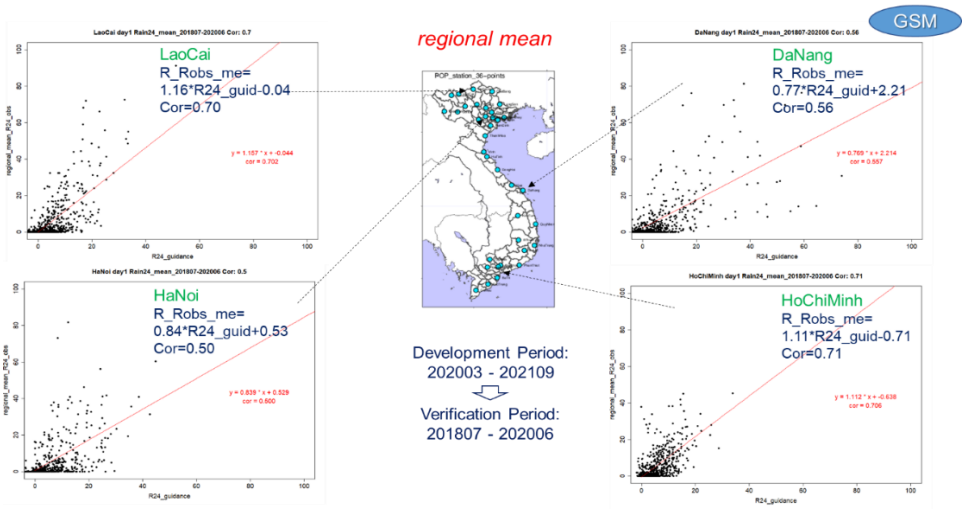

Figure 10. Scatter diagrams of regional mean 24-hour rainfall observations and regional mean 24-hour rainfall guidance in 4 regions for Day1.

3.4. Calculation of regional POP, regional mean and max 24-hour rainfall for 36 regions

In the preliminary investigation, Vietnam was divided into 21 regions to calculate regional mean rainfall etc. We however decided to subdivide Vietnam into 36 regions to make the regional allocation as close as possible to the forecast areas of NCHMF's city forecasts (5 municipalities and 58 provinces). It was desirable for a region to contain more than several stations, so if a province had only a few stations, it was combined with one or two neighboring provinces to form a region. New rainfall observation-GPV datasets for the 36 regions were created using 186 SYNOP station data for the period from Mar 2021 to Mar 2022 for IFS and from Mar 2020 to Mar 2022 for GSM, and regional POP, regional mean, and max rainfall guidance for the 36 regions were calculated and verified with the datasets.

3.4.1. Brier Skill Score of POP12 and POP24 for 36 regions

In line with the forecast period of NCHMF's city forecasts, we decided to prepare 12-hour precipitation guidance for tonight and tomorrow daytime, and 24-hour precipitation guidance after the day after tomorrow. Figure 11 shows BSSs of regional POP12 of IFS guidance and GSM guidance for tonight and tomorrow daytime in the 36 regions. BSSs of both IFS and GSM regional POP12 for tonight and tomorrow daytime were higher than 0.4 in most regions in the north and central. There were several regions with BSSs of less than 0.3 in the south for tonight in both IFS and GSM guidance. Comparing IFS and GSM, many regions had a slightly higher BSSs of POP12 in IFS, although the statistical periods were different.

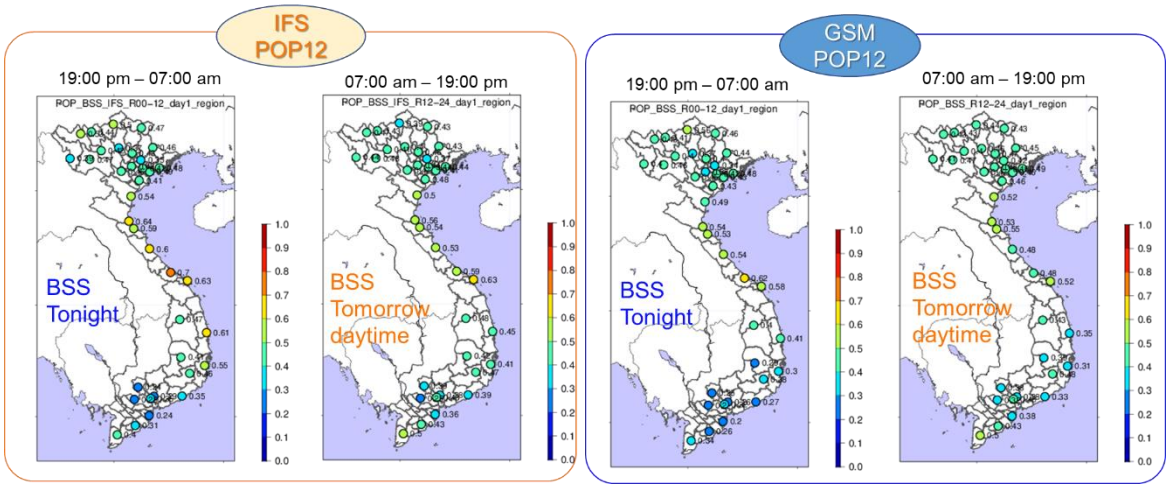

Figure 11. Distribution of Brier Skill Scores (BSSs) of regional IFS POP12 guidance and GSM POP12 guidance for tonight and tomorrow daytime for 36 regions. BSSs were calculated with dependent data (IFS: Mar 2021 to Mar 2022; GSM: Mar 2020 to Mar 2022).

Figure 12 shows BSSs of regional IFS POP24 and GSM POP24 for Day 1 and Day 5 in the 36 regions. BSSs of regional POP24 for Day 1 were higher than 0.5 in most regions in both IFS and GSM. Those for Day 5 were lower than POP24 for Day 1, but higher than 0.3 in most regions in both IFS and GSM. BSSs of IFS POP24 were a little bit higher than GSM POP24 in most regions, and BSSs of POP24 in the central were higher than those in the north and south.

In addition, POHP was calculated and verified similarly to the POP. However, BSSs of POHP were considerably lower than those of POP due to the small sample of heavy rainfall. BSSs were less than 0.2 in many regions even in the dependent data especially for long forecast periods (Figure not shown). It is considered necessary to accumulate heavier rain sample data for the development of POHP guidance.

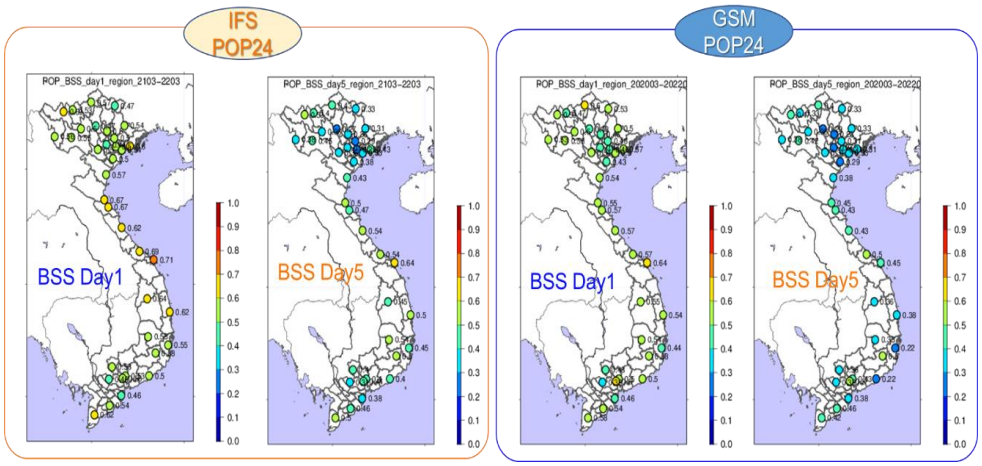

Figure 12. Distribution of Brier Skill Scores (BSSs) of regional IFS POP24 guidance and GSM POP24 guidance for Day1 and Day 5 for 36 regions. BSSs were calculated with dependent data (IFS: Mar 2021 to Mar 2022; GSM: Mar 2020 to Mar 2022).

3.4.2. IFS-GSM integrated precipitation guidance

We then developed IFS-GSM integrated precipitation guidance by using IFS and GSM predictors together. Figure 13 shows BSSs of POP and POHP with dependent data averaged over the 36 regions in IFS, GSM and IFS-GSM guidance for tonight, tomorrow daytime, Day 1 and Day 3. BSSs of POP12 and POP24 in IFS-GSM guidance were slightly higher than those in IFS and GSM guidance for all forecast periods. As for POHP12 and POHP24, BSSs in IFS-GSM guidance were higher than those in IFS and GSM guidance but were generally much lower than BSSs of POP guidance.

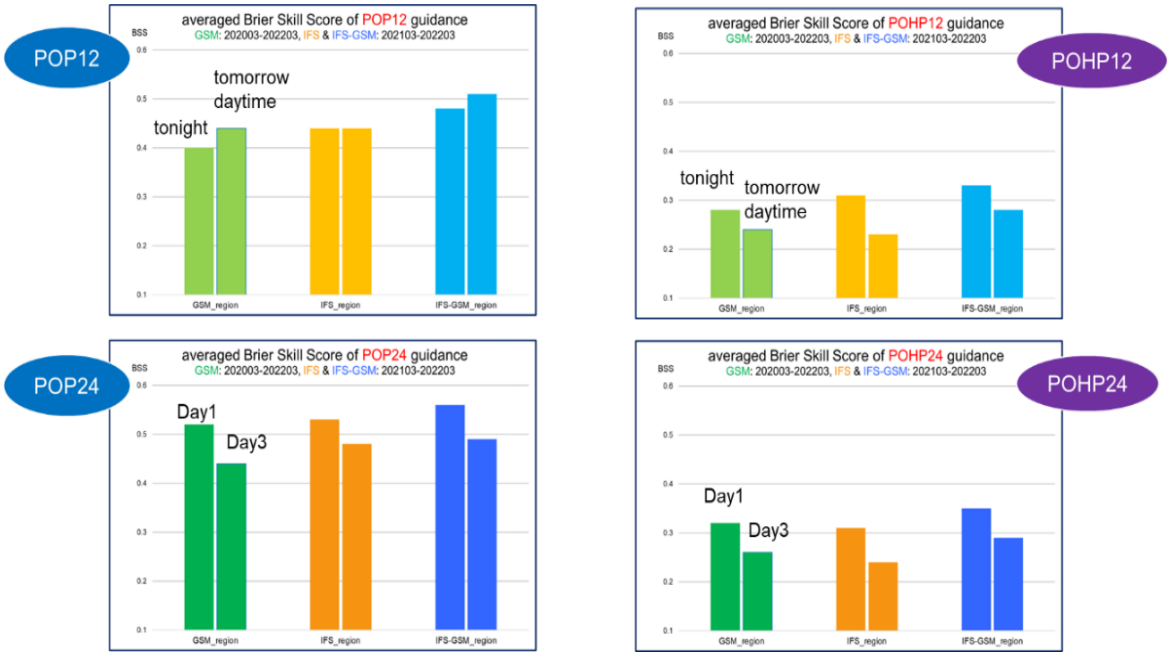

Figure 13. Averaged BSSs of POP12, POHP12, POP24 and POHP24 guidance by GSM, IFS and IFS–GSM for tonight, tomorrow daytime, Day1 and Day3.

Figure 14 shows scatter diagrams of regional mean and max 24-hour rainfall of IFS-GSM guidance in Hue region for Day 1. Correlation coefficients with dependent data were quite high at 0.88 and 0.83 for regional mean and max 24-hour rainfall respectively, but the variation was quite large, especially in maximum rainfall.

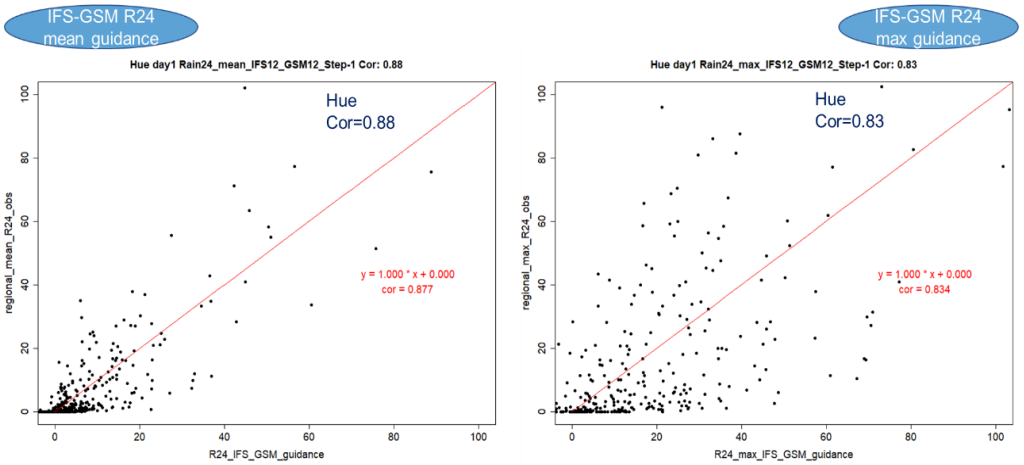

Figure 14. Scatter diagrams of regional mean/max 24-hour rainfall observations and IFS–GSM regional mean and max 24-hour rainfall guidance for Hue, Day1.

3.5. Daily calculation of precipitation guidance for 63 provinces

Based on the verification results, we decided to develop precipitation guidance on regional POP12 (tonight, tomorrow daytime) and POP24 (Day 2 to Day 5), regional mean and max 12-hour rainfall (tonight, tomorrow daytime) and 24-hour rainfall (Day 2 to Day 5) for 5 municipalities and 58 provinces up to 5-day ahead. Precipitation guidance is calculated for 36 regions and output for 5 municipalities and 58 provinces. Figure 15 is an example of precipitation guidance for August 19, 2022. It includes POP12, regional mean and max 12-hour rainfall for tonight and tomorrow daytime, POP24, regional mean and max 24-hour rainfall from the day after tomorrow to 5 days ahead. In addition, IFS and GSM regional mean rainfall predictions are included for forecaster's reference.

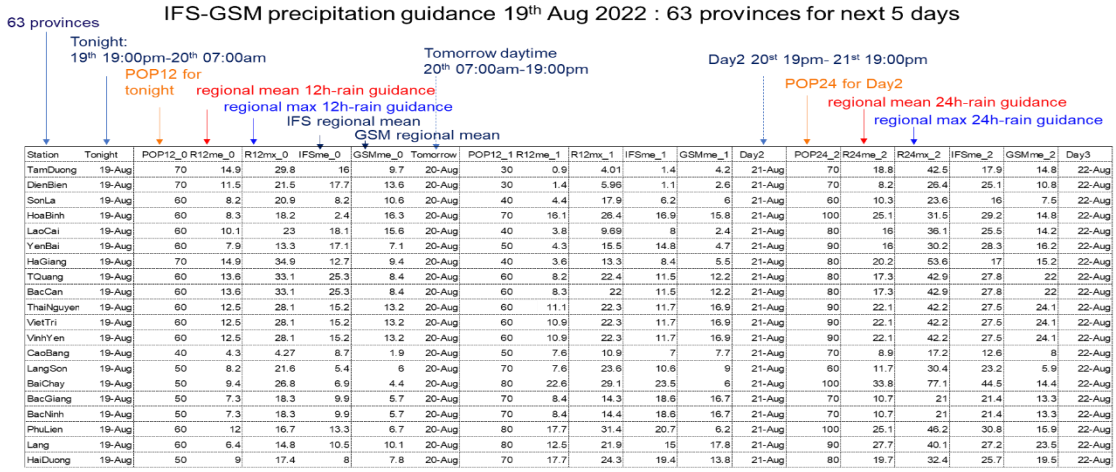

Station	Tonight	POP12_0	R12me_0	R12mx_0	IFSme_0	GSMme_0	Tomorrow	POP12_1	R12me_1	R12mx_1	IFSme_1	GSMme_1	Day2	POP24_2	R24me_2	R24mx_2	IFSme_2	GSMme_2	Day3
TamDuong	19-Aug	70	14.9	29.8	16	9.7	20-Aug	30	0.9	4.01	1.4	4.2	21-Aug	70	18.8	42.5	17.9	14.8	22-Aug
DienBien	19-Aug	70	11.5	21.5	17.7	13.6	20-Aug	30	1.4	5.96	1.1	2.6	21-Aug	70	8.2	26.4	25.1	10.8	22-Aug
SonLa	19-Aug	60	8.2	20.9	8.2	10.6	20-Aug	40	4.4	17.9	6.2	6	21-Aug	60	10.3	23.6	16	7.5	22-Aug
HoaBinh	19-Aug	60	8.3	18.2	2.4	16.3	20-Aug	70	16.1	26.4	16.9	15.8	21-Aug	100	25.1	31.5	29.2	14.8	22-Aug
LaoCai	19-Aug	60	10.1	23	18.1	15.6	20-Aug	40	3.8	9.69	8	2.4	21-Aug	80	16	36.1	25.5	14.2	22-Aug
YenBai	19-Aug	60	7.9	13.3	17.1	7.1	20-Aug	50	4.3	15.5	14.8	4.7	21-Aug	90	16	30.2	28.3	16.2	22-Aug
HaGiang	19-Aug	70	14.9	34.9	12.7	9.4	20-Aug	40	3.6	13.3	8.4	5.5	21-Aug	80	20.2	53.6	17	15.2	22-Aug
TQuang	19-Aug	60	13.6	33.1	25.3	8.4	20-Aug	60	8.2	22.4	11.5	12.2	21-Aug	80	17.3	42.9	27.8	22	22-Aug
BacCan	19-Aug	60	13.6	33.1	25.3	8.4	20-Aug	60	8.3	22	11.5	12.2	21-Aug	80	17.3	42.9	27.8	22	22-Aug
ThaiNguyen	19-Aug	60	12.5	28.1	15.2	13.2	20-Aug	60	11.1	22.3	11.7	16.9	21-Aug	90	22.1	42.2	27.5	24.1	22-Aug
VietTri	19-Aug	60	12.5	28.1	15.2	13.2	20-Aug	60	10.9	22.3	11.7	16.9	21-Aug	90	22.1	42.2	27.5	24.1	22-Aug
VinhYen	19-Aug	60	12.5	28.1	15.2	13.2	20-Aug	60	10.9	22.3	11.7	16.9	21-Aug	90	22.1	42.2	27.5	24.1	22-Aug
CaoBang	19-Aug	40	4.3	4.27	8.7	1.9	20-Aug	50	7.6	10.9	7	7.7	21-Aug	70	8.9	17.2	12.6	8	22-Aug
LangSon	19-Aug	50	8.2	21.6	5.4	6	20-Aug	70	7.6	23.6	10.6	9	21-Aug	60	11.7	30.4	23.2	5.9	22-Aug
BaiChay	19-Aug	50	9.4	26.8	6.9	4.4	20-Aug	80	22.6	29.1	23.5	6	21-Aug	100	33.8	77.1	44.5	14.4	22-Aug
BacGiang	19-Aug	50	7.3	18.3	9.9	5.7	20-Aug	70	8.4	14.3	18.6	16.7	21-Aug	70	10.7	21	21.4	13.3	22-Aug
BacNinh	19-Aug	50	7.3	18.3	9.9	5.7	20-Aug	70	8.4	14.4	18.6	16.7	21-Aug	70	10.7	21	21.4	13.3	22-Aug
PhuLien	19-Aug	60	12	16.7	13.3	6.7	20-Aug	80	17.7	31.4	20.7	6.2	21-Aug	100	25.1	46.2	30.8	15.9	22-Aug
Lang	19-Aug	60	6.4	14.8	10.5	10.1	20-Aug	80	12.5	21.9	15	17.8	21-Aug	90	27.7	40.1	27.2	23.5	22-Aug
HaiDuong	19-Aug	50	9	17.4	8	7.8	20-Aug	70	17.7	24.3	19.4	13.8	21-Aug	80	19.7	32.4	25.7	19.5	22-Aug

Figure 15. Example of IFS–GSM precipitation guidance for 63 provinces up to 5 days ahead for 19th Aug 2022.

3.6. Examples of precipitation guidance for heavy rain events in 2022

3.6.1. Heavy rain event caused by Typhoon NORU

Intense Typhoon NORU hit central Vietnam on the night of 27th September 2022 and brought heavy rainfall exceeding 300 mm in 12 hours in central Vietnam. Track forecasts of NORU by most NWP models fairly accurately predicted that it would make landfall in central Vietnam and bring heavy rainfall from the night of the 27th September to the next morning. Figure 16 shows the track of NORU analyzed by RSMC Tokyo, predictions of surface pressure and 6-hour rainfall around NORU for 28th 00UTC Sep by GSM 26th 12UTC initial.

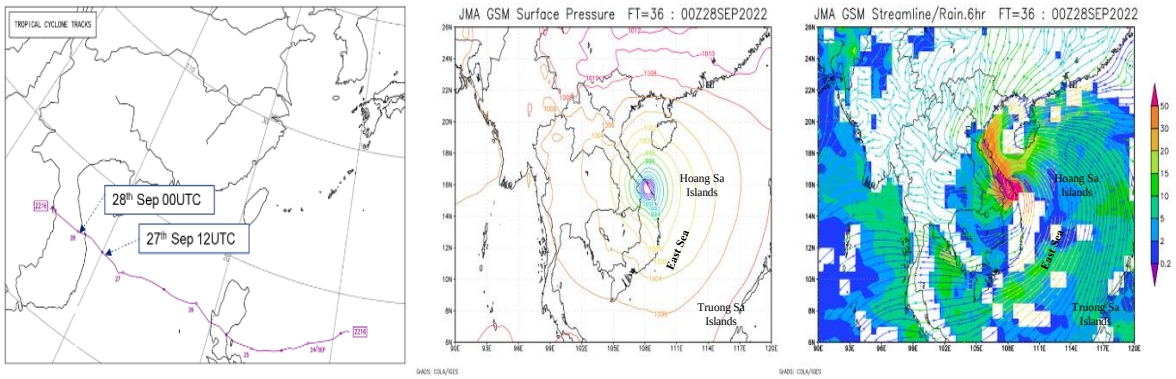

Figure 16. Track of TY NORU analyzed by RSMC Tokyo, 36–hour predictions of Surface pressure, streamline and 6–hour rainfall around NORU by GSM 26th 12UTC initial.

Three days prior to landfall, the 24-hour maximum rainfall predictions by IFS, NCEP GFS and GSM from the night of the 27th to the next day were 200-250 mm, 250-300 mm and 250-300 mm respectively, in central Vietnam (Figure 17). Figure 18 shows regional mean and max 24-hour rainfall guidance for 25th September 2022 based on IFS, GSM, and IFS-GSM predictions of 24th 12UTC initial. IFS guidance and GSM guidance had the highest rainfall of about 250 mm (IFS) and 420 mm (GSM) around Hue, while IFS-GSM guidance had the highest rainfall of about 350 mm around Da Nang.

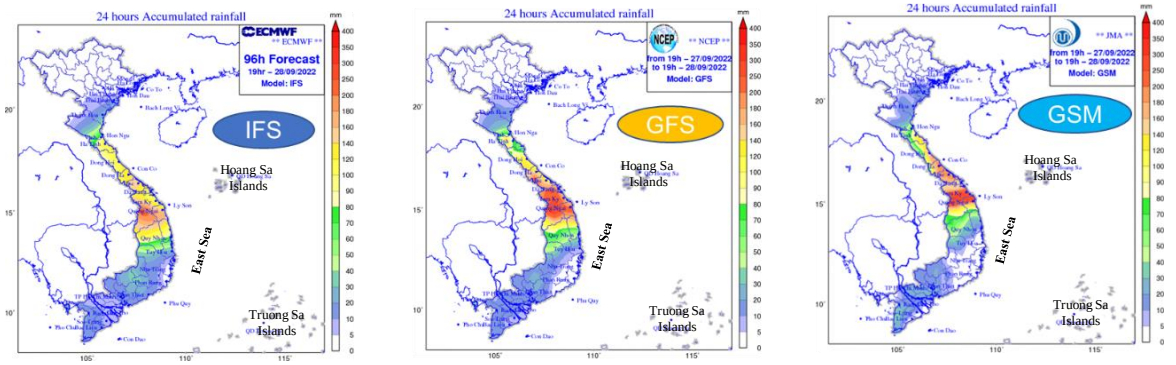

Figure 17. 24-hour rainfall predictions for 28th Sep by IFS, GFS and GSM of 24th 12UTC initial.

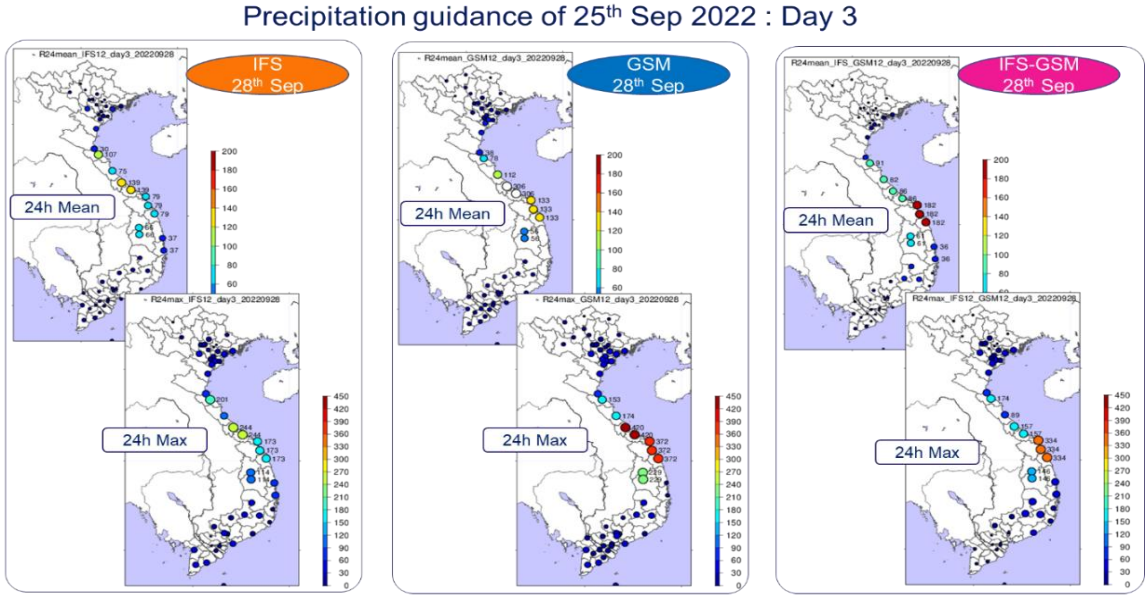

Figure 18. IFS, GSM and IFS-GSM precipitation guidance (regional mean/max 24-hour rainfall) of 25th Sep for Day 3 (28th Sep) based on 24th Sep 12 UTC initial.

Looking at 24-hour rainfall observations for the corresponding time period, the regional max rainfall in Hue and Da Nang was almost the same at 330 mm and 340 mm, respectively, and the regional mean rainfall was almost the same at 160 mm (Figure 19). Comparing the guidance to observations, IFS guidance had considerably too little rainfall in the Da Nang region and GSM guidance had considerably too much mean rainfall in the Hue region; IFS-GSM guidance had a fairly good representation of rainfall in the Da Nang region but less in the Hue region. All guidance was too little for rainfall in the Vinh region.

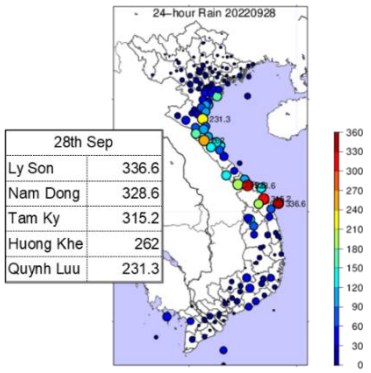

Figure 19. 24-hour rainfall observation for 19:00 27th – 19:00 28th Sep 2022.

One day prior to landfall, the 24-hour maximum rainfall predictions by IFS, GFS, GSM and VNMHA WRF for the night of the 27th and next day were 200-250 mm, 300-350 mm, 250-300 mm, and more than 400 mm respectively, in central Vietnam (Figure 20). Figure 21 shows regional mean and max 12-hour rainfall guidance of 27th for 27th tonight based on IFS, GSM, and IFS-GSM predictions of 26th 12UTC initial. Regional mean and max 12-hour rainfalls of IFS guidance were mean: 90 mm, max: 180 mm around Hue, mean: 60 mm, max: 180 mm around Da Nang, those of GSM guidance were mean:170 mm, max: 270 mm around Hue, mean: 120 mm, max: 280 mm around Da Nang and those of IFS-GSM guidance were mean: 90 mm, max: 250 mm around Hue, mean: 170 mm, max:430 mm around Da Nang.

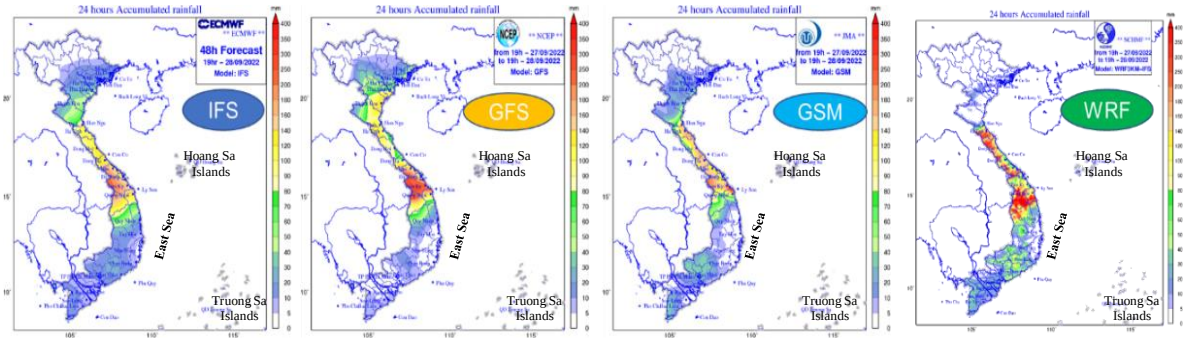

Figure 20. 24-hour rainfall predictions for 28th Sep by IFS, GFS and GSM of 26th 12UTC initial.

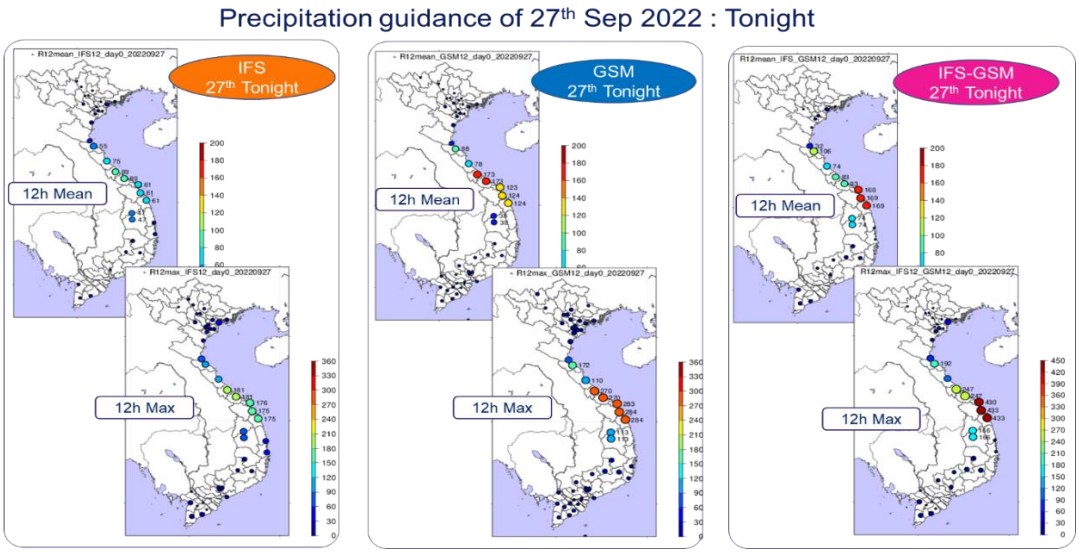

Figure 21. IFS, GSM and IFS-GSM precipitation guidance (regional mean/max12-hour rainfall) of 27th Sep for 27th tonight based on 26th Sep 12 UTC initial.

Looking at 12-hour rainfall observations, the regional max rainfall in Hue and Da Nang was almost the same at 330 mm, and the regional mean rainfall was also almost the same at 150 mm (Figure 22a). Comparing the guidance to observations, IFS guidance had considerably too little rainfall in the Da Nang region and GSM guidance was generally adequate rainfall in both Hue and Da Nang regions IFS-GSM guidance was slightly less for Hue region and more for Da Nang region. All guidance was generally adequate around Vinh region on the night of 27th September, but too little for the next daytime.

3.6.1. Heavy rain event with strong northeasterly winds blowing

Strong northeasterly winds blew into central Vietnam and heavy rainfall of 400-600 mm was observed in central Vietnam from the night of 9th to daytime of 10th October 2022. On that day, well-developed cloud systems and very strong radar QPE developed by Output 2 radar expert team were continuously observed over central Vietnam (Figure 22b) [13]. QPE provides detailed information on heavy rainfall that cannot be obtained from satellite imagery. Figure 23 shows predictions of surface winds and 6-hour rainfall and winds at 850hPa for 10th 00UTC Oct by GSM 7th 12UTC Oct initial.

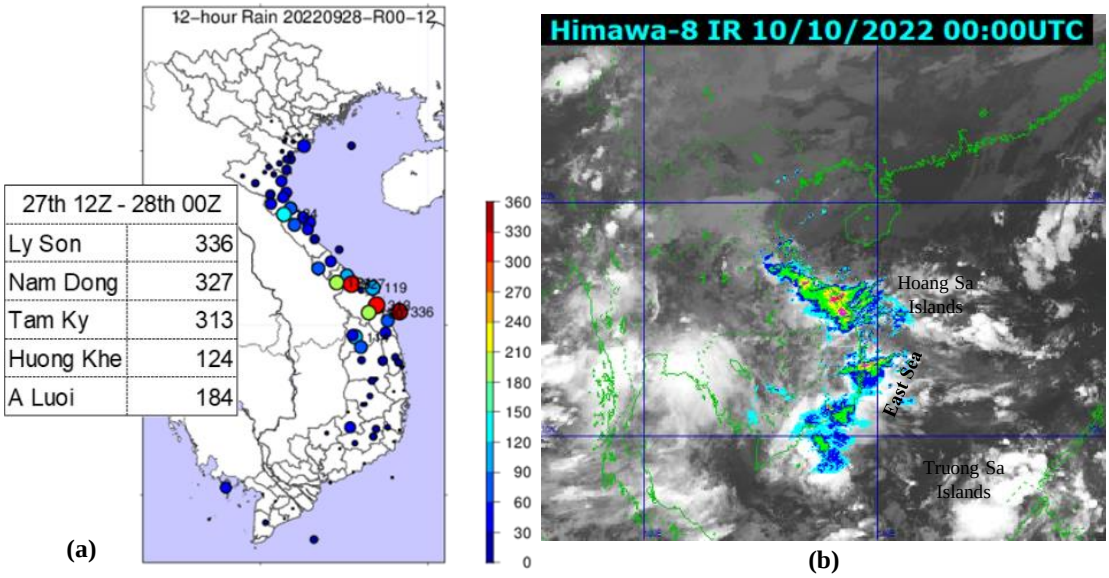

Figure 22. (a) 12-hour rainfall observation for 19:00 27th – 00:00 28th Sep 2022; (b) Radar QPE overlayed on IR image for 10th 00UTC Oct 2022.

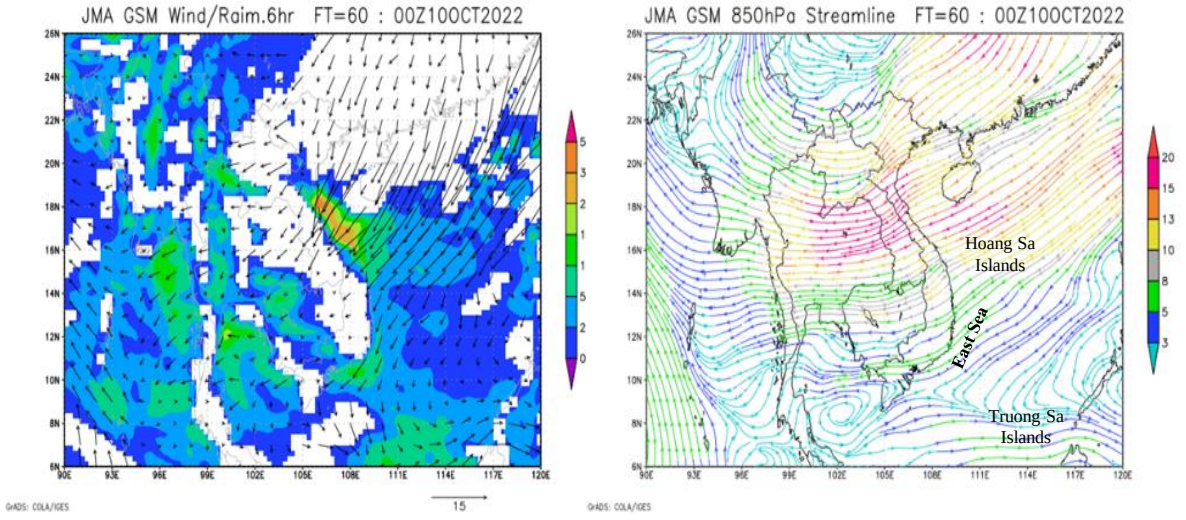

Figure 23. Surface winds and 6-hour rainfall, 850hPa stream lines for 10th 00UTC Oct 2022.

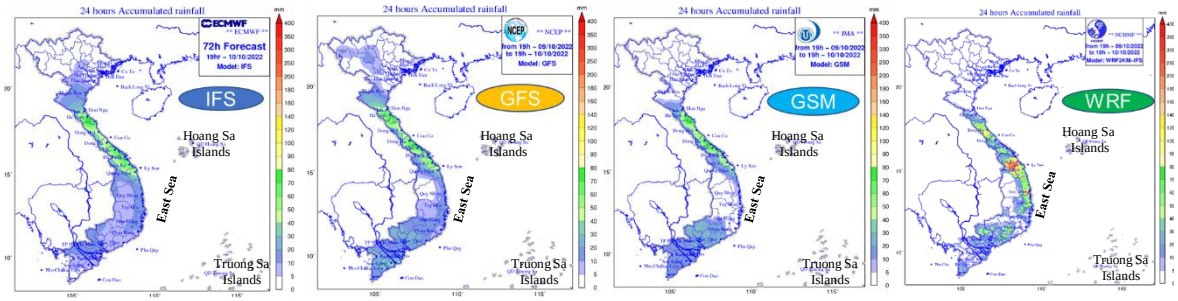

Figure 24. 24-hour rainfall predictions for 10th Oct 2022 by IFS, GFS and GSM of 7th Oct 12UTC.

IFS, GFS and GSM all predicted strong northeasterly winds blowing over central Vietnam, bringing 70-90 mm of rainfall during the time period, but they did not predict any heavy rains reaching 600 mm. WRF predicted heavy rainfall of 200-250 mm for some regions in central Vietnam (Figure 24). Regional max 24-hour rainfall of precipitation guidance for 8th Oct 2022 based on IFS-GSM predictions of 7th 12UTC initial was about 150 mm around Hue, much less than actual observations (Figure 25).

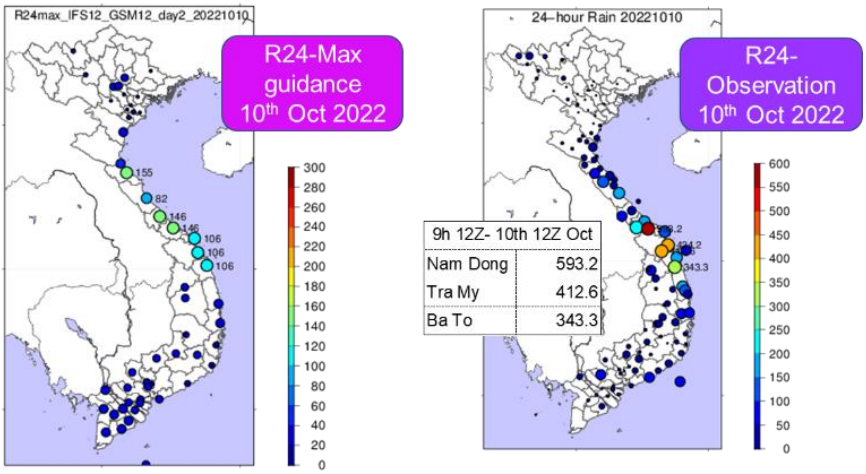

Figure 25. IFS-GSM precipitation guidance (regional max24-hour rainfall) of 8th Oct for 10th Oct 2022 based on 7th Oct 12 UTC initial.

In 2022, there were many heavy rain events caused by tropical cyclones. As for tropical cyclones, IFS and GSM predicted a little less rainfall but a reasonable amount, so precipitation guidance was generally able to predict a reasonable amount of rainfall for such heavy rain events caused by tropical cyclones. However as in the case of a heavy rain event with strong northeasterly winds blowing, there were several events where IFS and GSM rainfall predictions were quite low, and rainfall guidance was also quite low. Post-analysis of various heavy rainfall cases should be accumulated to improve rainfall precipitation guidance.

4. Conclusions

Precipitation guidance was developed with logistic regression and multiple linear regression for 36 regions up to 5 days ahead using JMA GSM GPV data and ECMWF IFS GPV data as an activity of the second phase of the JICA Project for Strengthening Capacity in Weather Forecasting and Flood Early Warning System. 2-year datasets of 24-hour rainfall observations and GSM/IFS predictions were first created at each station and in each region. Statistical analysis with the datasets showed correlation coefficients between 24-hour rainfall observations and IFS/GSM predictions were higher in the central region and lower in the

northern mountainous region and south region. The correlation coefficients of regional mean 24-hour rainfall were considerably higher than those of the stations in each region. Verification of POP trial guidance for 4 stations and 4 regions showed reliability diagrams were generally good for Day 1 for both at station and in region. BSSs of regional POP, which ranged from 0.39 to 0.58, were considerably higher than those of station POP ranged from 0.26 to 0.29. Scatter diagrams of regional mean 24-hour rainfall observations and guidance for 4 regions showed a large variation and correlation coefficients of them were relatively low in Hanoi and Da Nang (0.5 and 0.56) and relatively high in Lao Cai and Ho Chi Minh City (0.7 and 0.71).

Based on the verification results, we decided to develop precipitation guidance on regional POP12 (tonight, tomorrow daytime) and POP24 (Day 2 to Day 5), regional mean and max 12-hour rainfall and 24-hour rainfall for 36 regions (5 municipalities and 58 provinces) up to 5-day ahead. In addition to IFS and GSM guidance, we developed IFS-GSM-integrated precipitation guidance by using IFS and GSM predictors together and confirmed that its verification results were slightly better than those of IFS and GSM guidance. Test operation of the precipitation guidance started in September 2022.

Case studies of heavy rain events in September and October 2022 were conducted using observation data, NWP products and precipitation guidance. Precipitation guidance was generally able to predict a reasonable amount of rainfall for heavy rain events caused by tropical cyclones, however there were several events where IFS and GSM rainfall predictions were quite low, and rainfall guidance was also quite low. Post-analysis of various heavy rainfall cases should be accumulated to improve rainfall precipitation guidance.

Author Contributions: Conceptualization: K.S.; Methodology: K.S.; Software: K.S.; Observation and forecast data curation: V.T.A.; Verification: K.S.; Writing–original draft preparation: K.S.; Writing–review and editing: V.T.A.

Acknowledgments: Method of this work is based on training materials on guidance in the JICA group training course in meteorology being implemented by the Japan Meteorological Agency (JMA). We would like to thank JMA for their support. Ms. Do Thuy Trang of the NCHMF NWP division helped us in providing the IFS data. We would like to thank the Working Group 3 members, NCHMF staff members and JICA experts of this Project for their cooperation to our activities.

Conflicts of Interest: The authors declare no conflict of interest.

References

1. Tonouchi, M.; Kasuya, Y.; Tanaka, Y.; Akatsu, K.; Akaeda, K.; Nguyen, V.T. Activities of JICA on disaster prevention and achievement of JICA project in Period 1. *VN. J. Hydrometeorol.* **2020**, *5*, 1–12.
2. Sasaki, K.; Anh, V.T.; Hang, N.T.; Trang, T. Development of maximum and minimum temperature guidance with Kalman filter for 63 cities in Vietnam up to 10 days ahead. *VN. J. Hydrometeorol.* **2020**, *5*, 51–64.
3. Glahn, H.R.; Lowry, D.A. The use of model output statistics (MOS) in objective weather forecasting. *J. Appl. Meter.* **1972**, *11*, 1203–1211.
4. Klein, W.H.; Glahn, H.R. Forecasting local weather by means of model output statistics. *Bull. Amer. Meteor. Soc.* **1974**, *55*, 1217–1227.
5. Takada, S. Overview of Guidance. Special volume of numerical prediction division report. *Japan Meteorological Agency* **2018**, *64*, 1–18. (In Japanese)
6. Kudo, J. Guidance Development Techniques. Special volume of numerical prediction division report. *Japan Meteorological Agency* **2018**, *64*, 19–74. (In Japanese)

7. Shiroyama, Y. Precipitation Guidance. Special volume of numerical prediction division report. *Japan Meteorological Agency* **2018**, *64*, 95–118. (In Japanese)
8. Hoshina, M.; Yasutomi, Y.; Konoda, S. Guidance development techniques. research bulletin. *Japan Meteorological Agency* **1982**, *34*, 239–276. (In Japanese)
9. Ebihara, S. Improvement and verification of precipitation guidance. textbook for nwp training numerical prediction division. *Japan Meteorological Agency* **1999**, 23–33. (In Japanese)
10. Applequist, S.; Gahrs, G.E.; Pfeffer, R.L.; Niu, X.F. Comparison of methodologies for probabilistic quantitative precipitation forecasting. *Weather Forecasting* **2001**, *17*, 783–799.
11. Wilks, D.S. Statistical methods in the atmospheric sciences. 3rd Ed., Academic Press, Chapter 7, 2011, pp. 214–300.
12. Brier, G.W. Verification of forecasts expressed in terms of probability. *Mon. Wea. Rev.* **1950**, *78*, 1–3.
13. Kimpara, C.; Tonouchi, M.; Bui, T.K.H.; Nguyen, V.H.; Nguyen, M.C.; Akaeda, K. Quantitative precipitation estimation by combining rain gauge and meteorological radar networks in Viet Nam. *VN. J. Hydrometeor.* **2020**, *5*, 36–50.

JOURNAL OF
HYDRO-METEOROLOGY

Research Article

Development of a prototype system of the very short-range forecast of precipitation in Vietnam

Kazuo Saito[1,2,3]*, Mai Khanh Hung[4], Du Duc Tien[4]

[1] Japan Meteorological Business Support Center, Tokyo101-0054, Japan; k-saito@jmbsc.or.jp
[2] Atmosphere and Ocean Research Institute, University of Tokyo, Kashiwa 277-8564, Japan; k_saito@aori.u.tokyo.ac.jp
[3] Meteorological Research Institute, Japan Meteorological Agency, Tsukuba 305-0052, Japan; ksaito@mri-jam.go.jp
[4] National Center for Hydro-Meteorological Forecasting, Hanoi 10000, Vietnam; maikhanhhung18988@gmail.com; duductien@gmail.com

*Corresponding author: k-saito@jmbsc.or.jp; Tel.: +813–55772178

Received: 6 March 2023; Accepted: 14 April 2023; Published: 25 June 2023

Abstract: We developed a prototype system of the very short-range forecast of precipitation in Vietnam by merging kinematic extrapolations of composite hourly rainfall analysis and NWP, verified its performance for the case of a heavy rainfall event in July 2021 over central Vietnam. First, we produced hourly composite rainfall analysis over Vietnam with a grid distance of 5 km using AWS, radar, and satellite data. Next, we computed lag correlations between two hourly rainfall intensities at specific templates of 50 × 50 grids, and obtained lag indexes that maximize the lag correlation at 11 × 10 points. The moving vectors of precipitation areas at all grids are obtained by Cressman interpolation of the lag indexes, and a quality check using NWP horizontal winds at 700 hPa level was applied. Kinematic extrapolation of rainfall analysis was conducted using the above moving vectors and was merged with hourly rainfall prediction by a regional NWP model at NCHMF of VNMHA (WRF3kmIFS-DA) by weighted averaging. The magnitude of weight for the NWP in the merger was linearly increased from 0 to 1 for FT = 2 to 6 (from 03 UTC to 07 UTC, 12 July 2021). Verifications showed that the merged rainfalls outperformed both NWP and kinematically extrapolated precipitations for the time range of FT = 3 to 5.

Keywords: Precipitation analysis; Radar composite; Quantitative precipitation forecast; Very short-range forecast of precipitation.

1. Introduction

In most countries in southeast and east Asia including Vietnam and Japan, meteorological disasters occur every year. In particular, disasters by heavy rains often cause the greatest damage, and improvement of nowcasting and forecasting of intense precipitation is a key issue for disaster prevention and mitigation. Since June 2018, a bilateral cooperation project between the Japan International Cooperation Agency (JICA) and the Viet Nam Meteorological and Hydrological Administration (VNMHA) for "Strengthening Capacity in Weather Forecasting and Flood Early Warning System in the Social Republic of Vietnam" has been conducted. The Japan Meteorological Business Support Center (JMBSC) has been participating in the project as a main contributing organization of Japan. The project scopes are divided into four output targets: 1) surface meteorological observation; 2) radar

maintenance and products; 3) weather forecasting; and 4) regional weather dissemination. More detailed reviews of the JICA project are given by [1].

One of the main targets of the JICA project is quantitative precipitation estimation (QPE). QPE focuses on estimating precipitation levels over a relatively short period, such as a few hours in disaster prevention. QPE is useful in predicting the likelihood of flash floods or other weather–related hazards in a given area. Good QPE is attained by qualified networks of rain gauges and radars, and satellite data are used for supplementary information for filling data sparse areas as on the sea. In the first term of the JICA project, maintenance and installation of automated rain gauges for radar QPE calibration [2], and QPE by combining rain gauge and meteorological radar network [3] in Vietnam were conducted. At the National Center for Hydro-Meteorological Forecasting (NCHMF) of VNMHA, precipitation nowcasting for 3-hour precipitation is operationally conducted using a composite of rain gauge data at Automated Weather Stations (AWS), rainfall estimation by radars and satellite (Himawari-8 or GPS) [4–5].

Another important topic in disaster prevention is the quantitative precipitation forecast (QPF). QPF is typically based on numerical weather prediction (NWP), and short-term QPFs are used for decisions about pre-evacuation and emergency response. Although the accuracy of NWP has improved remarkably in recent years, the absolute accuracy of NWP is still not necessarily sufficient for disaster prevention, especially in a very short range of time (e.g., less than 6 hours), where the accuracy is often inferior to the kinematic extrapolation of the precipitation analysis. To bridge this gap between QPE and NWP, the Japan Meteorological Agency (JMA) operates its precipitation analysis and very short-range forecast of precipitation (VSRFP). The first one is the precipitation nowcast based on radar/rain gauge-analyzed precipitation with a spatial resolution of 250-1000 m, updated every 5 minutes [6].

VSRFP of JMA predicts precipitation with a spatial resolution of 1 km up to 6 hours ahead, updated every 10 minutes, whose basic concept is the merge of kinematic extrapolation of precipitation analysis and regional NWP model forecasts. Since performance of kinematic extrapolation deteriorates more rapidly than NWP, VSRFP with merging usually outperforms both extrapolation and NWP (Figure 1) [7–8].

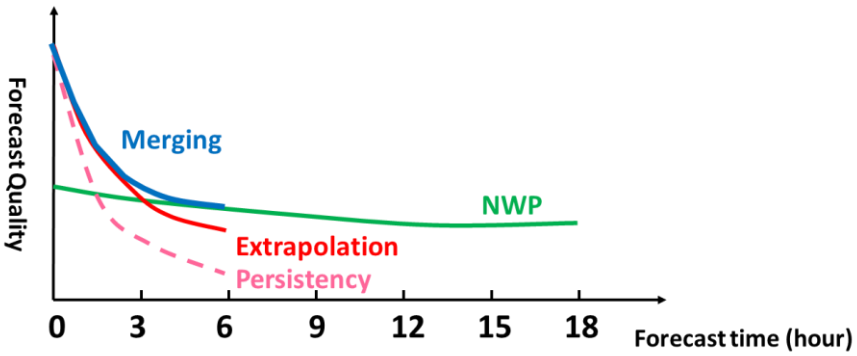

Figure 1. Concept of VSRFP: Reproduced from Saito and Makihara (2007) [7].

A similar precipitation nowcasting system, SWIRLS, has been in operation at the Hong Kong Observatory as well [9]. At JMA, both precipitation nowcast and VSRFP are essential information to issue advisories and warnings for rainfall and are used as input data for its hydrological model to compute soil water, surface water, and runoff indexes on risks of landslide, inundation, and river flood [10]. The importance of such the impact-based forecasting (IBF [11]) is increasing in several countries that suffer from natural disasters including Vietnam. Toward the realization of a very short-range rainfall prediction system in Vietnam similar to VSRFP of JMA, we developed a prototype system of the very short-range forecast of precipitation in Vietnam by merging kinematic extrapolations of composite hourly

rainfall analysis and regional NWP at NCHMF. Validation of the system was conducted for a heavy rainfall event that occurred in central Viet Nam in September 2021.

The organization of this paper is as follows. In Section 2, a heavy rainfall event in central Vietnam on 10-12 September 2021 is introduced. In Section 3, hourly composite rainfall analysis for this case using AWS, radar, and satellite data is described. The performance of persistency for this case is shown with verification scores. In Section 4, the kinematic extrapolation method for rainfall areas by moving vectors based on lag correlation is described. Quality control of moving vectors is performed by checking consistency against NWP winds. In section 5, a merge of extrapolated rains with regional NWP at NCHMF is described, with its verification scores. Summary and concluding remarks are given in Section 6.

2. Heavy rainfall event in central Viet Nam on 10-12 September 2021

On September 10-12, 2021, a heavy rainfall event occurred in central Vietnam, and at Danang, rain of 584 mm was observed in 48 hours from 12 UTC Sep 10 to Sep 12 (Figure 2). This heavy rainfall was brought by a weak tropical cyclone (T2113 Conson), which moved westward over the East China sea (Figure 3a). Although its intensity was not strong in terms of the central pressure (Figure 3b), this tropical cyclone was accompanied by a distinct cold dense overcast as seen in the Himawari satellite images (Figure 4).

As shown in Figure 2a, there were two peaks in this heavy rainfall event; 1012 UTC to 1112 UTC, and 1118 UTC to 1212 UTC. Here, we focus on the later peak of the rainfall in this study. Figure 5 indicates SYNOP and AWS 6h rains for 1118-1212 UTC. Generally, AWS rainfall well follows the rainfall pattern in SYNOP and indicates a more detailed distribution. Quality control of AWSs in Vietnam has been discussed by [11].

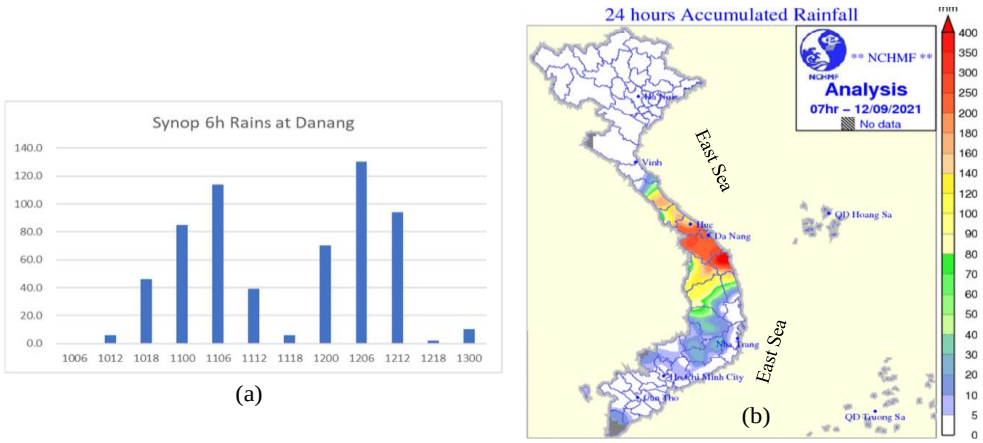

Figure 2. (a) SYNOP 6h observed rain at Danang 584 mm in 48h from 12 UTC Sep 10 to 12 UTC Sep 12; (b) SYNOP 24h accumulated rain at 12 UTC Sep 12.

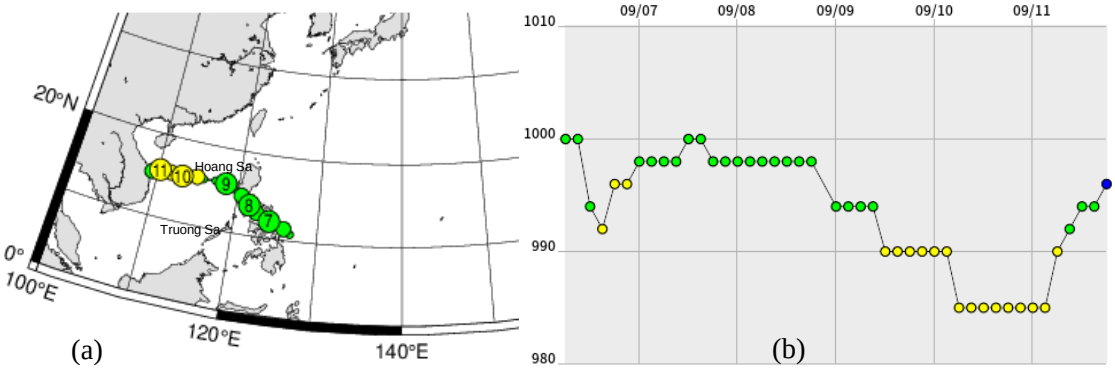

Figure 3. Track (a) and central pressure (b) of typhoon T2113 Conson. After the Digital Typhoon website of the National Institute of Informatics (http://agora.ex.nii.ac.jp/digital-typhoon/summary/wnp/s/202113.html.en).

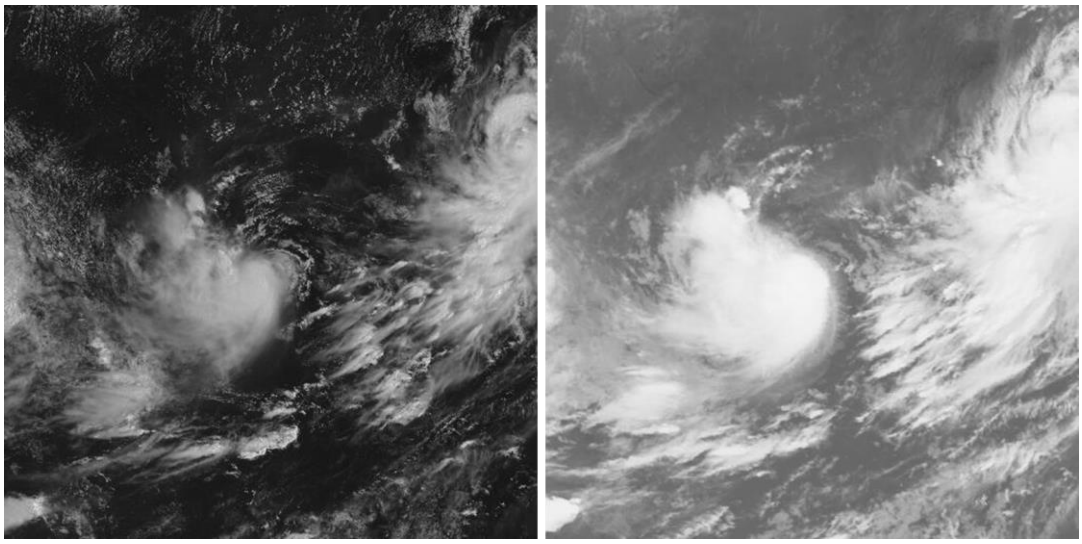

Figure 4. Himawari-8 satellite images at 202109 1103UTC for VIS (left) and IR (right).

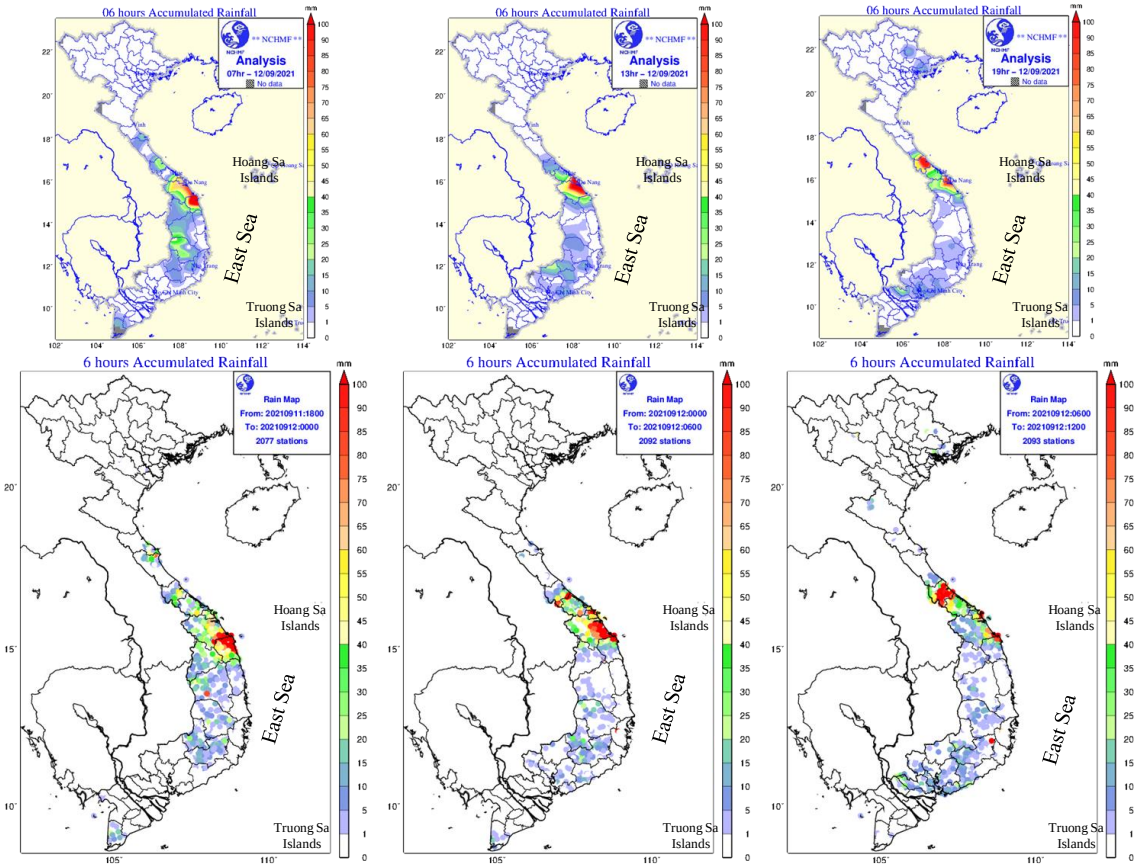

Figure 5. Upper) SYNOP 6h rains for 2021 September 11th 18 UTC to 12th 12 UTC. Lower) AWS 6h rains.

3. Hourly composite rainfall analysis

3.1. Hourly precipitation nowcast

VNMHA has operationally produced a 3-hour accumulated rainfall analysis using a composite of AWS, radar, and satellite estimated rainfall since August 2018. These observation data are collected by AMO of VNMHA daily, and binary-formatted precipitation amount data are prepared with a horizontal grid spacing of 0.05 degree. For details of meteorological radar observations at VNMHA and rainfall estimate from radars [2]. As

described by [4], two kinds of precipitation analysis ("Mean" and "Max") are produced at NCHMF. In "Mean", a priority order of data, AWS, radar and satellite, is prescribed, and precipitation amount at each analysis grid is determined by higher priority data source in order among the available data (e.g., a mean value of AWS precipitation is taken first if AWS rain gauge data are available). In "Max", the maximum value of the available data is selected.

In this study, to develop a very short-range forecast of precipitation system, first, we modified the rainfall analysis from three hourly to one hour. Figure 6 shows hourly rainfall at 00 UTC (07 LST; upper) and 01 UTC (08 LST; lower) of 2021 Sep 12 by AWS, radar, satellite, and their composite precipitation. Same as in Saito et al (2020), the composite rain map for the domain from 8.5 N to 23.5 N and 102.0 E to 116.0 E with a grid spacing of 0.05 degree is made with a priority in the order of AWS, radar, and satellite (i.e., same as "Mean"). Both the AWS and radar detected intense rains over central Vietnam. In the satellite estimated rainfall, very intense rains over 40 mm/h are seen not only over the central part of Vietnam, but in Thailand and over the South China Sea, corresponding to low TBB areas shown in the IR image in Figure 4. As discussed in [4–5], these very intense rainfalls are likely overestimation by using the statistical relationship between the cloud top temperature and rainfall by [12]:

$$R = 1.1183\times10^{11}\exp(-3.6382\times10^{-2}T_{BB}^{1.2}) \quad (1)$$

This relationship yields extremely intense rains (R) if the satellite-observed cloud top temperature (T_{BB}) is very low. This over-estimation by satellite is masked by AWS and radar rainfall in the composited rains over the mainland of Vietnam. Figure 7 indicates hourly composite rainfall analyses for successive 4 hours from 02 to 07 UTC, 2021 Sep 12.

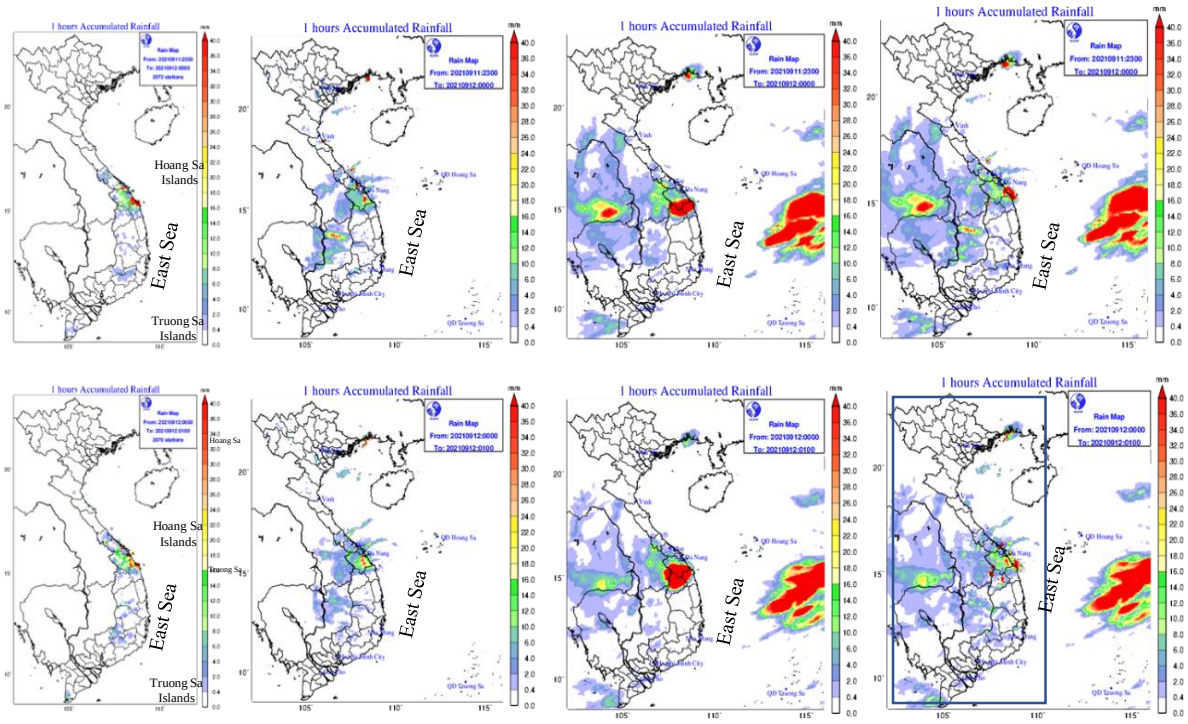

Figure 6. Upper) Hourly rainfall at 2021 Sep 12 00UTC (07LST) by AWS, radar, satellite, and composite precipitation. Lower) Same as upper but for 01 UTC (08 LST).

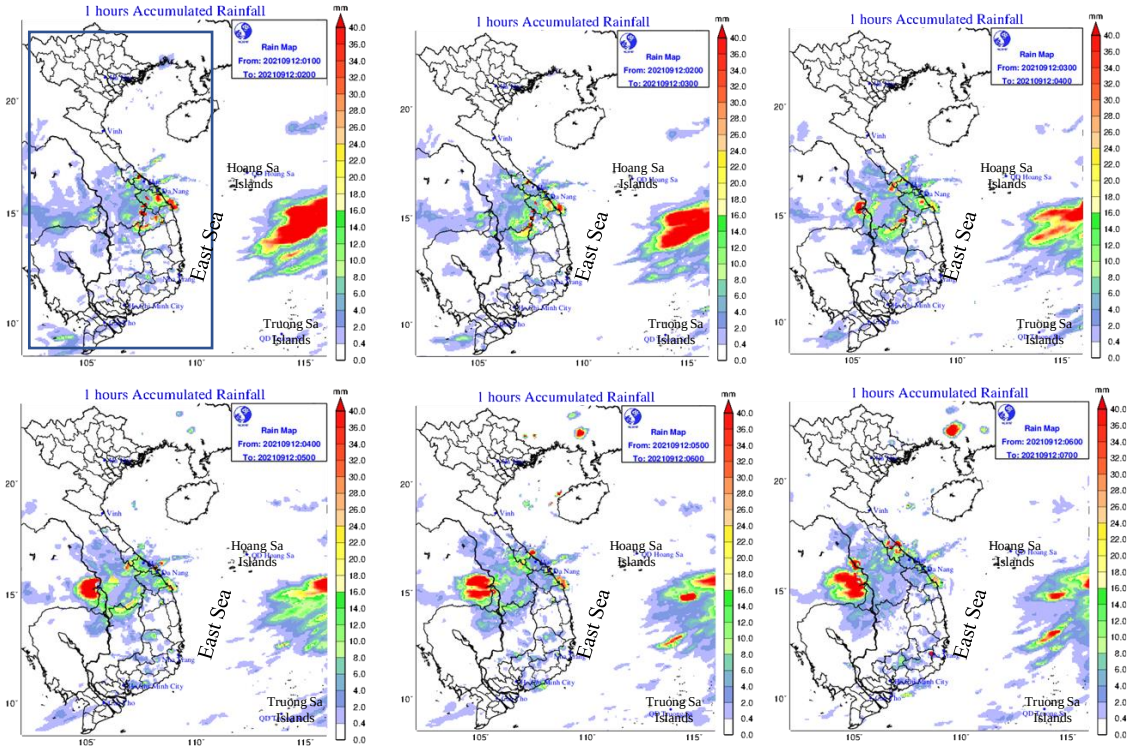

Figure 7. Composited hourly precipitation nowcast from 02UTC to 07 UTC, 2021 Sep 12.

3.2. Verification of persistency

Before the discussion on extrapolation of the rainfall areas, first we checked the performance of the persistency of hourly rainfall analysis in this heavy rainfall event. Considering the tendency of overestimation of intense rains in satellite rainfall estimation, the verification area is confined around the mainland of Vietnam, indicated by rectangles shown in Figures 6 and 7.

Figures 8 and 9 show scatter diagrams that indicate correlations of rainfall intensities from 02 UTC to 07 UTC against the rainfall intensity at 01 UTC in the verification domain. Needless to say, if we take the same time (01 UTC), the scatter plots are on the diagonal line of x = y. With the one-hour time lag (02 UTC), the scatter diagrams show a dispersion apart from the diagonal line, and this dispersion gradually increases with time. Middle and lower panels of Figure 8 show bias and threat scores of the persistency respectively, for different intensity thresholds from 0.5 to 20 mm/h, where the composite rains at 01 UTC are regarded as the forecast and the analyses at 02 to 07 UTC are regarded as the observation. At 02 to 03 UTC, bias scores are around 1.0 for all thresholds, while after 04 UTC, bias scores tend to decrease for intense rains. The threat scores tend to decrease with time, especially for intense rains. At 02 UTC, threat scores are about 0.55 at 0.5 mm/h and around 0.25 for rains over 5 mm/h. After 05 UTC, threat scores for intense rains over 10 mm/h become smaller than 0.1, however, in this case, threat scores for weak rains such as 0.5 mm/h keep their values around 0.4 (Figure 9).

Figure 10 shows the time evolution of bias scores (upper panels) and threat scores (lower panels) for weak (1 mm/h) and moderate (5 mm/h) rains from 01 to 07 UTC (FT = 0 to 6). In these rainfall intensity ranges, bias scores keep their values around unity for the whole verification period. Threat scores rapidly decrease at the first one to two hours but remain at a certain value even after FT = 3. Usually, in the middle latitude region such as in Japan, rainfall areas are advected eastward by the westerly, thus the threat scores persistency become very small with time. In this case study, the major rainfall areas by tropical cyclone remained over Vietnam, thus both bias and threat scores of the persistency kept its performance even after FT = 3.

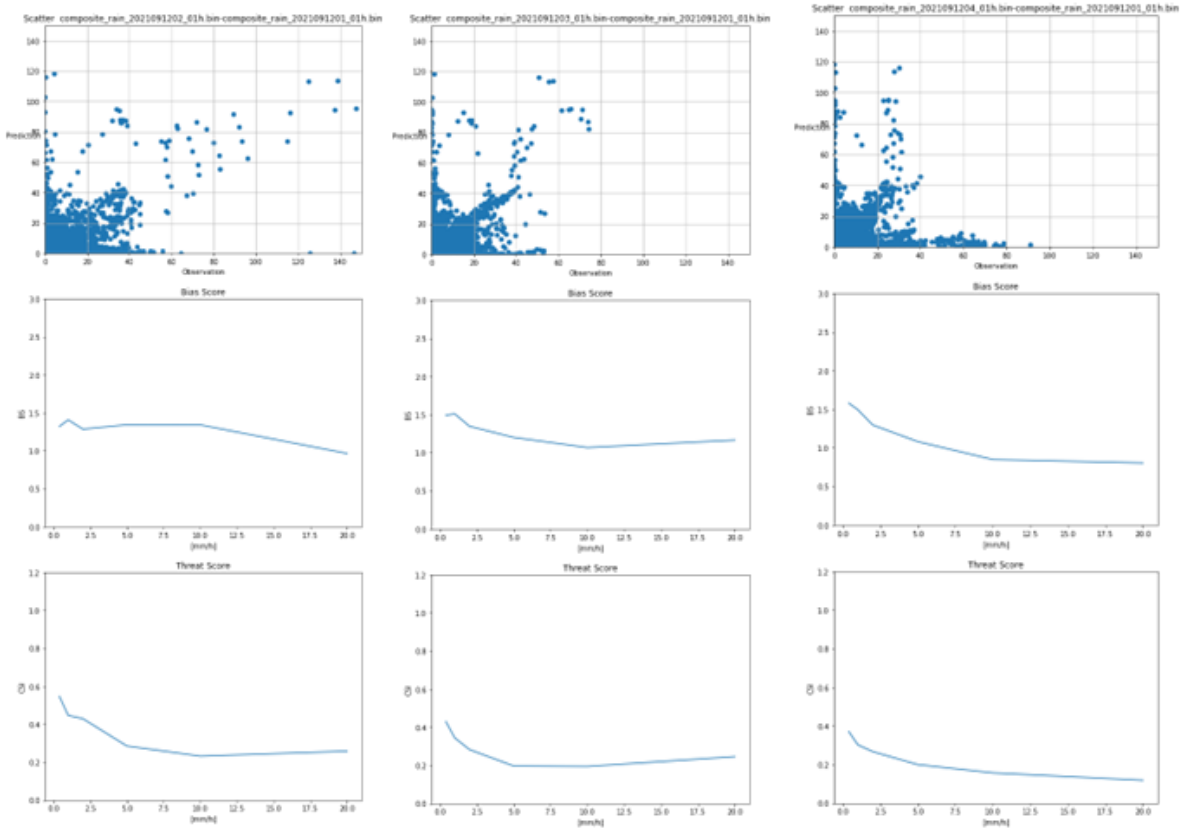

Figure 8. Upper) Scatter diagrams of persistency between the rainfall intensities at 02 to 04 UTC (horizontal axis) and 01 UTC (vertical axis) in the rectangles in Figure 6. Middle) Bias scores. Lower) Threat scores.

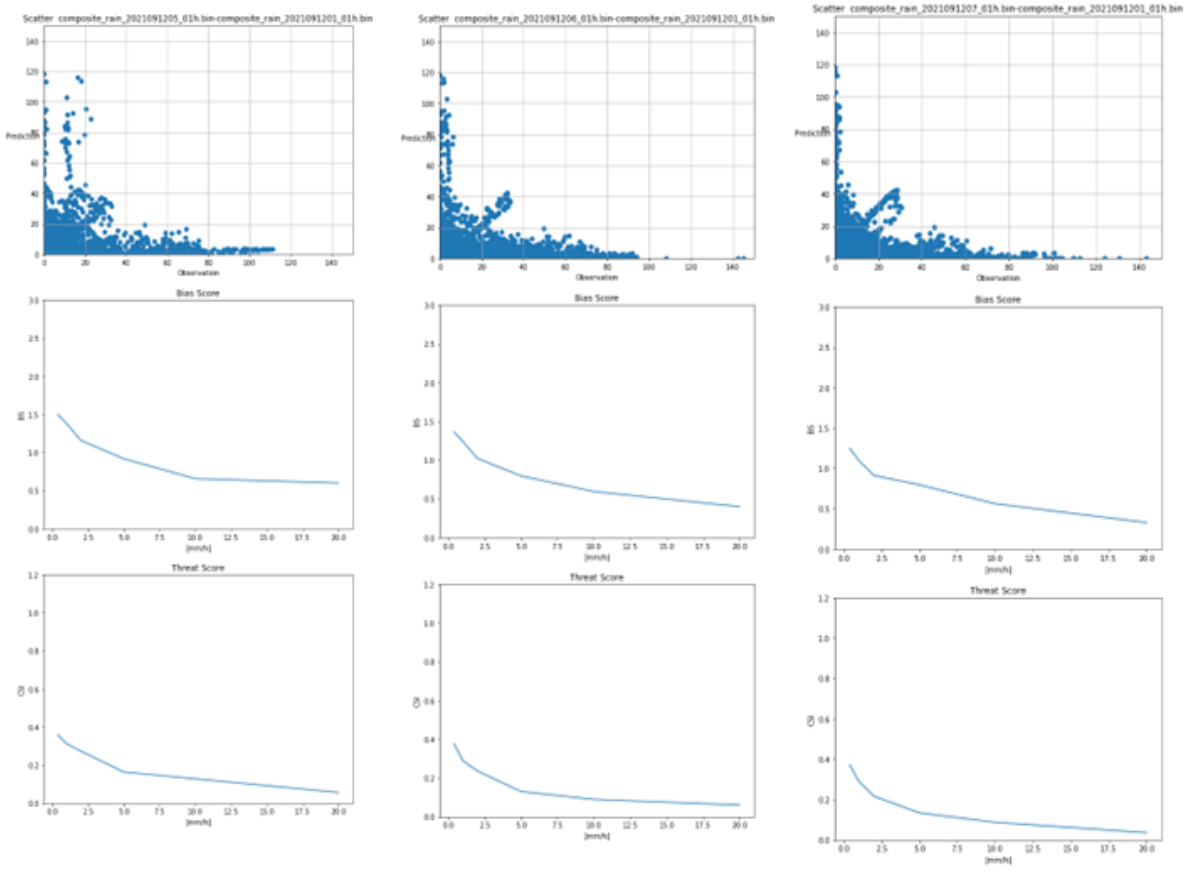

Figure 9. Same as in Figure 7 but for 05 to 07 UTC.

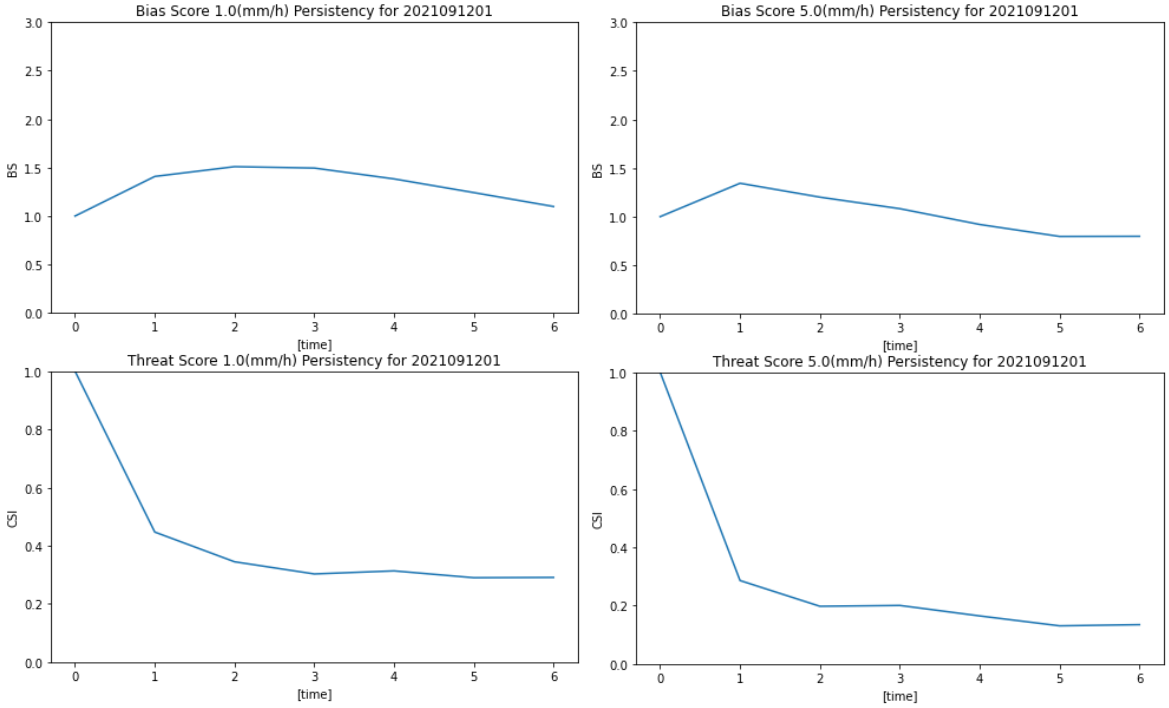

Figure 10. Time evolution of bias scores (upper) and threat scores (lower) of persistency for FT = 0 to 6 for 1 mm/h (left) and 5 mm/h (right) rainfall intensity threshold against 01 UTC, 2021 Sep 12.

4. Kinematic extrapolation by lag correlation

4.1. Computation of lag correlation

For kinematic extrapolation of rainfall analyses, we followed the cross correlation method for cell tracking [14], where initial array of radar reflectivity is correlated with later array. By location the second array with the bet correlation, a motion vector for the initial array is determined. This method is widely used to calculate cloud motion vectors from satellite images ass well [15–16]. In this study, cross (lag) correlations of precipitation between two rainfall maps (e.g., 00 and 01UTC) were computed to obtain a moving vector of the precipitation areas. For the analysis domain of 15×14 degrees (330×308 grids), we computed the lag correlations at 11×10 points of every 25 grids using a computation template of 50×50 grids.

Figure 11 shows the composite rainfall analyses at 00 and 01 UTC on September 12, 2021 (corresponding to Figures 6d and 6h). An example of the computational template is shown by the yellow square over the south of Vietnam in these figures.

Figures 12a and 12b show enlarged views of the templates indicated by the squares in the lower-left corner of the figures. Positional lag correlations of rainfall intensities in these templates were calculated by shifting the template in four directions (east, west, south, and north) up to 5 grids each:

$$r_{xy} = \frac{\sum_{i=1}^{n}(x_i - \bar{x})(y_i - \bar{y})}{\sqrt{\sum_{i=1}^{n}(x_i - \bar{x})^2}\sqrt{\sum_{i=1}^{n}(y_i - \bar{y})^2}} \quad (2)$$

where x_i and y_i represent (the square root of) rainfall intensity at the same grid of two templates and r_{xy} the correlation.

To avoid correlation coefficients being too sensitive to a few extremely intense rain grids, we applied the square root function to the rainfall intensity R before calculating the correlation coefficients. Applying the square root function in rainfall intensity in the calculation (2) is corresponding to the use of the absolute deviation in the least square

method, and this approach is known as the Huber norm in data assimilation to make the system less sensitive to outliers [17]. We also tested several functions such as the logarithm function (log(1+R)), but the results (indexes that maximize the correlation coefficients) were not so different.

Figure 12c shows the distribution of the magnitude of lag correlation coefficients when this template is shifted up to 5 grids from the center to the east, west, south, and north directions. In this figure, the correlation coefficient reaches a maximum value of 0.75 when the precipitation areas at 00 UTC are shifted to four grids to the west (x = –4) and two grids to the south (y = –2). In other words, the moving vector of the precipitation area obtained from these two figures is approximately 4.5 (2√5) grids to the west-southwest.

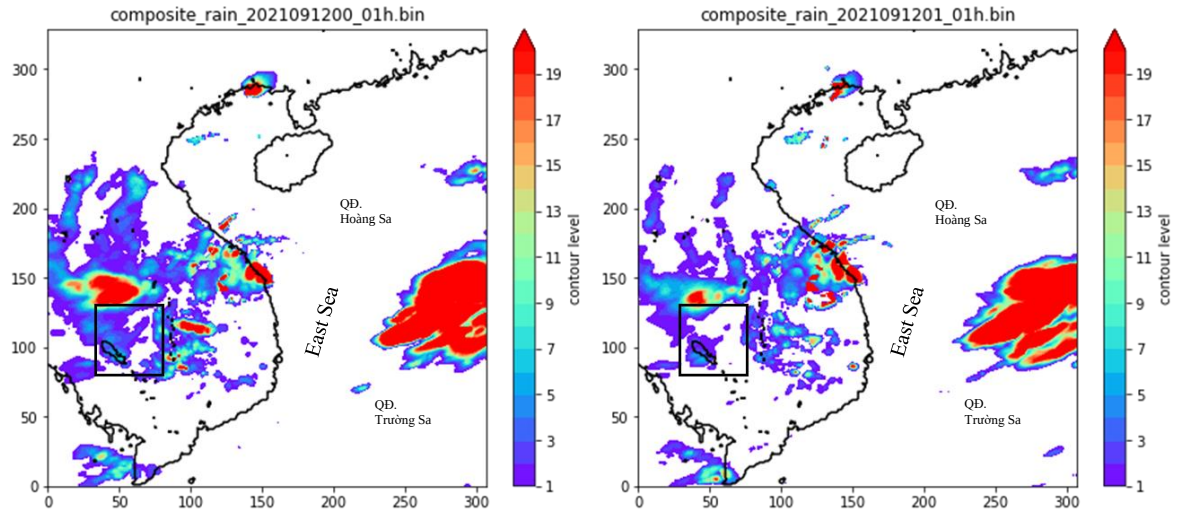

Figure 11. Composite rain at 00 UTC and 01 UTC, 2021 Sep 12. Black squares indicate the template to compute the lag correlation. Black lines indicate the contour of 0.5 of the land use in the WRF3kmIFS–DA model.

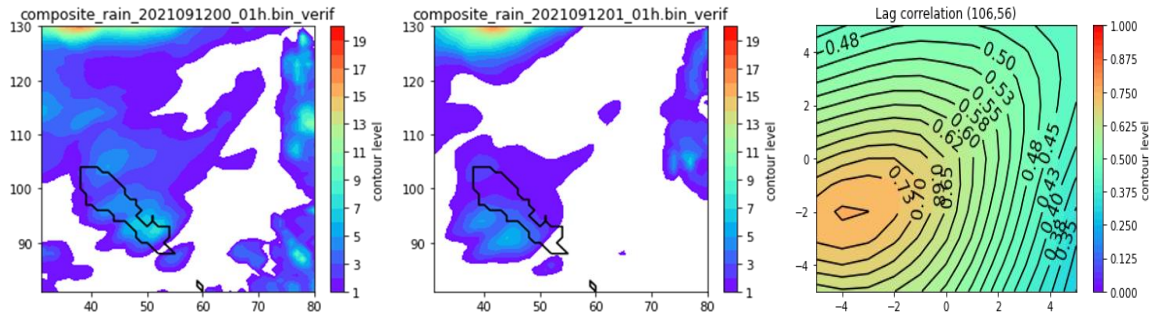

Figure 12. Enlarged view of composite rain in the template at 00 UTC and 01 UTC, 2021 Sep 12, and lag correlation coefficients at a grid point of (106, 56).

The computation points were changed by 25 grids to find the amount of movement with similar maximum correlation coefficients at 11×10 points in the region. The Cressman interpolation to the original grids is used:

$$z_p = \frac{\sum_{i=1}^{n} w_i z_i}{\sum_{i=1}^{n} w_i} \tag{3}$$

where w_i is the weight expressed by the following function of the square of the distance between the interpolated points and rainfall grids:

$$w_i = 1 + (x_i - x_p)^2 + (y_i - y_p)^2 \quad (4)$$

Here, the weights of the calculation points at which the maximum correlation coefficient value was less than 0.3 or the number of rainfall grids in the template was less than 10% were set to zero (shown by white masks in Figure 13). Figure 14 indicates the distribution of the indexes interpolated to the original analysis grids of 330×308.

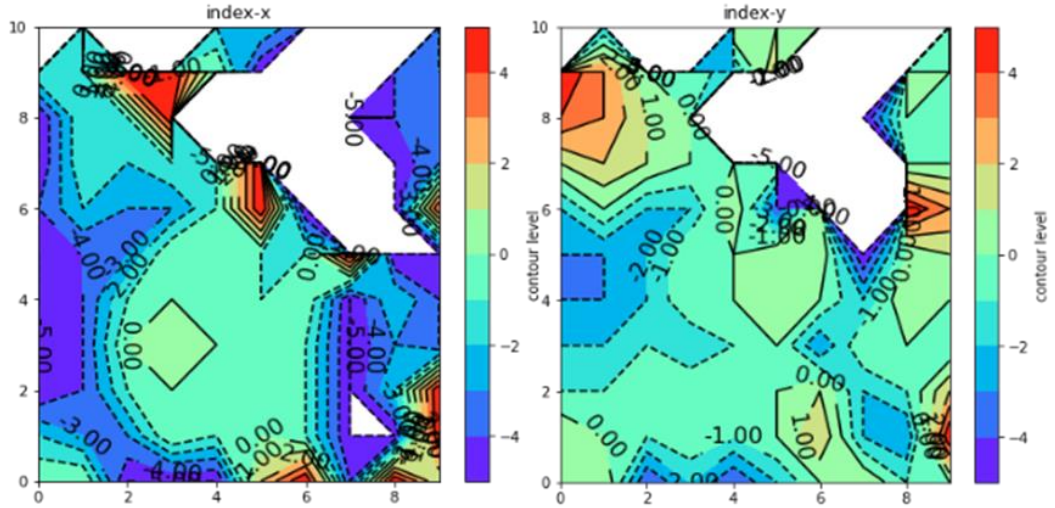

Figure 13. Distribution of lag-indexes which maximize the correlation coefficients at 11×10 points with intervals of 25 grids. White masks indicate the points at which the maximum correlation coefficient value was less than 0.3 or the number of rainfall grids in the template was less than 10 %.

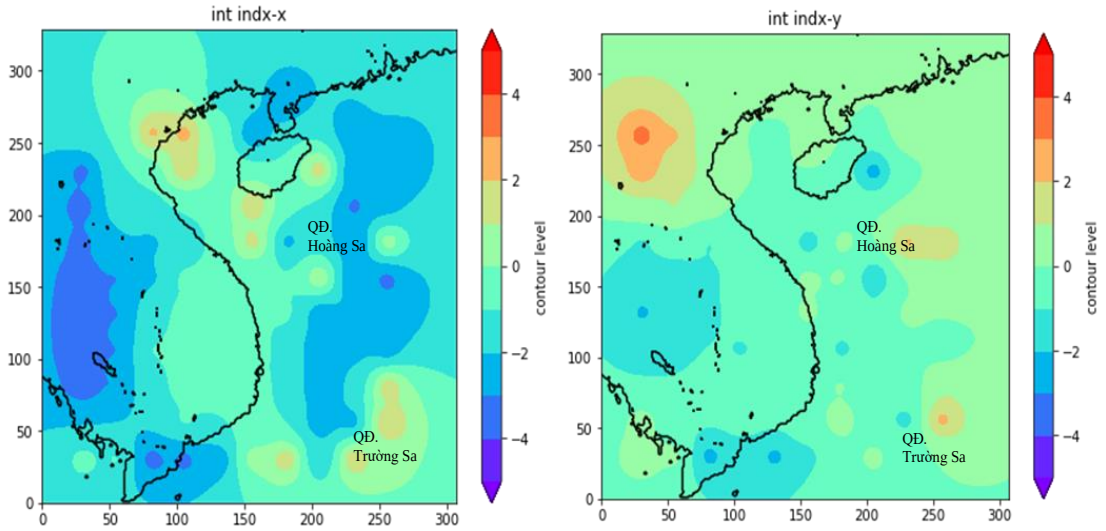

Figure 14. Interpolated lag indexes between 00 and 01 UTC rain map.

4.2. Consistency check with NWP winds

The lag indexes that maximize the correlation coefficients may have erroneous patterns due to local extremum. To discard such unrealistic movement of rainfall area, we applied quality control using the NWP model to forecast winds. Moving vectors in the opposite directions to the NCHMF regional NWP (WRF3kmIFS-DA) winds at 700-hPa level were considered to be zero. Figure 15 indicates 700 hPa wind at 01 UTC September 12 predicted by WRF3kmIFS-DA, whose initial time is 12 UTC September 11 (FT = 13). Corresponding

to the weak tropical cyclone in the central part of Vietnam, both zonal winds (U700; left panel) and meridional winds (V700; left panel) show dipole patterns which suggest counterclockwise rotation. Figure 16 shows the resultant quality-controlled lag indexes corresponding to the moving vector components of rainfall areas. Some westward movements in the south of the tropical cyclone and northward movements in the northwest of the tropical cyclone are removed.

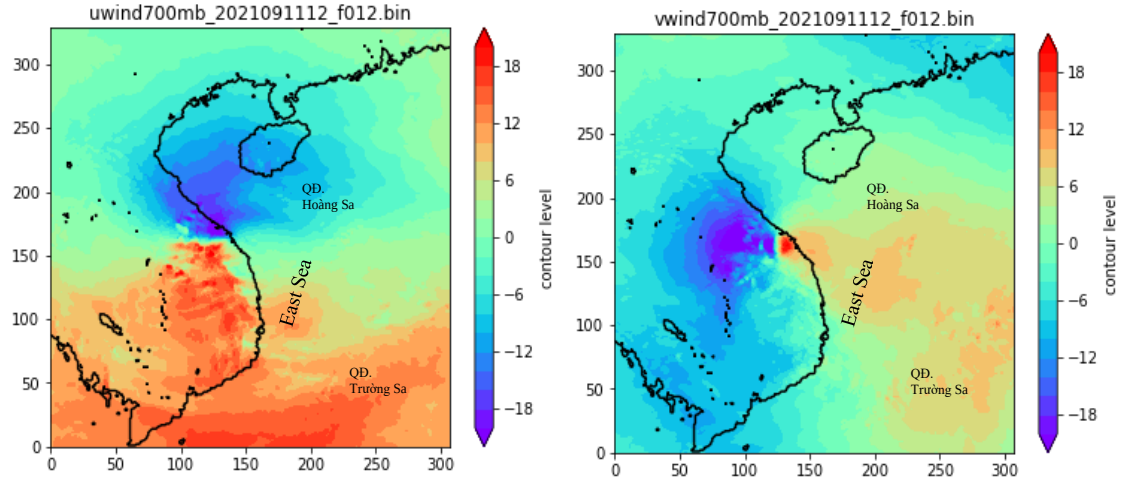

Figure 15. WRF3kmIFS-DA 700 hPa winds at 01 UTC: (a) U700, (b) V700.

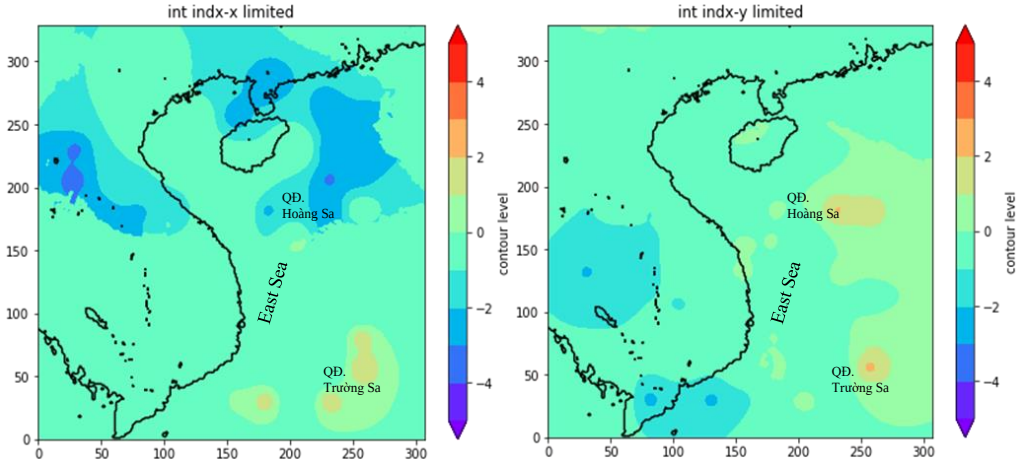

Figure 16. Same as Figure 13, but quality-controlled by consistency with the sign of (U700, V700).

4.3. Kinematic extrapolation

The aforementioned moving vector components are used to kinematically extrapolate the rainfall areas at 01 UTC. For extrapolation, we determine an upstream point for each grid by multiplying the moving vector components by extrapolation time (i.e., linear extrapolation), and then replace the rainfall amount at the grid with the value at the corresponding upstream point.

Figure 17 shows a map of precipitation for 02-07 UTC (FT = 1-6) on 12 September 2021, obtained by the kinematic extrapolation. Corresponding to the counterclockwise rotation around the tropical cyclone, rainfall areas in the eastern part of the figure extend northward or westward slightly while most of rainfall areas over Vietnam remain or slowly move southward.

We conducted a verification of the kinematic extrapolation similar to the persistency. Figures 18 and 19 show scatter diagrams, bias scores, and threat scores for extrapolation

against rainfall analysis from 02 UTC (FT = 1) to 07 UTC (FT = 6). Seemingly these figures are not so different from the corresponding figures for persistency (Figures 7 and 8), but small differences are seen in the scatter diagrams and scores. Since kinematic extrapolation does not change the frequency of rainfall intensity, no significant differences are seen in the bias scores. On the other hand, threat scores of extrapolation for 1 mm/h and 2 mm/h at FT = 1 were slightly better than persistency. Figure 20 shows the time evolution of bias scores (upper) and threat scores (lower) of extrapolation for 1 mm/h and 5 mm/h rainfall intensity against the rainfall analysis at the same time. Threat scores of extrapolations for 1 mm/h at FT = 1 were slightly better than persistency, but no improvements are obtained in other time ranges in this case.

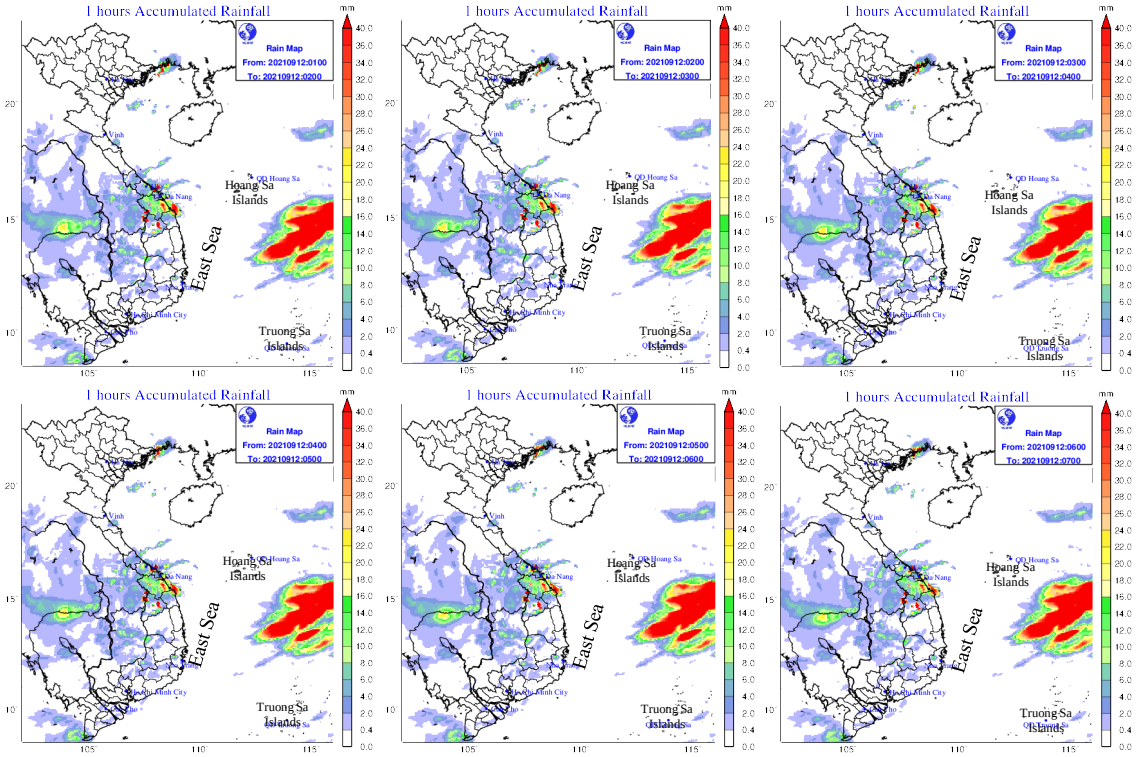

Figure 17. Composite rains by kinematic extrapolation for 02 to 07 UTC, 2021 September 12.

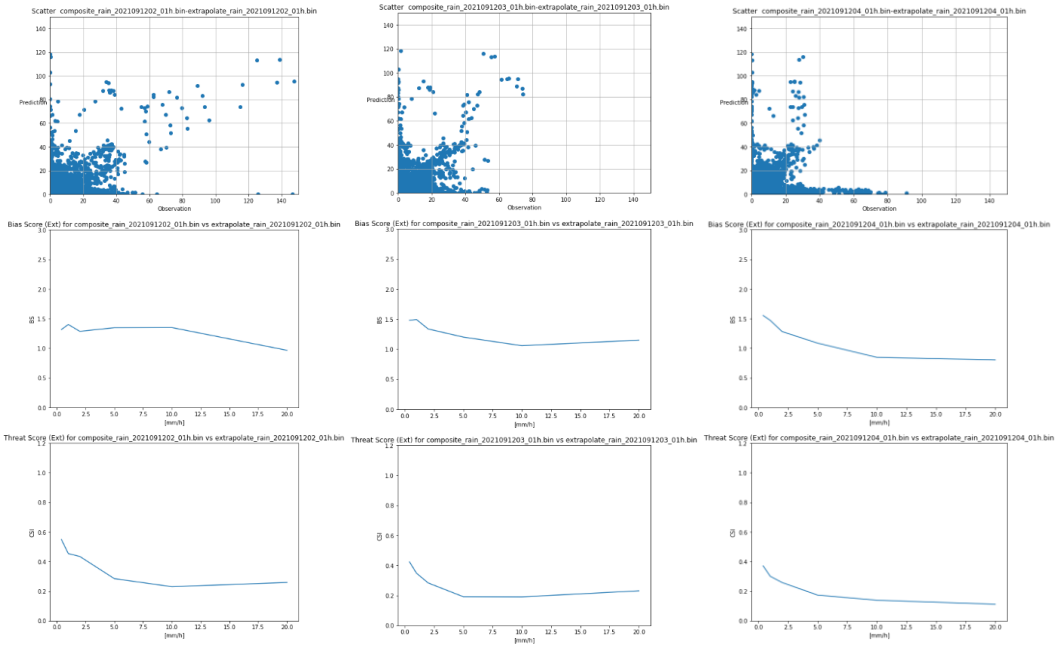

Figure 18. Same as Figure 8 but for extrapolation for 02 to 04 UTC (FT = 1 to 3).

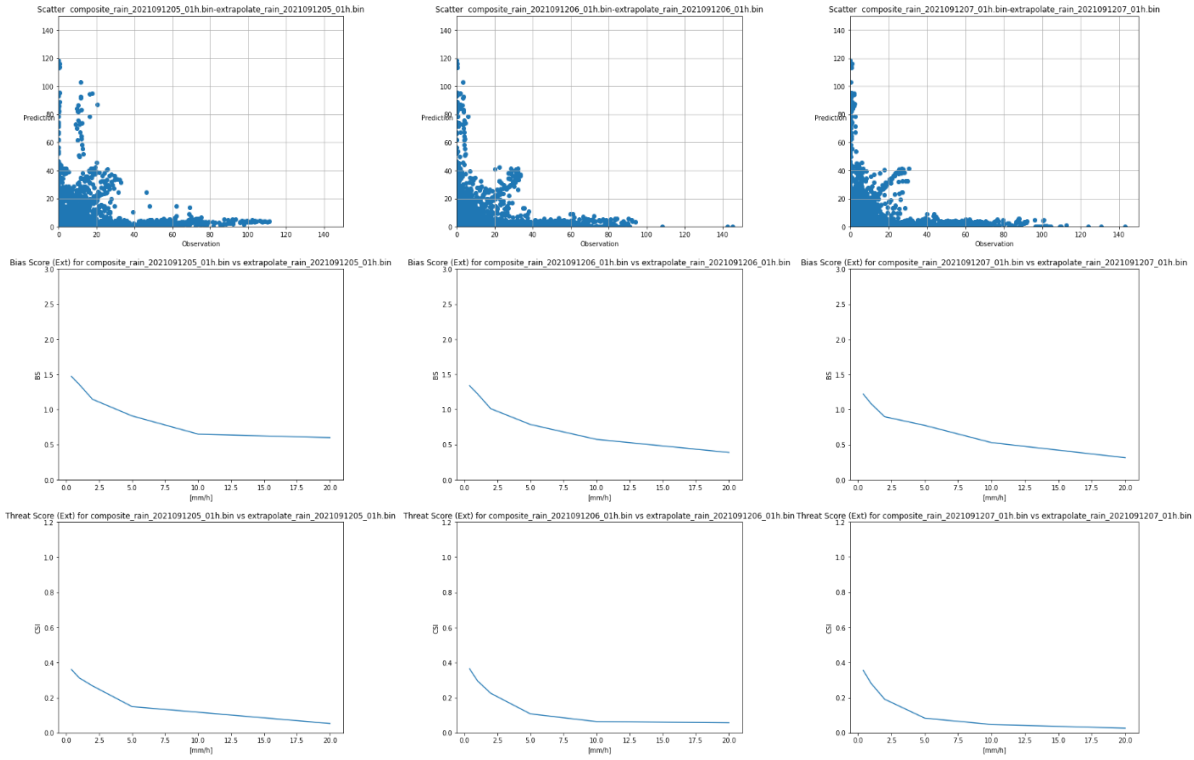

Figure 19. Same as Figure 18 but for 05 to 07 UTC (FT = 4 to 6).

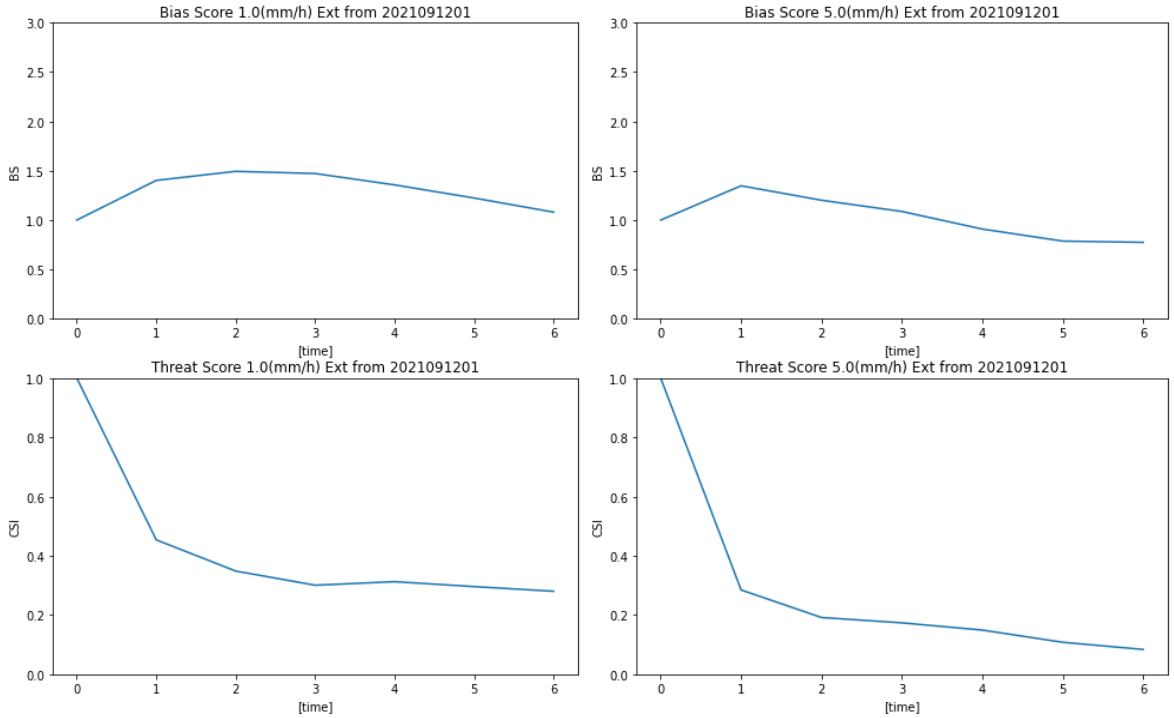

Figure 20. Same as Figure 10 but for extrapolated rains.

5. Merge with NWP

5.1. Regional NWP at NCHMF

At NCHMF of VNMHA, 72-hour forecasts by a regional NWP model (WRF-ARW) with a horizontal resolution of 3 km are conducted operationally four times a day. The initial condition is prepared by 3D-VAR at 00, 06, 12, and 18 UTC, assimilating observations (SYNOP) in Vietnam and NCEP observation data (PREPBUFR), whose first guess is given

by a 6-hour assimilation cycle (WRF3kmIFS-DA). The lateral boundary condition is given by the ECMWF's global forecast model (IFS). Due to the data latency of IFS forecasts, the WRF 3 km uses IFS forecasts from the previous 12UTC for 00 and 06 UTC forecasts, and IFS forecasts from the previous 00 UTC for 12 and 18 UTC forecasts. For the 00 UTC initial forecast, the data assimilation starts at 04 UTC, the forecast starts at 05 UTC, and computation and post-processing end at around 0630 UTC.

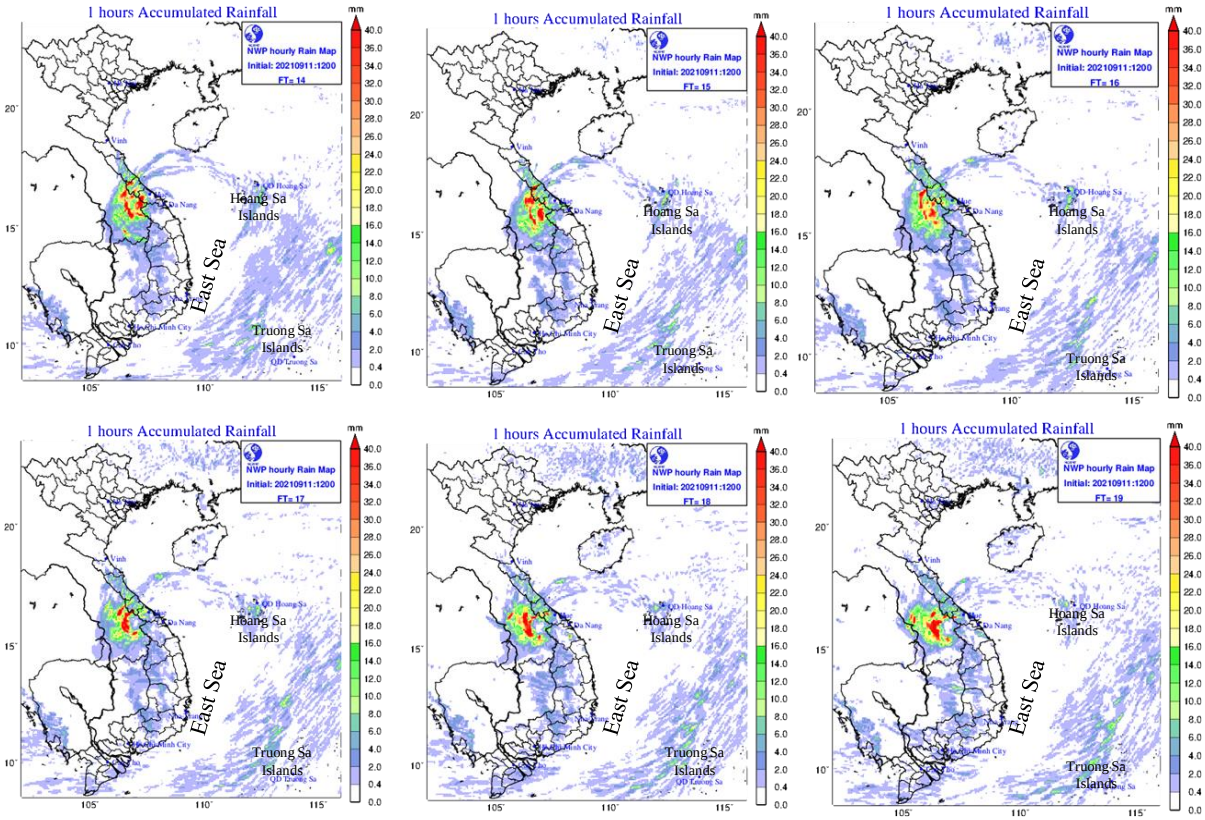

Figure 21. Hourly precipitation forecast by WRF3kmIFS-DA for 02 to 07 UTC, 2021 September 12.

Considering the timing to obtain the forecast of WRF3kmIFS-DA, we assume that for 00 UTC's VSRFP, we use WRF3kmIFS-DA whose initial time is 12 UTC of the day before. For the development of the VSRFP system, we re-ran WRF3kmIFS-DA from 12 UTC, 2021 September 11 with hourly outputs of the precipitation data. Figure 21 shows the hourly precipitation forecast by WRF3kmIFS-DA for 02 to 07 UTC (FT = 14 to 19), 2021 September 12. Comparing the corresponding rainfall analysis (Figure 6), intense rains overestimated by satellite are not seen over the sea in NWP-predicted rains. Scatter plot and verification scores for 01 UTC to 07 UTC (FT = 13 to 19 from 12 UTC the day before) against the rainfall analysis are shown in Figures 22 and in 23. The correlation between the analysis and NWP is not as good as extrapolation for early time ranges. The bias scores of NWP are around 1.0 for weak rains, but it decreases for intense rains after 05 UTC. Since this verification does not allow any positional lags in the computation of the scores, threat scores for intense rains are very small.

Figure 24 shows the time evolution of bias scores (upper) and threat scores (lower) of NWP for 1 mm/h and 5 mm/h rainfall intensity. Both bias and threat scores of NWP are relatively flat. For 1 mm/h, bias scores are around 1.0 and threat scores are around 0.2. For 5 mm/h, bias scores are in the range of 0.5 to 1.0 but threat scores are around 0.1 after FT = 3.

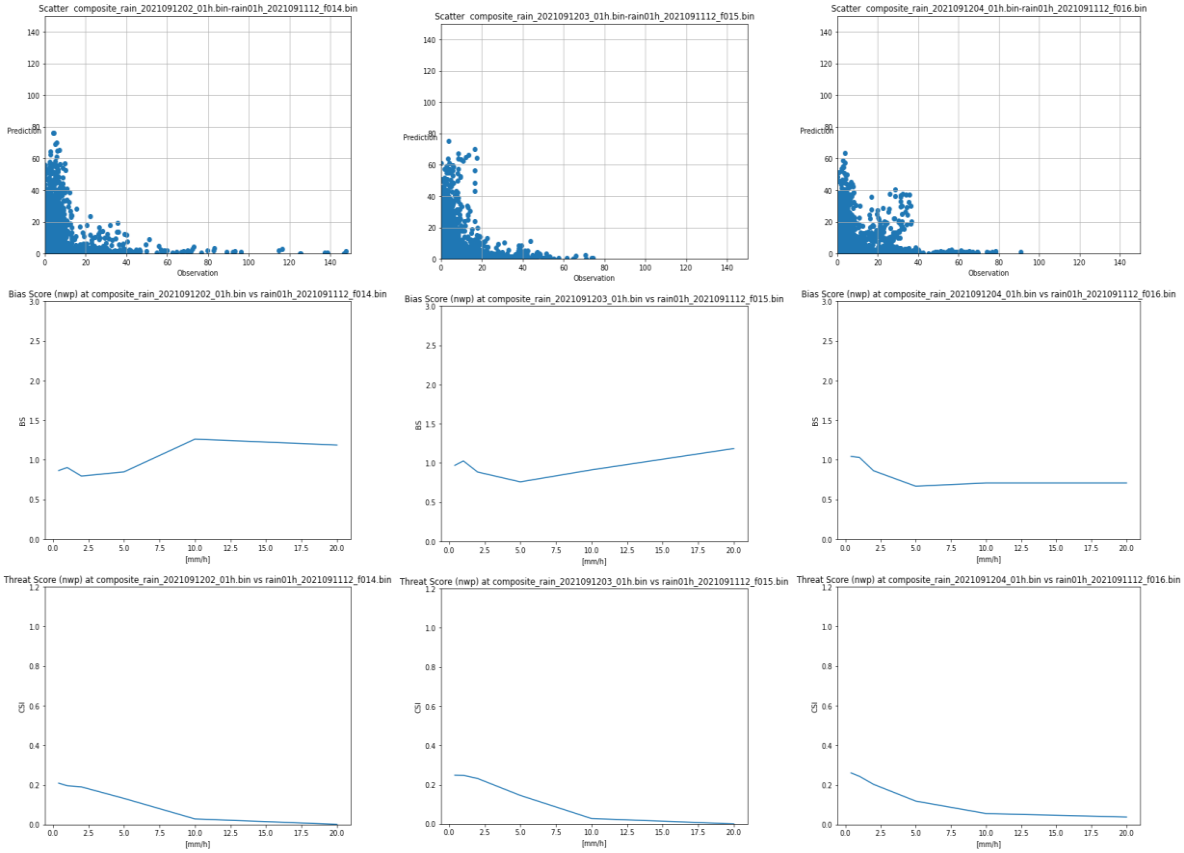

Figure 22. Same as Figure18 but for NWP rains for 02 to 04 UTC (FT = 14 to 16 from 12 UTC of the day before).

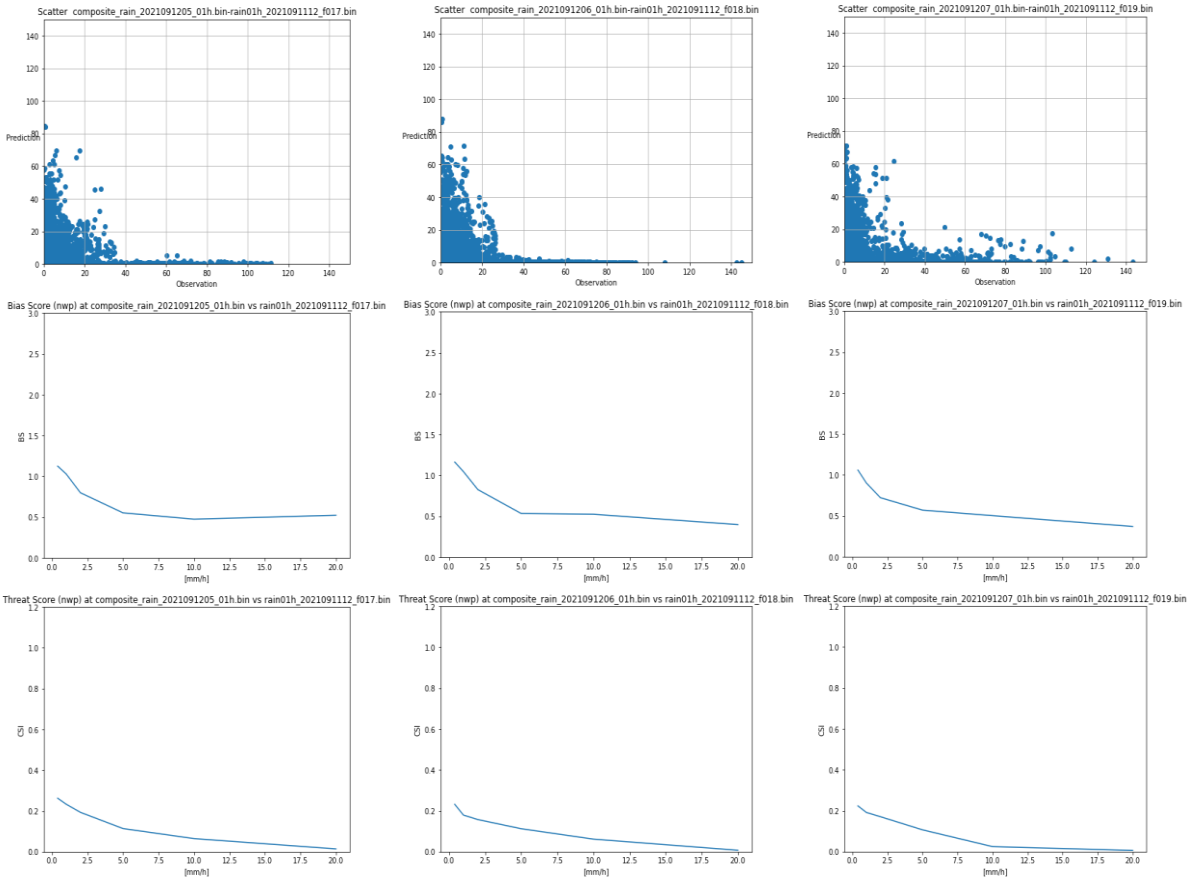

Figure 23. Same as Figure 22 but for 05 to 07 UTC (FT=17 to 19 from 12 UTC of the day before).

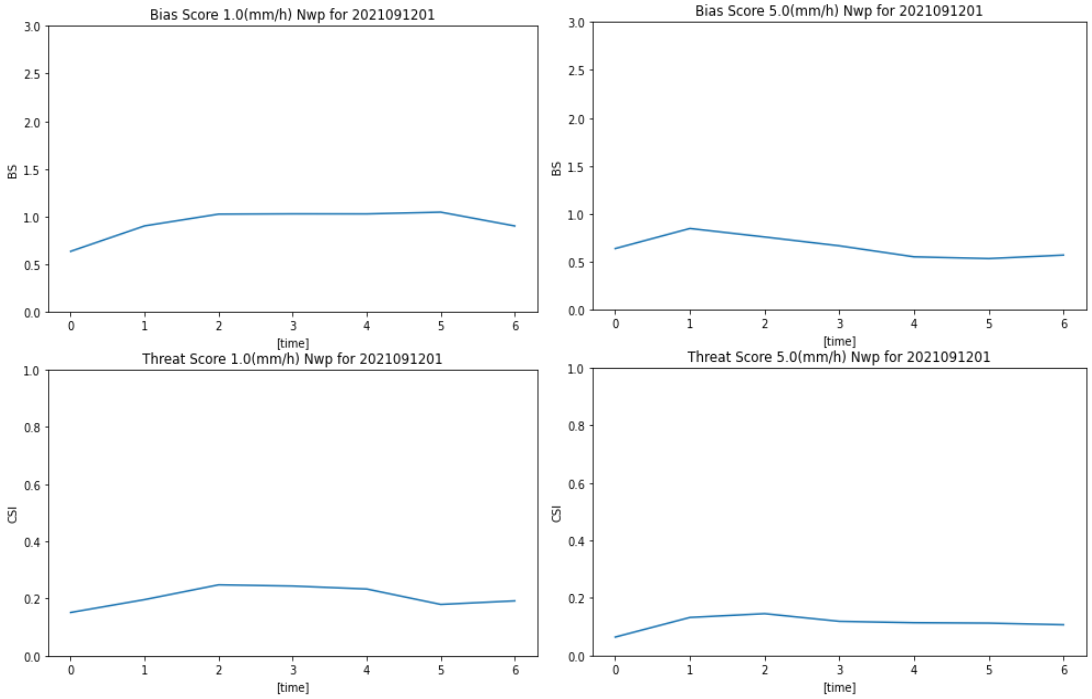

Figure 24. Same as Figure 20 but for NWP rains by WRF3kmIFS-DA.

5.2. Merge of extrapolated rains and NWP

As the development of a very short-range forecast of precipitation system (Figure 1), we merged kinematically extrapolated precipitation rainfall with NWP model-predicted rainfall by the WRF3kmIFS-DA. The merged intensity (Mrg) is given by a weighted mean of kinematic extrapolation (Exp) and numerical weather prediction (Nwp):

$$\mathrm{Mrg} = \mathrm{Exp} \times w + \mathrm{Nwp} \times (1 - w) \quad (5)$$

where w is the weight parameter. In JMA's VSRFP, the magnitude of w is dynamically determined based on the local accuracy of NWP (Figure 25).

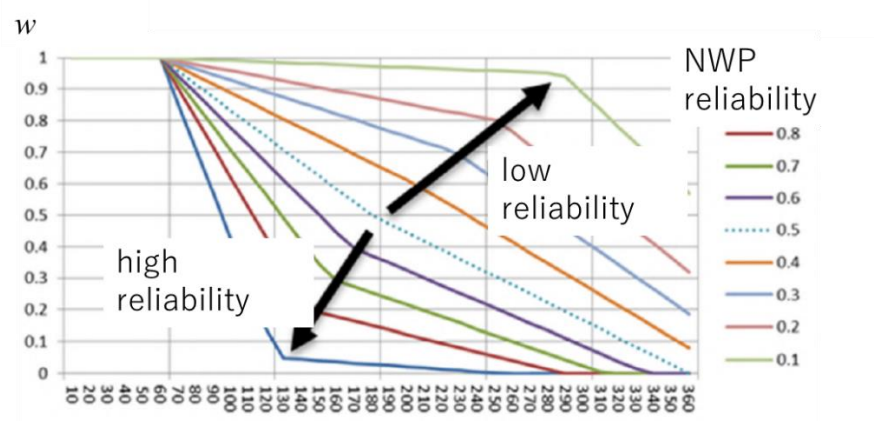

Figure 25. Weight parameter in JMA7s VSRFP. Reproduced from Tsujimura (2019) [8].

Here, the NWP reliability is determined by the ratio of NWP and Extrapolation scores (for detail, see [8]). In our prototype system, we reduced the weight parameter w linearly from 1.0 at FT = 2 to 0.0 at FT = 6 for simplicity, i.e., 0.75 at 04 UTC (FT = 3), 0.5 at 05 UTC (FT = 4) and 0.25 at 06 UTC (FT = 5). This procedure roughly corresponds to assuming the NWP reliability around 0.4. As shown in Figure 26, the merged rains are identical to the extrapolation until FT = 2, and then gradually approach NWP rains from FT = 3 to 5, and finally agree with NWP at FT = 6.

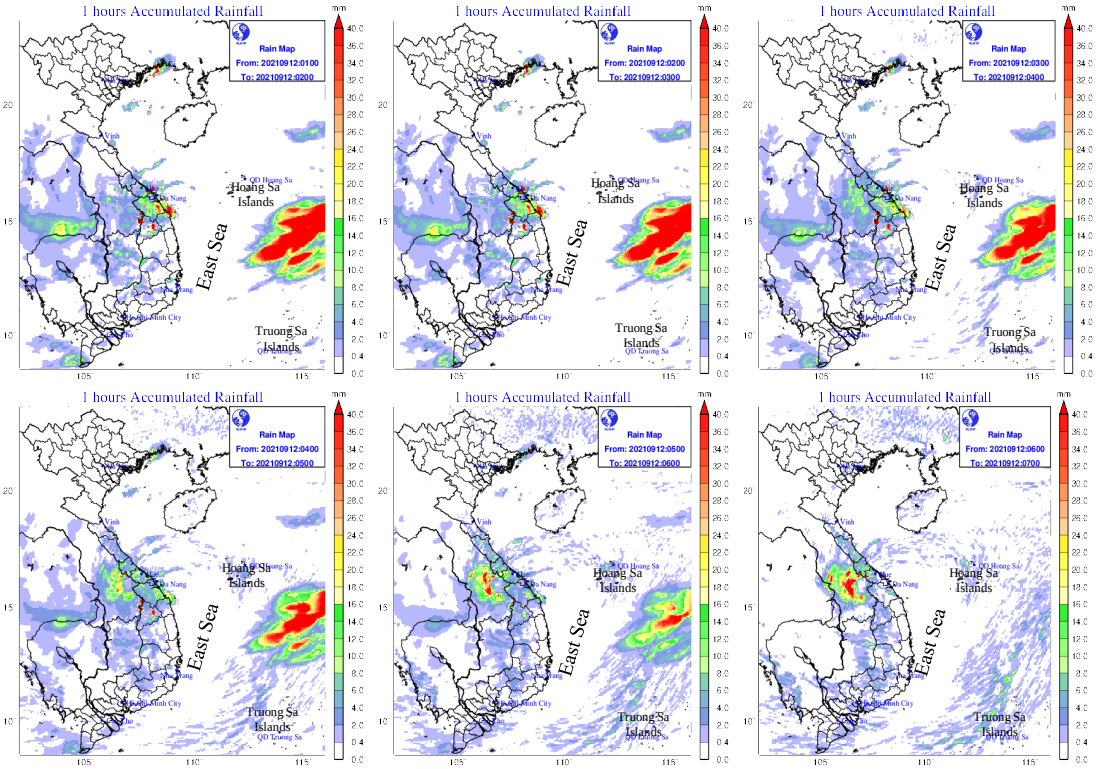

Figure 26. Same as Figures 15 and 18 but by very short-range forecast of precipitation.

Figure 27 shows the scatter plot and verification scores of merged rains at 04, 05 and 06 UTC (FT = 3 to 5) against the rainfall analysis. The bias scores of merged rains are slightly larger than extrapolation or NWP for weak rains but smaller for intense rains. This is due to the weighted averaging of two values, which moderates intense rains. Threat scores are better than extrapolation for weak rains. This improvement is attributable to the effect of the ensemble mean in the weighted average.

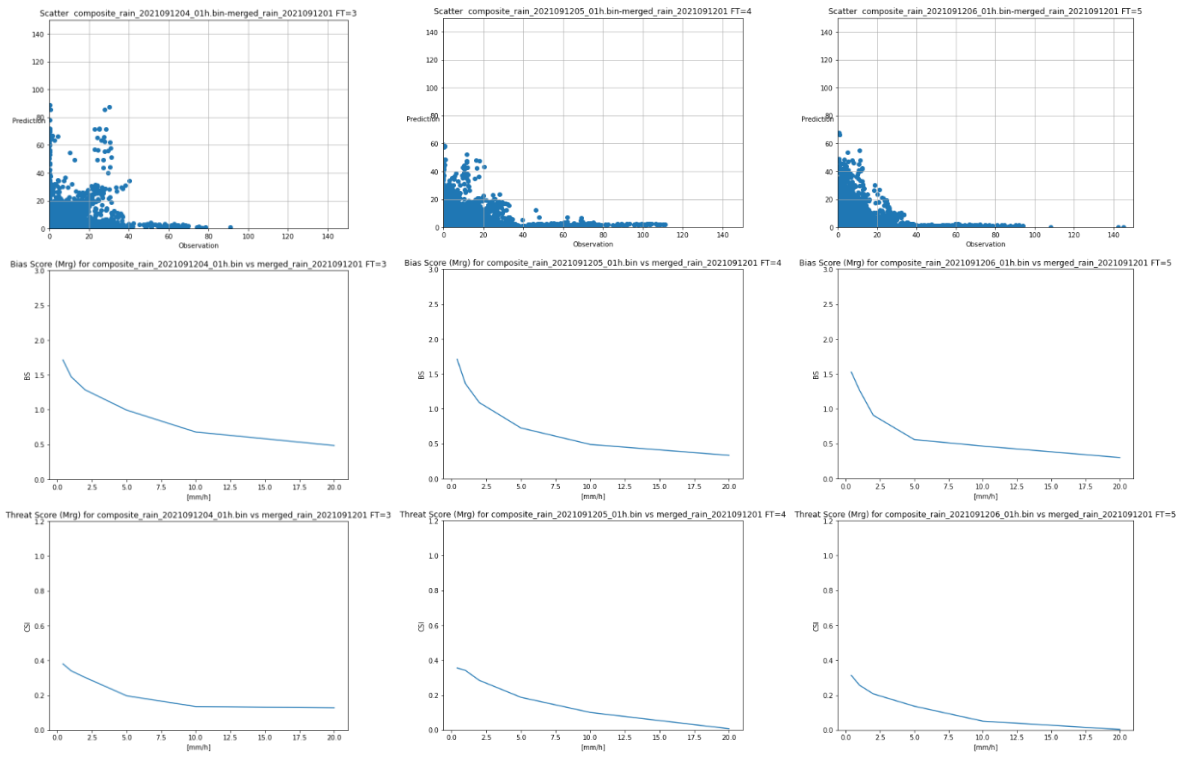

Figure 27. Same as Figure 17 but for VSRFP for 04 to 06 UTC (FT = 3 to 5).

Figure 28 shows the time evolution of bias scores (upper) and threat scores (lower) of merged rains for 1 mm/h and 5 mm/h intensities. Bias scores for 1 mm/h are almost the same as an extrapolation and larger than NWP. Threat scores for 1 mm/h are better than extrapolation for FT = 3 and 4, and better than NWP for all time ranges. Threat scores for 5 mm are better than both extrapolation and NWP for all time ranges.

5.3. Verification for the different initial time

In the former subsections, we computed the lag correlation between the two composited hourly rainfall distributions at 00 and 01 UTC and extrapolated the rains from 02 to 07 UTC. To check the performance of this system for a different initial time, we conducted similar lag correlation procedures for two composited rain fields at 01 and 02 UTC, and extrapolated the rain fields at 02 UTC for 03 to 08 UTC. As for NWP forecast, forecast from the same NWP whose initial time of 12 UTC 11 September was used (FT = 15 to 20).

Figure 29 indicates time evolution of threat scores of extrapolations (upper) and merged rains (lower) for FT = 0 to 6 (02 to 08 UTC) for 1 mm/h (left) and 5 mm/h (right) rainfall intensity. The same tendencies as in the initial time of 01 UTC were obtained; for 1 mm/h merged rains were better than extrapolation at FT = 3 and 4, and for 5 mm/h merged rains were better than extrapolation at after FT = 3-time ranges.

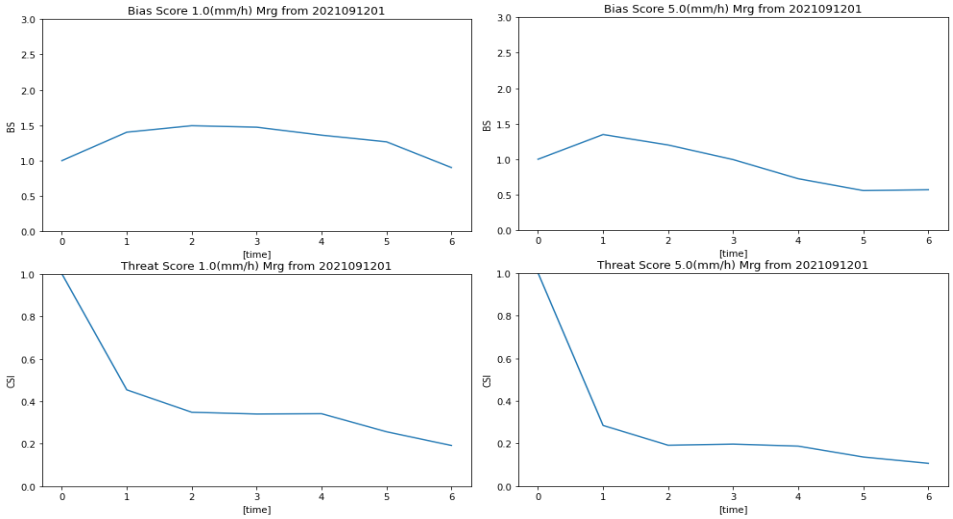

Figure 28. Same as Figure 20 but by VSRFP.

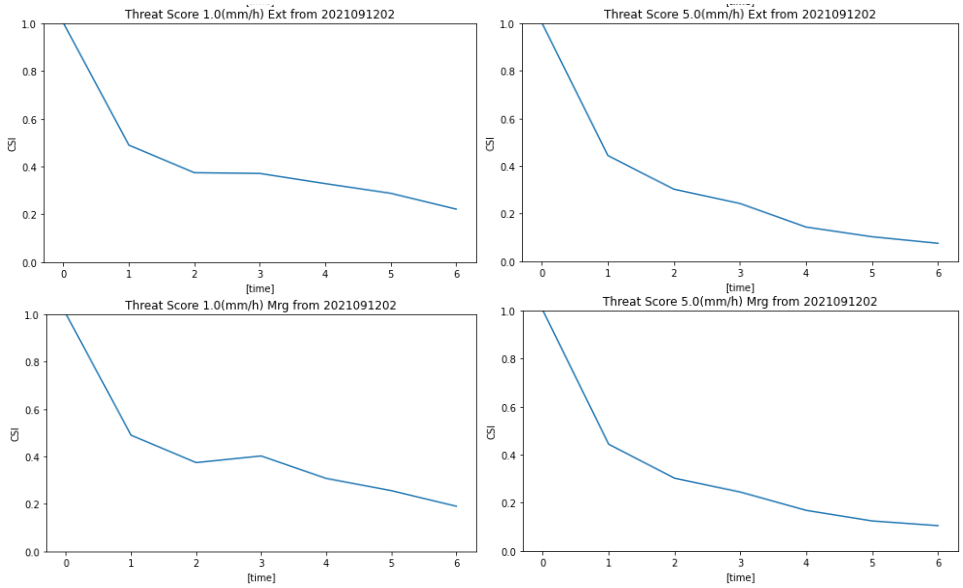

Figure 29. Upper) Time evolution of threat scores of extrapolations from 02 UTC to 08 UTC for FT = 0 to 6 for 1 mm/h and 5 mm/h rainfall intensity threshold against rainfall analysis. Lower) Same as in upper panels but by VSRFP.

6. Summary and concluding remarks

Toward the very short-range forecast of precipitation, we prepared a one-hour composite rainfall analysis using AWS, radar, and satellite data for the case of heavy rainfall event over central Vietnam on 11 to 13 July 2021. Moving vectors of rainfall area were estimated by computing lag correlation coefficients in the template between the two rainfall distributions at 00 and 01 UTC, and the indexes which maximize the lag correlation were interpolated to the original grid of 5 km. Quality control of the moving vectors was made by checking the consistency between the moving directions and NWP winds at 700 hPa level. Extrapolated rains were merged with rainfall forecast by VNMHA's operational NWP (WRF3kmIFS-DA), with a weight function which increases the weight of NWP linearly from FT = 2 to FT = 6. Merged rainfall outperformed extrapolation at least weak to moderate rains such as 1 and 5 mm/h.

In this paper, we selected a heavy rainfall case in July 2021 brought by a weak tropical cyclone which slowly approached central Vietnam. Different from mid-latitude synoptic disturbances which move eastward by the prevailing westerly, the major rainfall areas did not move eastward and stalled over the central Vietnam, though individual clouds around the tropical cyclone rotate counterclockwise. Generally, if the major rainfall area is advected by synoptic winds, the performance of the persistency is soon deteriorated, however in this case, the persistency kept its performance, and the extrapolation did not clearly outperform the persistency. More cases need to be studied to show the advantage of extrapolation based on the lag correlation method. In this first trial, we applied a simple linear method for extrapolation to detect the upstream point. Recently, [18] proposed a new method for cell tracking, where the cross-correlation method is used to obtain average moving vectors and the optimal over lapping area method is applied to modify the vector for each cell motion. A more sophisticated method may improve the performance of kinematic extrapolation. In the merger process, we used a simple linear function for weight parameters. As in the JMA's VSRFP system [8], there is room for much improvement in this approach as well.

As shown in threat scores, the precipitation forecast by WRF3kmIFS-DA was not necessarily good in this case. If the performance of NWP improved, the merit of a merger should become larger. As additional tests, by considering the data latency at the timing of 01 UTC (and 02 UTC), we used the NWP forecast whose initial time is 12 UTC of the day before (11 July 2021) for the merger process. This means that NWP forecasts with FT = 16 to 19 (17 to 20) were used. Supposing an operational time schedule, where the computation and post processing ends at around 6.5 hours later from the initial time, we can use the 18 UTC initial forecast after 02 UTC. In the near future, we will test the use of the latest NWP forecasts in the daily operational test.

Author Contributions: Author Contributions: Conceptualization, K.S.; methodology, K.S.; validation, K.S., M.K.H.; AWS data curation, M.K.H., K.S.; Radar data curation, M.K.H., K.S.; Satellite data curation, M.K.H., K.S.; NWP data curation, M.K.H., K.S.; writing–original draft preparation, K.S.; writing–review and editing, D.D.T., M.K.H.; supervision, D.D.T.; project administration, K.S., D.D.T.; All authors have read and agreed to the published version of the manuscript.

Funding: This research was performed under the Japan International Cooperation Agency (JICA) Project for "Strengthening Capacity in Weather Forecasting and Flood Early Warning System in the Social Republic of Vietnam". Kazuo Saito was partly supported by Grant-in-Aid for Scientific Research (C) (21K03657K; Study on the mechanisms of the pre-typhoon precipitation enhancement) from the Japan Society for the Promotion of Science (JSPS). Mai Khanh Hung and Du Duc Tien were sponsored by the Ministry of Natural Resources and Environment (intervention code TNMT.2022.06.02, title of the project "Research and innovate technology to the quantitative forecast of precipitation due to typhoon, tropical

depressions by high-resolution numerical model combining data assimilation of radar, satellite, surface and upper-air observations").

Acknowledgments: The authors thank Nguyen Vinh Thu and Mai Van Khiem of the Viet Nam Meteorological and Hydrological Administration, Kenji Akaeda, leader of JICA team, and Michihiko Tonouchi, Kiichi Sasaki of the Japan Meteorological Business Support Center (JMBSC) for their support on the JICA project. Thanks are extended to Yasutaka Makihara of JMBSC for their comments on the kinematic extrapolation of rainfall areas. Comments by two anonymous reviewers improved the quality of this paper.

Conflicts of Interest: The authors declare no conflict of interest.

References

1. Tonouchi, M.; Kasuya, Y.; Tanaka, Y.; Akatsu, K.; Akaeda, K.; Nguyen, V.T. Activities of JICA on disaster prevention and achievement of JICA project in Period 1. *VN J. Hydrometeorol.* **2020**, *5*, 1–12. Doi:10.36335/VNJHM.2020(5).1-12.
2. Mikami, M.; Ichijo, H.; Matsubara, M.; Nguyen, H.A.; Duc, L.X. A proposal of AWS maintenance and periodic calibration tools and installation of ARGs for Radar QPE calibration. *VN J. Hydrometeorol.* **2020**, *5*, 13–35. Doi: 10.36335/VNJHM.2020(5).1-35.
3. Kimpara, C.; Tonouchi, M; Hoa, B.T.K.; Hung, N.V.; Cuong, N.M.; Akaeda, K. Quantitative precipitation estimation by combining rain gauge and meteorological radar network in Vietnam. *VN J. Hydrometeorol.* **2020**, *5*, 36–50. Doi:10.36335/VNJHM.2020(5).36-50.
4. Saito, K.; Hung M.K.; Hung N.V.; Vinh N.Q.; Tien D.D. Heavy rainfall in central Viet Nam in December 2018 and modification of precipitation analysis at VNMHA. *VN J. Hydrometeorol.* **2020**, *5*, 65–79. Doi:10.36335/VNJHM.2020(5).65-79.
5. Hung, M.K.; Saito, K.; Khiem, M.V.; Tien, D.D.; Hung, N.V. Verification of GSMaP data in precipitation nowcasting at Vietnamese National Center for Hydro-Meteorological Forecasting. *VN J. Hydrometeorol.* **2020**, *5*, 80–94. Doi: 10.36335/VNJHM.2020(5).80-94.
6. Kigawa, S. Analysis and forecasting techniques of high-resolution precipitation nowcasting. *Sokko-jiho* **2014**, *81*, 55–76. Available online: https://www.jma.go.jp/jma/kishou/books/sokkou/81/vol81p055.pdf. (In Japanese)
7. Saito, K.; Makihara, Y. On the very short range forecast of precipitation at JMA. *J. Water Env. Japan* **2007**, *30(5)*, 230–235. Available online: https://www.jswe.or.jp/publications/journals/contents/2007/index.html) (In Japanese)
8. Tsujimura, Y. Modification of very short range forecast of precipitation. *Forecasting Technology Training Textbook, JMA* **2019**, *24*, 146–153. Available online at https://www.jma.go.jp/jma/kishou/books/yohkens/24/chapter7.pdf. (In Japanese)
9. Li, P.W.; Wong, W.K.; Cheung, P.; Yeung, H.Y. An overview of nowcasting development, applications, and services in the Hong Kong Observatory. *J. Meteor. Res.* **2014**, *28*, 859–876. Doi:10.1007/s13351-014-4048-9.
10. Japan Meteorological Agency website. https://www.jma.go.jp/jma/kishou/know/bosai/riskmap.html.
11. World Meteorological Organization. WMO guidelines on multi-hazard impact-based forecast and warning services. WMO No.1150. 2015, pp. 34. ISBN: 978-92-63-11150-0.
12. Kobayashi, R.; Duc, L.X.; Tien, P.M. Attempt to detect maintenance-need rain gauge station by double–mass analysis. *J. Hydro-Meteorol.* **2023**, *15*, 10–20.

13. Vicente, G.; Scofield, R.A.; Mensel, W.P. The operational GOES infrared rainfall estimation technique. *Bull. Amer. Meteor. Soc.* **1998**, *79*, 1881–1898. Doi:10.1175/1520-0477(1998)079<1883:TOGIRE>2.0.CO;2.
14. Rinehart, R.E.; Garvey, E.T. Three-dimensional storm motion detection by conventional weather radar. *Nature* **1978**, *273*, 287–289.
15. Hamada, T. Cloud wind estimation system summary of GMS system. *Tech. Note Meteor. Satt. Cent.* **1979**, *II–2*, 14–42.
16. Takano, I.; Saito, K. Statistical analyses of wind field obtained from short interval VISSR observations. *Tech. Note Meteor. Satt. Cent.* **1986**, *14*, 29–37.
17. Tavolate, C.; Isaksen, L. On the use of a Huber norm for observation quality control in the ECMWF 4D-Var. *Quart. J. Roy. Meteor. Soc.* **2015**, *141*, 1514–1527. Doi:10.1002/qj.2440.
18. Shimizu, S.; Ueda, H. Algorithm for the identification and tracking of convective cells based on constant and adaptive threshold methods using a new cell-merging and - splitting scheme. *J. Meteor. Soc. Japan* **2012**, *90*, 869−889. Doi:10.2151/jmsj.2012-602.

JOURNAL OF
HYDRO-METEOROLOGY

Research Article

Development of mobile services for weather observation information

Hiroyuki Ichijo[1]*, Ngo Van Manh[2], Vuong Minh Phuong[2], Nguyen Viet Huy[2], Phan Vu Thanh Nhan[3]

[1] Japan Meteorological Business Support Center; ichijo@jmbsc.or.jp
[2] Viet Nam Meteorological and Hydrological Administration; manh.ngovan@gmail.com; vuong.mphuong@gmail.com; viethuy076@gmail.com
[3] Earth System Science Co., Ltd (ESS); thanhnhan1211@gmail.com

*Corresponding author: ichijo@jmbsc.or.jp; Tel.: +81−8021673647
Received: 2 March 2023; Accepted: 01 April 2023; Published: 25 April 2023

Abstract: NCHMF and JICA team decided development of mobile services as an activity of the JICA Project. The mobile service system displays the data of Automatic Rain Gauge (ARG) stations, radars and meteorological satellites and the extreme weather warning messages disseminated from the system are aimed at users nationwide. The system is designed using modern technologies with high stability to meet the technical requirements of the project. The system's database is MongoDB, which is flexible in storing different data sizes. The user interfaces of both the website and mobile app are programmed using React (ReactJS and ReactNative). The system is designed with two servers connected in a cluster, so it has high stability. Alerts are delivered to users quickly using push notification technology, suitable for personal computers and iOS and Android mobile devices. The system is in line with the trend of Vietnamese people using mobile devices to monitor weather information today. Therefore, this will be an effective source of extreme weather warnings that VNMHA can use.

Keywords: Radar; Meteorological satellite; Weather observation information.

1. Introduction

In late years, disaster damages by severe weather increases rapidly in Vietnam. Especially heavy rain and the flood caused a serious situation for people's life. To prevent the serious damages weather Warnings and flood alerts must be quickly delivered to the people in the correspond area in addition to provision of understandable weather information. When we think about how to deliver information, mobile users are increasing day by day. More and more applications (apps) are continuously launching every day. In the year 2019, there were approximately 2.6 million Android apps and 2.2 million iOS apps available for users in the world. National Centre for Hydro-Meteorological Forecasting (NCHMF) and the Japan International Cooperation Agency (JICA) team considered the necessity to improve warning delivery and weather information provision and taking the opportunity of the mobile service trend. Then they decided on the development of mobile services as an activity of the JICA Project. The target information was observation data from weather radar, Automatic Rain Gauge (ARG), and satellite, in addition to forecast and warnings.

The development has been carried out mainly by Working Group 4 of the JICA Project and a contractor since December 2020. There were several processes, such as technical research, system design, prototyping and developing individual functions, functional test and

verification, and comprehensive evaluation for operation. Then the development was mostly completed in December 2022 despite delay due to COVID-19.

2. Materials and Methods

2.1. Description of study area

The mobile service system displays the data of ARG stations, radars, and meteorological satellites. While ARG stations installed in the project are concentrated in the Northeast and North Central regions, radar and satellite images are spread throughout Vietnam. The extreme weather warning messages disseminated from the system are aimed at users nationwide. Therefore, the database in the system is designed to target the entire territory of Vietnam in the display. This is an advantage, i.e., there is no need to modify the system when the data from other ARG stations are provided for the system.

The system processes and displays four types of input data, i.e., observation data of weather radar, ARG and meteorological satellite, and extreme weather forecast and warnings. These data are quite diverse such as from real-time monitoring to forecast, from time series to grid form, and from coded to unstructured. A few software modules below the service layer have been built to ensure the integration and conversion of data to suit the system so that data can be displayed to users quickly and conveniently.

2.2. Development conditions

The system development process is related to several units in the Viet Nam Meteorological and Hydrological Administration (VNMHA). The roles of the units during the system development are as follows:

- Hydro-Meteorological Information and Data Center (HMIDC) is a centralized data and equipment management unit for the system. The unit advises on technical solutions so that the system can be connected to the existing information systems of the VNMHA.
- Aero Meteorological Observatory (AMO) is a unit that provides radar data and manages data of ARG stations used in the radar data calibration algorithm. The unit advises solutions on data display to suit users.
- NCHMF is the unit that provides extreme weather forecast and warning bulletins.
- Northeast and North central regional HMSs are units directly managing ARG stations located in the field.

The system was developed to provide operational services for quickly and conveniently receiving observation and warning information on mobile devices with different screen sizes and operating systems. The main requirements for the system are as follows:

- Timely data dissemination: observed data must be displayed in real-time, and dangerous weather warnings must be quickly distributed to users by data push technology.
- Easy access by widespread mobile users: the system must consist of a mobile website and mobile apps for iOS and Android devices with a friendly interface and easy-to-use concepts.

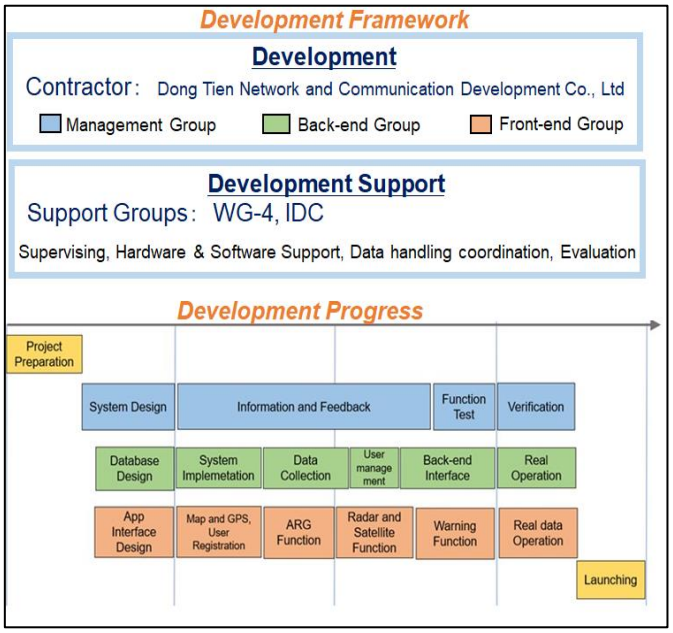

Figure 1. Mobile services system development diagram.

- Easily understandable visualization: it is required that data can be displayed in tabular, graph and map form, and station map and grid data must be displayed on top of the base map and be able to represent animation as well as perform operations to zoom in and out.

Based on the requirements, the system was developed under the collaboration framework shown in Figure 1.

2.3. Materials

Since the input data differs in format and data source, they need to be analyzed and processed separately.

2.3.1. Radar data

The input radar data are stored in NetCDF format [1]. Figure 2 shows an example of parameters of a data file in NetCDF format. This common format makes it convenient to share and store meteorological data.

```
dimensions:
        latitude = 1600 ;
        longitude = 1100 ;
        time = UNLIMITED ; // (1 currently)
variables:
        double latitude(latitude) ;
                latitude:units = "degrees_north" ;
                latitude:long_name = "latitude" ;
        double longitude(longitude) ;
                longitude:units = "degrees_east" ;
                longitude:long_name = "longitude" ;
        double time(time) ;
                time:units = "seconds since 1970-01-01 00:00:00.0 0:00" ;
                time:long_name = "verification time generated by wgrib2 function verftime()" ;
                time:reference_time = 1673595600. ;
                time:reference_time_type = 1 ;
                time:reference_date = "2023.01.13 07:40:00 UTC" ;
                time:reference_time_description = "analyses, reference date is fixed" ;
                time:time_step_setting = "auto" ;
                time:time_step = 0. ;
        float var0_1_200_surface(time, latitude, longitude) ;
                var0_1_200_surface:short_name = "var0_1_200_surface" ;
                var0_1_200_surface:long_name = "desc" ;
                var0_1_200_surface:level = "surface" ;
                var0_1_200_surface:units = "unit" ;

// global attributes:
                :Conventions = "COARDS" ;
                :History = "Fri Jan 13 14:55:41 2023: ncatted -a _FillValue,var0_1_200_surface,d,f,0.0 rdr_202301130740.nc\n",
                        "Fri Jan 13 14:55:41 2023: ncatted -a _FillValue,var0_1_200_surface,o,f,0.0 rdr_202301130740.nc\n",
                        "created by wgrib2" ;
                :GRIB2_grid_template = 0 ;
                :NCO = "netCDF Operators version 4.7.5 (Homepage = http://nco.sf.net, Code = http://github.com/nco/nco)" ;
```

Figure 2. Parameters of a radar data file in NetCDF format.

To display radar data (NetCDF format) into the website, we use a technique to convert this data to GeoTiff format [2], this format helps display radar on the website. We use a script module to download and convert data from NetCDF format to GeoTiff format.

2.3.2. ARG data

ARG data from stations are transmitted to a centralized server in text file format shown in Figure 3, with 2 frequencies of 10 minutes and 1 hour, each station has one data file equivalent to each frequency. The system has collected these data and put them into a decoding module to extract the corresponding rain values and put them into the database. During the processing, the total daily rainfall has been calculated by the system to display result statistics.

```
171569  00010,6,14.20.00,13,01,2023,0,M02,2,B,0.0,2,X,12594,#15
171570  00010,6,14.30.00,13,01,2023,0,M02,2,B,0.0,2,X,12594,#15
171571  00010,6,14.40.00,13,01,2023,0,M02,2,B,0.0,2,X,12594,#15
171572  00010,6,14.50.00,13,01,2023,0,M02,2,B,0.0,2,X,12594,#15
171573  00010,6,15.00.00,13,01,2023,0,M02,2,B,0.0,2,X,12594,#15
171574  00010,6,15.10.00,13,01,2023,0,M02,2,B,0.0,2,X,12594,#15
171575  00010,6,15.20.00,13,01,2023,0,M02,2,B,0.0,2,X,12594,#15
171576  00010,6,15.30.00,13,01,2023,0,M02,2,B,0.0,2,X,12594,#15
171577
```

Figure 3. Data text transmitted from an ARG station.

2.3.3. Satellite data

The satellite data used in the system are Himawari satellite data provided by the Japan Meteorological Agency (JMA). They are used at the VNMHA in several different formats shown in Table 1.

Table 1. Himawari Satellite data formats.

Data format	Data Source	Available at VNMHA in development progress
HSD	HimawariCloud	Yes
SATAID	HimawariCast	Yes
NetCDF	Central Data Hub	Not yet

HSD (Himawari Standard Data) format [3] is the original binary one provided through "HimawariCloud" which is a client-server network service operated by JMA. All other formats are converted from this format. Original data in HSD format are large in volume due to no clipping process. SATAID (Satellite Animation and Interactive Diagnosis) format is commonly used in desktop applications at the VNMHA. Data in SATAID format are provided to the VNMHA through "HimawariCast" which is a satellite broadcast system operated by JMA.

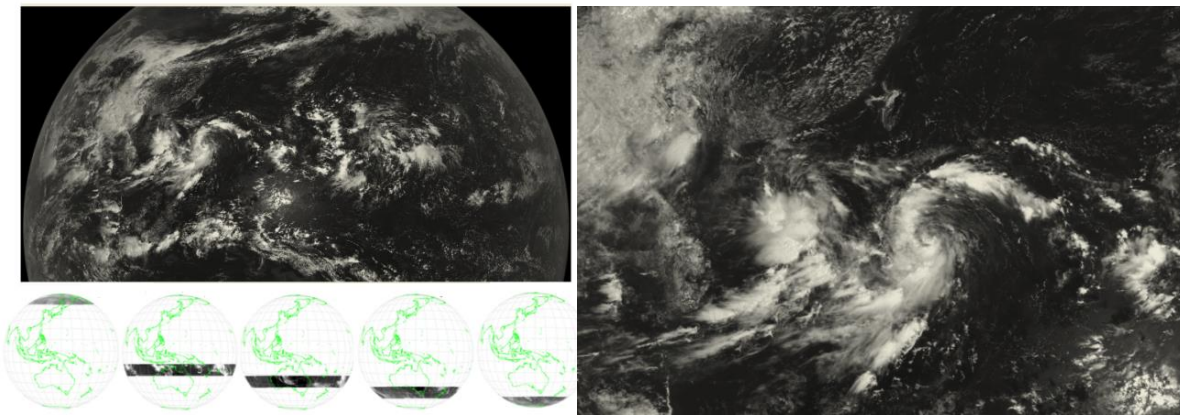

(a) **(b)**

Figure 4. Himawari satellite data: (a) HSD; (b) Data converted to Geotiff and clipped area.

The NetCDF format is a popular one for grid data worldwide. Therefore, the initial design of the system is to use input satellite data in NetCDF format. Another software module has been built to convert satellite data from HSD format to Geotiff format for display on the system. Figures 4 and 5 show the comparison between HSD and Geotiff formats in visual image, and the processing scheme of Himawari satellite data, respectively.

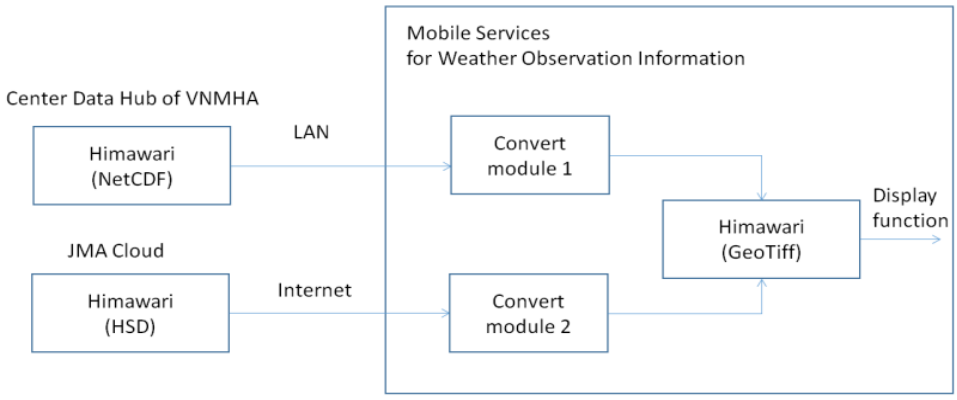

Figure 5. Processing scheme of Himawari satellite data in the system.

The system collects and processes two out of 16 bands of the Himawari satellite imagery, i.e., one visible band and one IR band. Because the system must rapidly provide local people with warnings at a high priority, other bands are not processed to reduce the system load.

2.3.4. Forecasts and warnings

Warnings provided through the system are generated based on two sources. The first source is created by local administrators registered on the website, and the second one is the extreme weather forecast and warning bulletins from NCHMF.

2.4. Methods

The system is designed using modern technologies, with high stability to meet the project's technical requirements. The system's database is MongoDB [4], which is flexible in storing different data sizes. Because it is stored as JSON [5], the system can easily insert the information as needed. The process to check compatibility when adding, deleting, or updating data for this type of database is quick and timesaving.

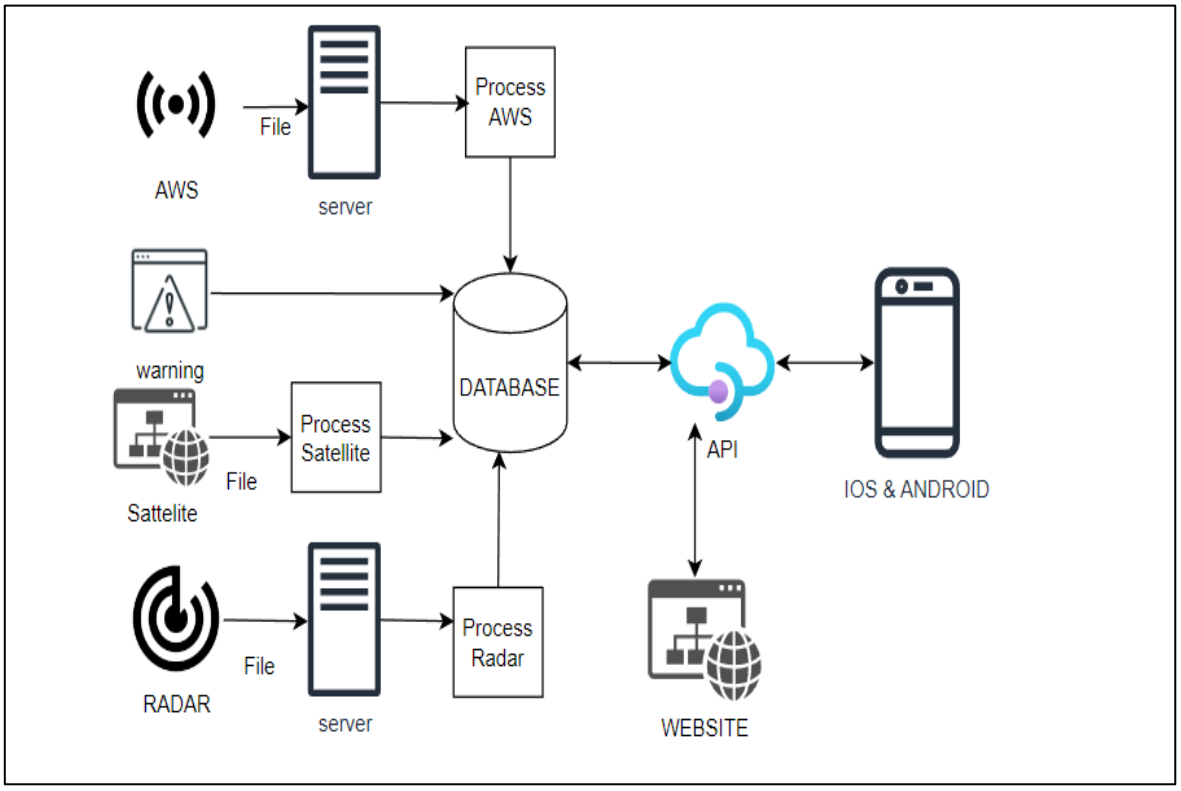

Figure 6. System functional diagram.

The system uses APIs to get data from the database provided to the website and mobile app as shown in Figure 6. The user interface of both the website and mobile app is programmed using React (ReactJS [6] and ReactNative [7]). This is a widely used framework today due to its many advantages such as flexibility, ease of maintenance due to modular architecture, high performance even with complex applications.

Two servers of the system (Worker Server 1 and 2) are connected and run Docker to form a cluster. The advantage of Docker Swarm is that it allows automatic routing and load balancing so that the application can operate with high stability. Figure 7 shows the system component based on two servers.

The system follows the user-friendly interface design concept. The system uses HTML5, CSS3, and JavaScript to move, resize, hide, and display elements based on the device. It is compatible with different operating systems and web browsers.

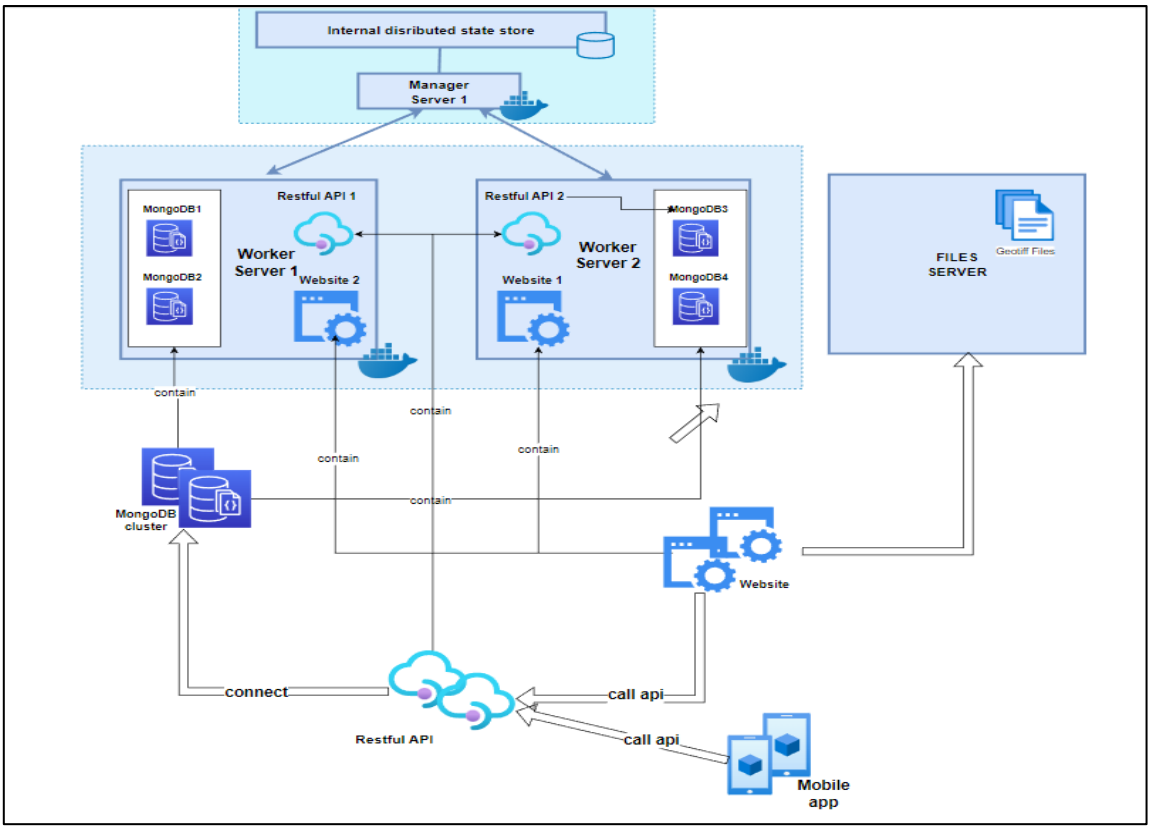

Figure 7. System component diagram.

3. Results and Discussion

3.1. ARG data display function

Rain data of ARG stations are automatically displayed as icons with numbers and colored according to warning scales. This makes it easy for users to track rain data during the day, and quickly identify areas with heavy rain, and can monitor the operating status of the station. Users can view detailed station information by pointing at the corresponding station icon. Precipitation data are displayed graphically at a frequency of 1 hour or 10 minutes. Figure 8 shows an example of ARG display.

The system also provides a detailed view of rainfall in the form of a table with a search function by a combination of station code, period, frequency, and total rainfall statistics, and warnings when the rainfall exceeds the threshold shown in Figure 9.

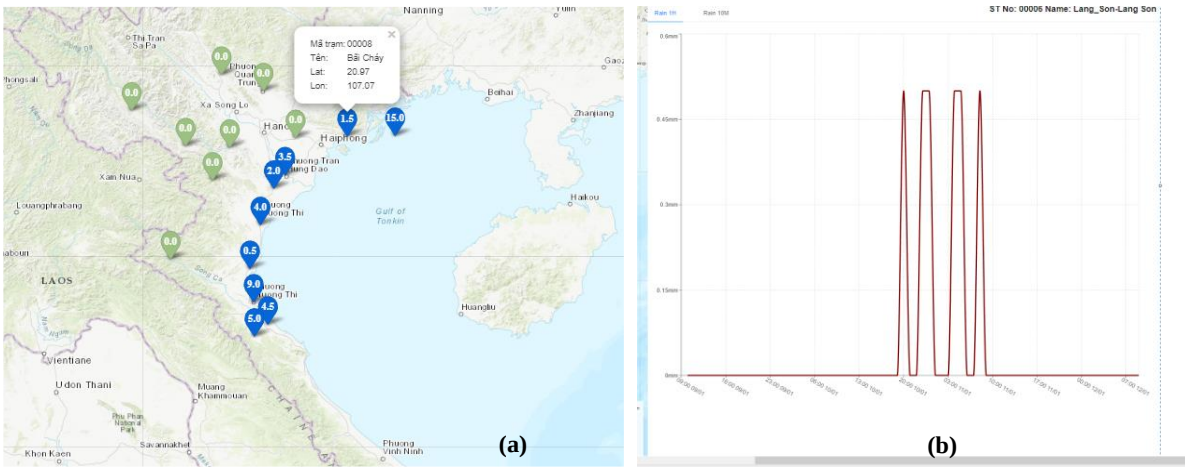

Figure 8. Precipitation display: (a) on the map; (b) graph mode.

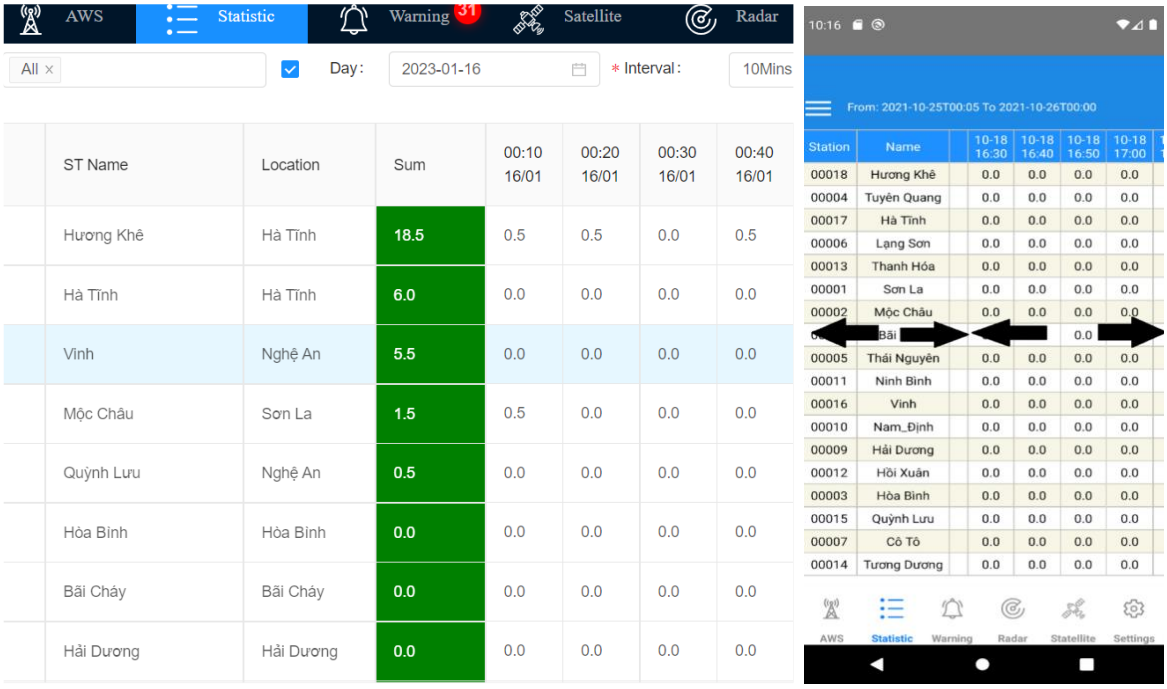

(a) **(b)**

Figure 9. ARG statistics interface: (a) on the website; (b) on the mobile app.

3.2. Satellite data display function

The system provides a viewing function of a real-time satellite cloud image in GeoTiff format, which can determine the data value of each point on the map as shown in Figure 10. Users have a view of a series of animated images or a single image, which can overlay the radar layer and/or ARG layer.

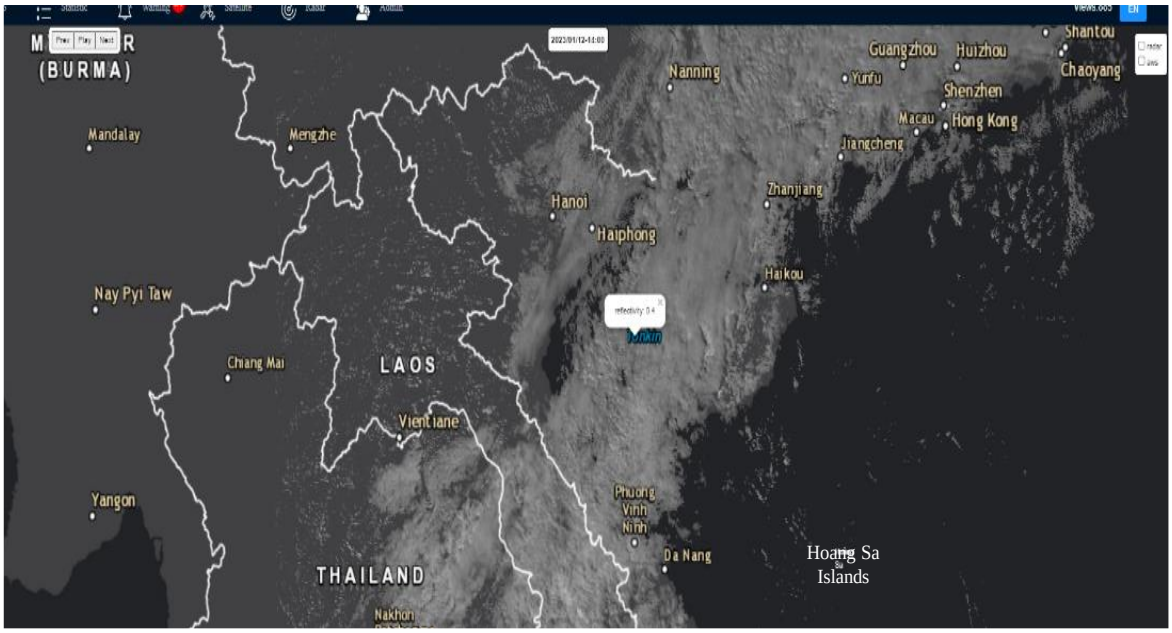

Figure 10. Himawari satellite image.

When in overlay mode, users can click a point to view both radar (estimated precipitation) and satellite (reflectivity) values and ARG stations which are automatically displayed as an icon with values and colors equivalent to the rain warning levels are easy to monitor as shown in Figure 11. Full-featured mobile app interface is similar to the mobile website.

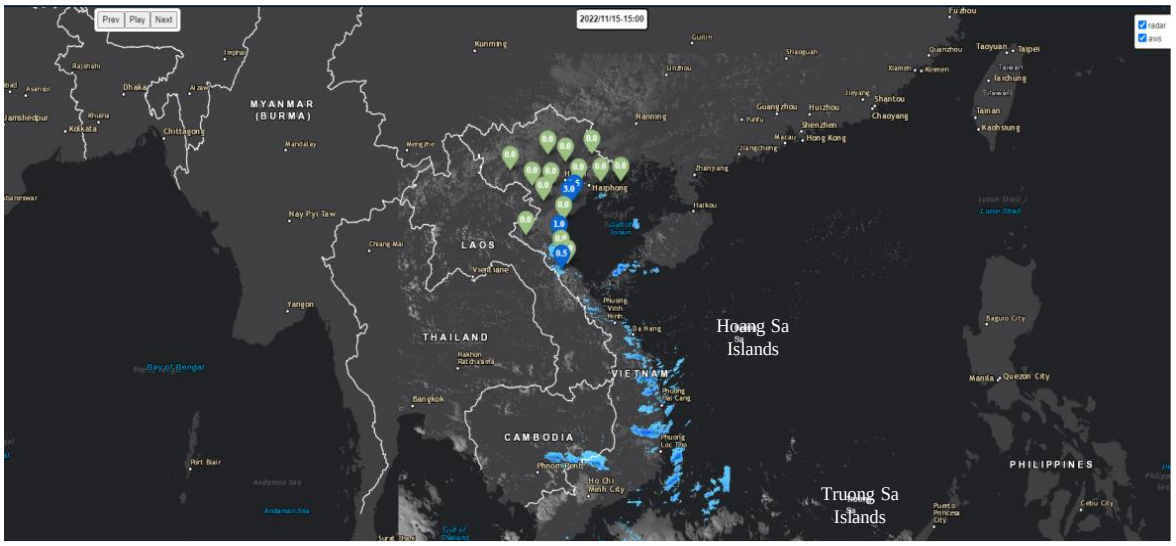

Figure 11. Overlay of ARG, radar and satellite.

3.3. Radar data display function

The system provides a viewing function of a real-time radar data in GeoTiff format shown in Figure 12, users can click on any point on the image to get the estimated rainfall value from the radar. Users have a loop view of images or individual images. The interface is capable of overlaying can overlay the satellite layer and/or ARG layer (on both the website and mobile app).

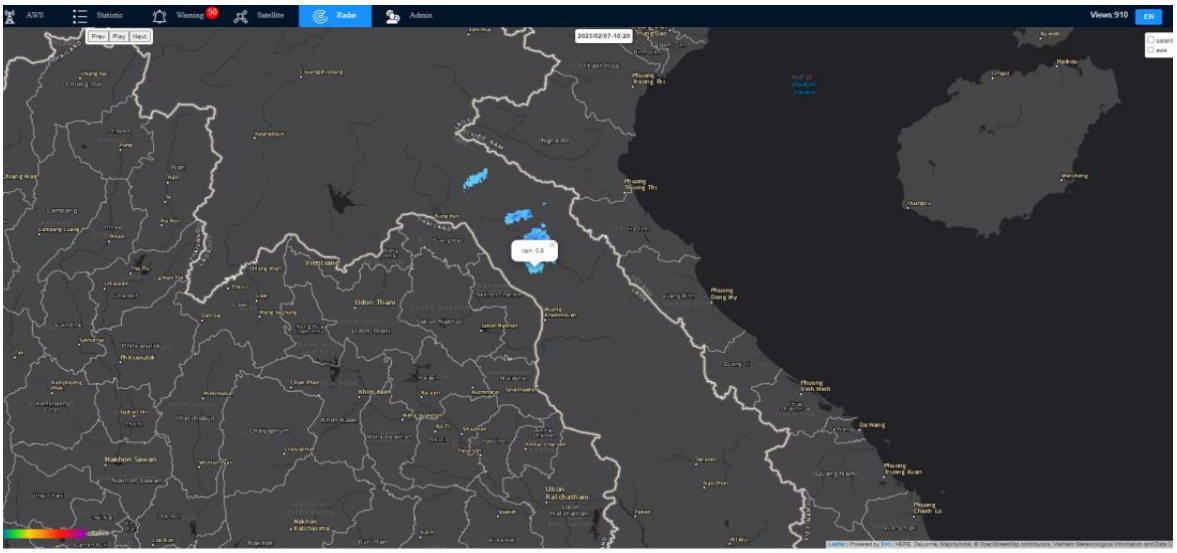

Figure 12. Radar data display.

When in overlay mode, Users click on a point to view both radar (estimated precipitation) and satellite (reflectivity) values, and ARG stations which are automatically displayed as icons with values and colors equivalent to the rain warning levels are easy to monitor, it is the same as Satellite Tab. Full-featured mobile app interface is similar to the mobile website.

3.4. Real-time warning function

The system provides a warning function to users by data push technology. Users will receive a warning when accessing the website or the mobile App. The interface displays the number of available warning messages and can view the content of the warning messages in real-time shown in Figure 13.

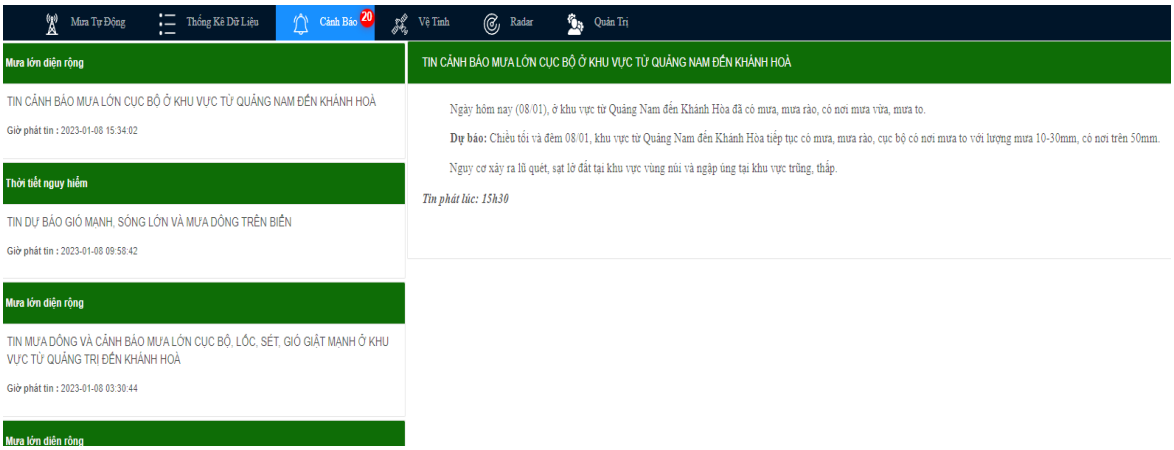

Figure 13. Real-time warning function on the website.

There are 2 types of users. Regular users only can view and receive alert messages. Administrative users can create, edit, and post warning-bulletin. The administrative interface is fully functional like a regular text editor shown in Figure 14, so users can easily use it.

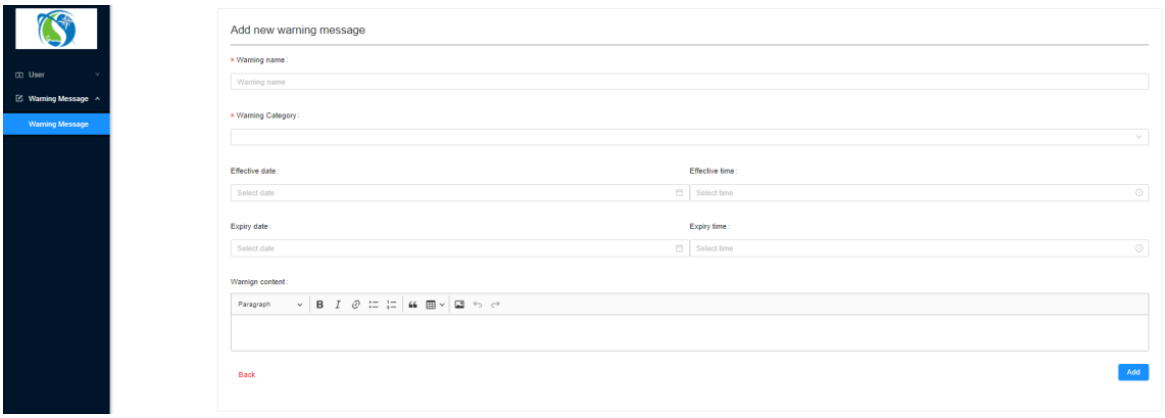

Figure 14. Administrative interface for creating bulletins on the website.

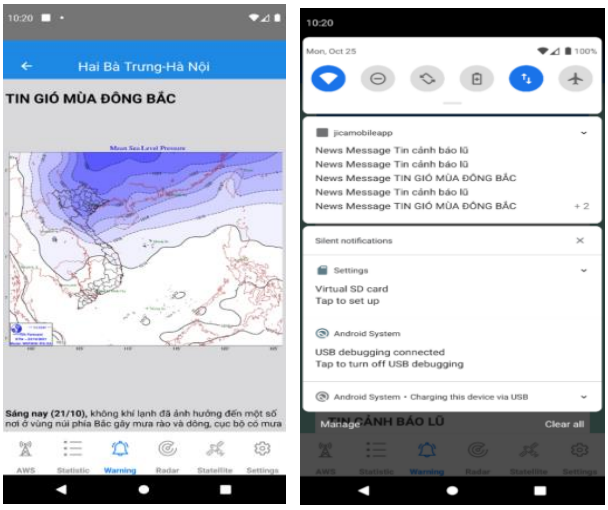

Figure 15. Real-time warning function on the mobile app.

The mobile app has information according to the registered user's location shown in Figure 15. Users can add multiple locations to receive warning messages related to the locations when there is a new dangerous weather warning.

The weather observation information app is available in both Apple Store and Google Play shown in Figure 16.

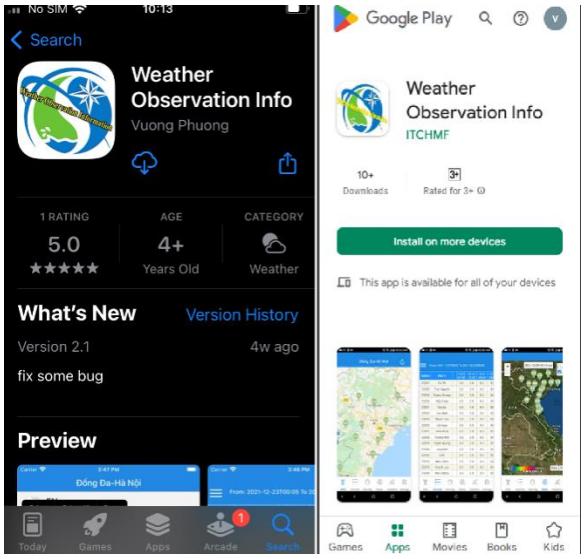

Figure 16. Weather observation information app in both Apple Store and Google Play.

4. Further consideration

The system has been fully deployed under the HMIDC management. Most of the system's modules operate automatically, except for the module that enters the warning message manually for the administrator. However, due to the requirement to notify users in real-time in dangerous weather conditions, a regular data monitoring process for the system's stable operation by the center's administrators is still required.

Since the system is designed to display rain data from automatic stations throughout Vietnam, it is possible to expand the display of data from other rain gauges. In addition, additional layers of satellite imagery can be added to the system to provide the user with more information.

Both monitoring data and warning information are provided in real-time allowing users to receive accurate and fast weather information. However, the volume of radar and satellite image data is relatively large, therefore some low-capability devices may have slow data display.

5. Conclusions

The technical report presented the methods used in the development of mobile services for weather observation information and the results of the development.

The mobile services consist of a mobile web site and a mobile application. They are running on two servers connected in a cluster to realize high stability and accessibility. Push notification technology and database-oriented APIs are introduced to quickly deliver alerts to users, whatever they use any devices such as personal computers, tablet, and iOS and Android mobile phones. Therefore, this will be an effective source of extreme weather warnings that VNMHA can use.

The following user-friendly functions have been developed.

- Rain data of ARG stations are automatically displayed as icons with numbers and colored according to warning scales. The system also provides a detailed view function of rainfall in the form of a table with a search function by a combination of station code, period, frequency, and total rainfall statistics, and warnings when the rainfall exceeds the threshold.

- The system provides a viewing function of a real-time satellite cloud image, which can determine the data value of each point on the map.

- The system provides a viewing function of real-time radar data; users can click on any point on the image to get the estimated rainfall value from the radar. The interface can overlay the satellite layer and/or ARG layer on both the website and mobile app.
- The system provides a warning function to users by data push technology. Users will receive a warning when accessing the website or the mobile app.

Author Contributions: Analysis and writing–original draft preparation: H.I., N.V.M., V.M.P., N.V.H.; writing–review and editing: P.V.T.N., H.I.; All authors have read and agreed to the published version.

Acknowledgments: The JICA technical cooperation project was supported by the people of Japan as JICA projects and technical assistance by JMA as DRR technical cooperation of WMO international cooperation frame for Southeast Asian countries. Specific thanks to JICA Tokyo experts who support the project and the Viet Nam Meteorological and Hydrological Administration (VNMHA) who have joined in the JICA Project for Strengthening Capacity in Weather Forecasting and Flood Early Warning System in the Social Republic of Vietnam.

Conflicts of Interest: The authors declare no conflict of interest.

References

1. UCAR-NetCDF. Network Common Data Form (NetCDF). Online Available: https://www.unidata.ucar.edu/software/netcdf/. Accessed 01/01/2021.
2. OGC-GeoTiff. OGC GeoTIFF Standard, 2020. Online Available: https://www.ogc.org/standards/geotiff. (Accessed 01/01/2021).
3. JMA. Himawari User Guide. Version 1.1. Japan Meteoroligical Agency, 2015. Online Available: https://www.data.jma.go.jp/. Accessed 08/12/2016.
4. MongoDB. Mongodb. Online Available: https://www.mongodb.com/. (Accessed 01/01/2021).
5. JSON. Online Available: https://www.json.org/json-en.html. (Accessed 01/01/2021).
6. ReactJS. A JavaScript library for building user interfaces. Online Available: https://reactjs.org/. (Accessed 01/01/2021).
7. Native, R. React Native. Online Available: https://reactnative.dev/. (Accessed 01/01/2021).

JOURNAL OF
HYDRO-METEOROLOGY

Technical Report

Training courses and seminars in the JICA technical cooperation project

Kenji Akaeda[1]*, Kazuo Saito[2,3,4], Kiichi Sasaki[5], Ryohei Kobayashi[6], Hiroyuki Ichijo[7]

[1] Japan International Cooperation Agency, Viet Nam Meteorological and Hydrological Administration, Hanoi, Viet Nam; akaeda191@yahoo.co.jp
[2] Japan Meteorological Business Support Center, Tokyo101-0054, Japan; k-saito@jmbsc.or.jp
[3] Atmosphere and Ocean Research Institute, University of Tokyo, Kashiwa 277-8564, Japan; k_saito@aori.u.tokyo.ac.jp
[4] Meteorological Research Institute, Japan Meteorological Agency, Tsukuba 305-0052, Japan; ksaito@mri-jam.go.jp
[5] Japan Meteorological Business Support Center, Tokyo 101-0054, Japan; k-sasaki@jmbsc.or.jp
[6] Japan Meteorological Business Support Center, Tokyo 101-0054, Japan; kobayashi@jmbsc.or.jp
[7] Japan Meteorological Business Support Center, Tokyo 101-0054, Japan; ichijo@jmbsc.or.jp

*Correspondence: akaeda191@yahoo.co.jp; Tel.: +829–761096

Received: 8 May 2023; Accepted: 23 June 2023; Published: 25 June 2023

Abstract: The JICA technical cooperation project has provided a wide range of training courses and seminars covering basic to applied topics to contribute to meteorological observation, forecasting, telecommunication, and disaster prevention. In this report, we describe the titles of training courses and seminars conducted during the project period and some summaries of them. The materials of these training and seminars can be used to organize knowledge for staff working in these fields.

Keywords: JICA; Training courses and seminars; Disaster risk reduction; International cooperation.

1. Introduction

In the Japan International Cooperation Agency (JICA) technical cooperation project [1], various training courses, seminars, on-the-job training (OJT), and technology transfer of products and software have been implemented to improve capacity. Among these, training courses and seminars have been the focus of efforts to improve the knowledge of many staff members. In this project, four outputs have been set. These are (1) maintenance and management of observation equipment, (2) radar data analysis technology, (3) utilization of observation data for forecasting, and (4) information dissemination technology. Various training programs were conducted for each of these outputs. For (1), (2), and (3), training in Japan was conducted in addition to training in Vietnam. For (1), the training was not limited to classroom lectures but also included OJT. The training was conducted not only by project members but also by dispatched Japan Meteorological Agency (JMA) officials.

This technical report has been prepared to provide an overview of the training and seminar activities in this project and to facilitate access to the materials for those who need

them. The training materials used for the training were prepared in PPT files in English and Vietnamese for the convenience of the participants. These materials are stored at the project office and will be available for future use as needed.

2. Training courses and seminars in 2018

Table 1. List of training courses and seminars in 2018.

Title of training course	Place	Date	Lecturer	Number of participants
Seminar on Utilization of Radar and Satellite data for disaster prevention in Japan	Hanoi	02 Aug 2018	Kenji Akaeda	40
Training course on extracting and displaying Japanese radar data	Hanoi	24 - 25 Sep 2018	Michihiko Tonouchi	14
Training course for the radars' software and data errors.	Hanoi	15 - 16 Oct 2018	Chiho Kimpara	
Seminar on Mesoscale Weather Prediction for Disaster Prevention (Section 2.1)	Hanoi	17 Oct 2018	Kazuo Saito	40
Training course on monitoring heavy rainfall and typhoon by using radar data, satellite data, ARG data and GPV data (Section 2.2)	Hanoi	17 - 19 Oct 2018	Kiichi Sasaki	24
Training course on basic knowledge of meteorological observation according to the guidance of WMO (Section 2.3)	Hanoi	06 - 09 Nov 2018	Koji Matsubara and Masao Mikami	24
Training course on controlling the quality of observation system, comparing the AWS data and Synop data	Hanoi	20 - 23 Nov 2018	Masao Mikami and Tsutomu Jomura	8
Training course on operation and maintenance of Phu Lien and Vinh radar	Phu Lien & Vinh	PL: 26 Nov - 05 Dec 2018 Vinh: 06 Dec - 14 Dec 2018	Masaru Wakabayashi	6
Seminar on Strategy to improve weather forecast information for disaster prevention	Hanoi	12 Dec 2018	Kazuo Saito	40

2.1. Seminar on utilization of radar and satellite data for disaster prevention in Japan

The first seminar in this project was held on 2 August 2018 to overview the JMA's effort to utilize radar and satellite data for disaster prevention. A combination of observation, analysis and forecasting is important to issue effective warnings related to heavy rainfall. Radar and satellite data are especially important to know the evolution of heavy rain-producing systems and to derive precise rainfall distribution. Radar is useful to catch the rainfall distribution, but some techniques are necessary to convert radar reflectivity data to accurate rainfall intensity. Quantitative precipitation estimation (QPE) products calculated from radar and rain gauges are useful to get precise rainfall distribution. QPE products produce some other products such as quantitative precipitation forecasting (QPF) or various indexes. These products contribute to the issuance of warnings.

2.2. Training course on monitoring heavy rainfall and typhoon by using radar data, satellite data, ARG data and GPV data

Introductory training courses on monitoring heavy rainfall and typhoon were conducted by output 3 (K. Sasaki of JMBSC) from 17 to 19 Oct 2018. First, a presentation and hands-on practice on typhoon monitoring with SATAID was given using Typhoons Mangkhut and Barijat of 2018 as actual examples. Second, a presentation and hands-on practice on heavy rainfall and typhoon monitoring with AWS, radar, and satellites using Typhoon Jebi as an example, which caused extensive damage to Japan in September 2018. Finally, hands-on practice on typhoon monitoring with NWP GPV data was given. A total of 24 staff from Aero-Meteorological Observatory (AMO) and National Center for Hydro-Meteorological Forecasting (NCHMF) participated in the training.

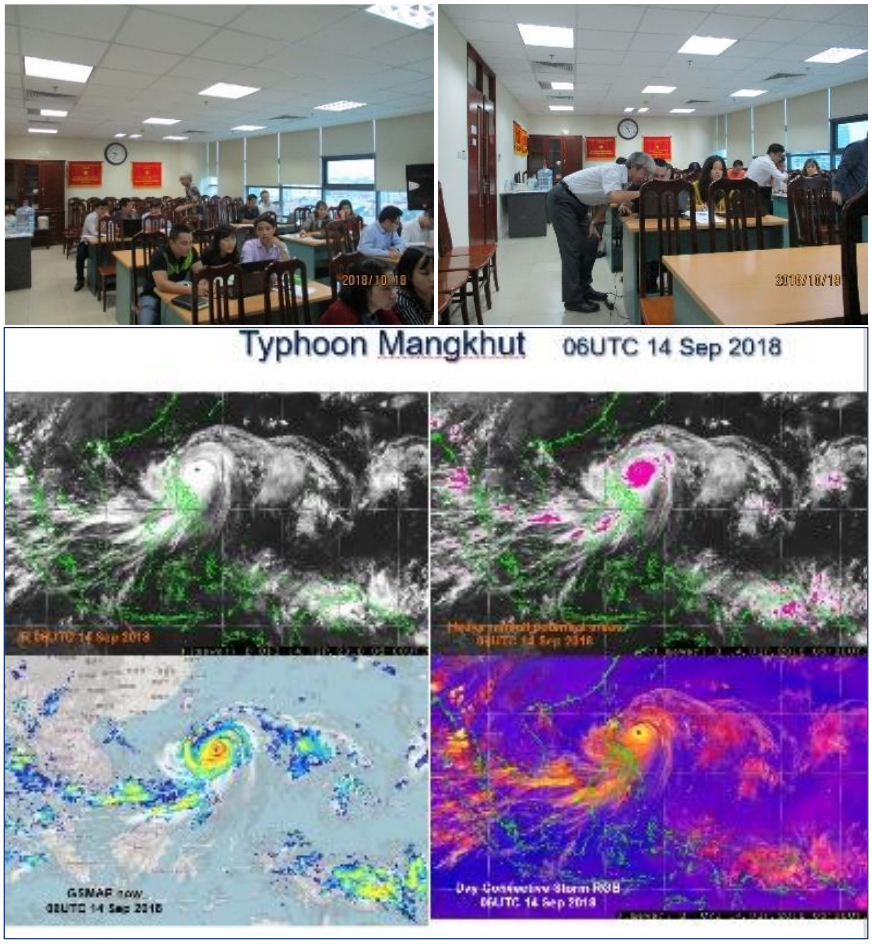

Figure 1. Training course on monitoring heavy rainfall and typhoon.

2.3. Training course on basic knowledge of meteorological observation according to the guidance of WMO

Introductory training courses on surface observation and its quality assurance were conducted by output 1 (M. Mikami and K. Matsubara of JMBSC) from 6 to 9 Nov. 2018. The accuracy of surface observation is highly dependent on the maintenance and calibration of surface instruments. Periodic maintenance and calibration are essential to keep the instruments in good condition. The observational environment is another factor to get good observational data. WMO showed several guidelines for the siting of observation and keeping its environment. Automatic quality control (AQC) is a useful method to detect anomaly data. We focus on the instruments or the environment of the observation site by utilizing the result of detection by AQC.

3. Training courses and seminars in 2019

Table 2. List of training courses and seminars in 2019.

Title of training course	Place	Date	Lecturer	Number of participants
Training course on the application of SATAID software in weather forecasting (Section 3.1)	Hanoi	18 - 22 Mar 2019	Shuji Nishimura and Marika Ono	31
Training course on Linux utilization	Phu Lien & Vinh & Hanoi	PL: 25-26 Mar 2019 Vinh: 28-29 Mar 2019 Hanoi: 01-02 Apr 2019	Chiho Kimpara	
Training on Operational Use of Kalman Filter Guidance for the Improvement of City forecasts & Outline of GSM KF guidance program "temp_guidance.bat"	Hanoi	25 & 28 Mar 2019	Kiichi Sasaki	
Training on Maintenance and Quality Control of Surface Meteorological Observation	Phu Lien & Vinh	Vinh: 28 Mar 2019 PL: 29 Mar 2019	Masao Mikami	20
Workshop on Integrating the hydro-meteorology system and orienting the development of improving forecast quality in Vietnam (Section 3.2)	Hanoi	10 Apr 2019	Kazuo Saito	40
Training course on Measurement of Meteorological Elements & Maintenance and Quality Control of Surface Meteorological Observation	Hanoi	16 - 17 Apr 2019	Masao Mikami	6
Training course for QC and QPE package of radar.	Japan	08 - 10 May 2019	JMA	2
OJT on radar maintenance at Phu Lien and Vinh radar sites	Phu Lien & Vinh	PL: 13 - 17 May 2019 Vinh: 20 - 24 May 2019	Tsutomu Jomura and Kenji Akaeda	
Training course on surface observation as part of output 1	Japan	24 Jun - 06 Jul 2019	JMA & JICA experts	6
Seminar on operational use of guidance for improvement of quantitative forecasts (Section 3.3)	Hanoi	25 Jul 2019	Kiichi Sasaki	22
Seminar on Heavy rainfall in Central Vietnam on 9th December 2018 and GSMaP data for precipitation nowcasting	Hanoi	20 Aug 2019	Kazuo Saito	25
Seminars: On the Northward Ageostrophic Winds Associated with a Tropical Cyclone Application of GSMaP data for precipitation nowcasting for the Heavy rainfall event in Central Vietnam on 9th December 2018	Hanoi	05 Sep 2019	Kazuo Saito	25

Title of training course	Place	Date	Lecturer	Number of participants
Seminar at Development Partners Conference on Hydro-Meteorological Services in Viet Nam	Hanoi	18 Sep 2019	Kenji Akaeda	50
Seminar on Disaster Management in Japan and effective usage of meteorological information	Hanoi	18 Oct 2019	Michihiko Tonouchi	25
Seminar on Natural Disaster prevention caused by heavy rainfall	Hanoi	23 Oct 2019	Kenji Akaeda, Yasutaka Makihara and Nguyen Vinh Thu	40
Seminar on quality control procedure of AWS data	Hanoi	25 Oct 2019	Tsutomu Jomura	40
Training course on evaluating the result of Japanese radar data with ARG data	Hanoi	04 - 06 Nov 2019	Chiho Kimpara	24
Seminar for improving rainfall observation accuracy and reliability for use in QPE/QPF application	Hanoi	07 Nov 2019	Masao Mikami	20
Training course on weather radar as part of output 2	Japan	10 - 23 Nov 2019	JMA & JICA experts	6
Training course on Development of Regional Quantitative Forecasts with Weather Guidance (Section 3.4)	Hanoi	02 Dec 2019	Kiichi Sasaki	

3.1. Training course on the application of SATAID software in weather forecasting

A satellite training course by JMA experts (S. Nishimura and M. Ono) was held from 18 to 22 March 2019 in the AMO conference room. 31 VNMHA staff members; 11 were from the Regional Hydro-met Centers, 6 were from NCHMF and 14 were from AMO participated in the Seminar. Lectures on the use of SATAID, the use of RGB images and on the basics of satellite image analysis and several event analyses were conducted.

Figure 2. Satellite training course by JMA experts.

3.2. Workshop on Integrating the hydro-meteorology system and orienting the development of improving forecast quality in Vietnam

On April 10, VNMHA hosted a special workshop on “Integration of Meteorology and Hydrology system and orientation for improving forecasting quality in Vietnam”. The workshop was held at conference room 210 of VNMHA and chaired by Mr. Le Cong Tanh, Vice Minister of MONRE. Most leaders of VNMHA including, Prof. Dr. Tran Hong Thai,

Administrator of VNMHA, Mr. Le Thanh Hai, Deputy Director General, and Assoc. Prof. Dr. Nguyen Van Thang, Director of the Viet Nam Institute of Meteorology, Hydrology and Climate Change(IMHEN), attended the workshop. As one of the two invited speakers, K. Saito gave a presentation on "Evaluation of heavy rainfall in Central Vietnam in 2018 and recommendations on the orientation for improving forecasting quality in Vietnam". Another speaker at the workshop was Dr. Marcel Marchand, an expert in flood risk and coastal management from Deltares (https://www.deltares.nl/en/), a hydrological research and consultancy firm based in the Netherlands. He gave a talk on 'Frame of integrated system for weather forecasting and early warning (Table 3).

Table 3. Agenda of workshop on integration of meteorology and hydrology system and orientation for improving forecasting quality in Vietnam.

Time	Content	Speaker
15h30-15h35	Introduction	
15h35-15h55	Frame of integrated system for weather forecasting and early warning	Marcel Machand
15h55-16h25	Evaluation of heavy rainfall in Central Vietnam in 2018 and recommendations on the orientation for improving forecasting quality in Vietnam	Kazuo Saito
16h25-16h50	Discussion	Tran Hong Thai - VNMHA Administrator
16h50-17h00	Remarks by MONRE leader	Le Cong Thanh - MONRE Vice Minister

Saito's presentation (Figure 3) was: 1) The heavy rainfall in Central Vietnam on December 9th; 2) Precipitation nowcasting; 3) Numerical Weather Prediction; and 4) Recommendations on the orientation for improving forecasting quality for short, middle, and long-range. Mr. Le Cong Thanh, Deputy Minister of MONRE, commented that Mr. Saito's presentation gave VNMHA very important points regarding its direction of future plans.

Figure 3. Example of presentation slides at the workshop.

3.3. Seminar on operational use of guidance for improvement of quantitative forecasts

A seminar on the operational use of guidance for the improvement of quantitative forecasts was held on 25 Jul 2019 at the AMO conference room with 22 participants. Output 3 (K. Sasaki of JMBSC) gave a presentation on temperature guidance with multiple linear regression method and Kalman filter method using JMA-GSM GPV data and ECMWF-IFS GPV data. Verification results of the temperature guidance with both models were also presented, as well as the results of city forecasts issued by NCHMF.

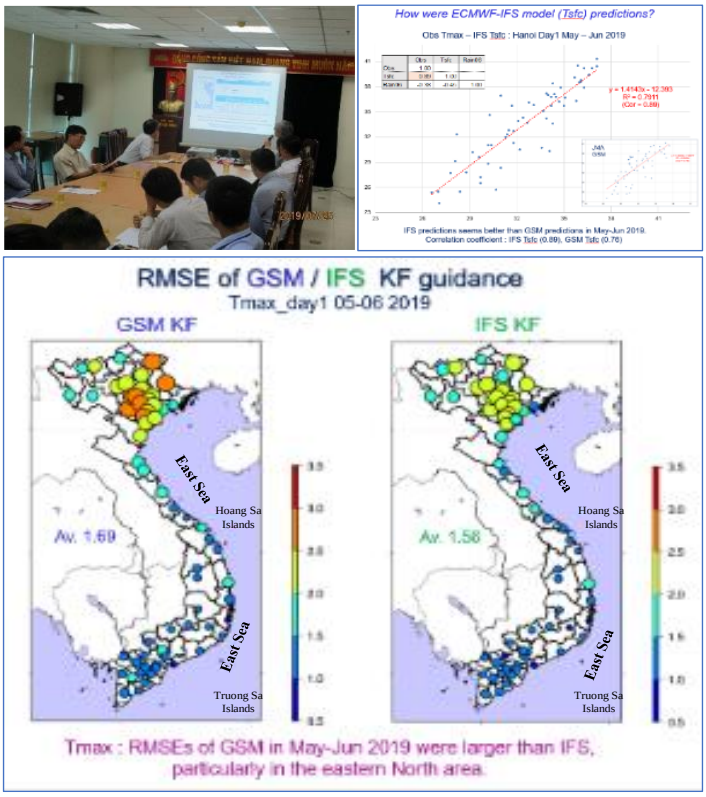

Figure 4. Seminar on operational use of guidance for improvement of quantitative forecasts.

3.4. Training on Development of Regional Quantitative Forecasts with Weather Guidance

Training on the development of regional quantitative forecasts with weather guidance was conducted at Vinh RFC on 2 Dec 2019 and at Phu Lien RFC on 5 Dec 2019. Output 3 (K. Sasaki of JMBSC) gave a presentation on the concept of MOS (multiple linear regression) guidance and Kalman filter temperature guidance. Hands-on practice on downloading GPV, visualization of GPV data with GrADS, and statistical analysis with Excel and R was also provided.

Figure 5. Training at Vinh RFC (left), and at PhuLien RFC (right).

4. Training courses and seminars in 2020 and 2021

Table 4. List of training courses and seminars in 2020 and 2021.

Title of training course	Place	Date	Lecturer	Number of participants
Training course on the basic principle of radar and radar data analysis guidance (Section 4.1)	Hanoi	02 - 06 Mar 2020	Yasutaka Makihara	40

Title of training course	Place	Date	Lecturer	Number of participants
Training course on application of numerical model products to support weather forecasting	Hanoi/Online	09 - 10 Mar 2020	JMA experts	42
Seminar at 9th Aero-Meteorology Conference	Hanoi	16 Dec 2020	Kenji Akaeda	30
Training course on operation of ARG system (Section 4.2)	Hanoi	22 Jul and 17 Aug 2021	Hiroyuki Ichijo	6
Advance training course on management of ARG system	Hanoi	18 Aug 2021	Hiroyuki Ichijo	2
OJT on maintenance with meteorological calibration equipment (Section 4.3)	Hanoi	21, 23 Dec 2021 and 5 Jan 2022	Ryohei Kobayashi	3 to 7
Seminar on Context of VNMHA's QPE and improvement & short-range precipitation forecast (Section 4.4)	Hanoi	27 Dec 2021	Chiho Kimpara and Kazuo Saito	19
Training course on setting clutter maps in JMA-QC Package	Hanoi	28 - 30 Dec 2021	Chiho Kimpara	5

4.1. Training course on the basic principle of radar and radar data analysis guidance

This 5-day training course covers a wide range of radar fundamentals as well as applied matters such as QPE calculations. Fundamentals include radar principles, characteristics of radar observation data, and quality control of anomalous and non-precipitation echoes. Applied topics include algorithms for calculating QPE using a combination of rain gauge and radar, characteristics of QPE products in Vietnam, and how to utilize QPE products. The training course also included an exercise to compare QPE products analyzed in Vietnam with rain gauge-only data and satellite data. The lecturer, Y.Makihara, who used to develop QPE products at the JMA, has a deep knowledge of QPE, and the training materials were well organized.

4.2. Training courses on operation and management of ARG system

Two training courses for operational staff and administrators toward full operation of the ARG system were held for 3 days from July to August 2021. The courses were comprised of technical lectures and practical instructions. The participants learned the comprehensive structure of the ARG system, functions of dataloggers and data collection servers, ARG data flow, and ARG maintenance issues.

Figure 6. ARG training courses: technical lecture (left), practical instruction (right).

4.3. OJT on maintenance with meteorological calibration equipment

The project provided equipment for meteorological calibration. This training provided handling the equipment and procedure to calibrate instruments at the calibration laboratory and at Ha Dong observatory. Since a thermal water chamber was installed at the calibration laboratory of the headquarters, the laboratory staff in charge of thermometers attended the training. Other equipment; digital barometers, digital Assmann psychrometers, and rain gauge checkers were introduced to technical staff at the laboratory and in the field.

Figure 7. Handling training for clibration equipment. (a) Training at the Headquarters; (b) Training at Ha Dong observatory.

4.4 Seminar: Context of VNMHA's QPE and improvement & Short range precipitation forecast

A seminar, Context of VNMHA's QPE and improvement & Short range precipitation forecast was held on 27 December 2021. In addition to JICA and VNMHA members, participants came from IMHEN, Hanoi University Science School (HUS), and a private meteorological company (Weather Plus). The first seminar on 27 December 2021 was conducted in a combination of online and onsite with a lecture from output 2 (C. Kimpara of JWA, online) and output 3 (K. Saito of JMBSC) (Figure 8).

Figure 8. The First Seminar is on 27 December 2021. (Left) AMO conference room, (Right) Screenshot of the online lecture.

5. Training courses and seminars in 2022 and 2023

Table 5. List of training courses and seminars in 2022 and 2023.

Title of training course	Place	Date	Lecturer	Number of participants
Seminar on short-range precipitation forecast (Part 2)	Hanoi	11 Jan 2022	Kazuo Saito	15
Seminar on Strengthening the development and innovation of	Hanoi	19 May 2022	Kenji Akaeda	40

Title of training course	Place	Date	Lecturer	Number of participants
heavy rainfall technology in disaster reduction				
Advanced training course on periodic maintenance AWS calibration tools at Phu Lien and Vinh	Phu Lien & Vinh	Vinh: 18 - 19 Oct 2022 PL: 25 - 27 Oct 2022	Ryohei Kobayashi	V:15 & P:12
Training course on QPE quality improvement and quantitative precipitation forecast (QPF) by using weather radar data and ARGs data (Section 5.1.1)	Hanoi	16-24 November 2022	Kenji Akaeda, Chiho Kimpara, Kazuo Saito, Bui Thi Khanh Hoa, Michihiko Tonouchi	40
Training course on short term weather forecast (Section 5.1.2)	Hanoi		Kazuo Saito, and Kiichi Sasaki	40
Training course on practicing the assessment of meteorological elements observed by AWS system	Hanoi	05 - 07 Dec 2022	Ryohei Kobayashi	8
Training course on inspection and quality control of AWS/ARG (Section 5.2)	Hanoi	13 - 15 Dec 2022	Hiroumi Shigeoka, Masaki Kuroiwa, and Hirokatsu Onoda	40
Training course on weather forecasting as part of output 3 (Section 5.3)	Japan	07 - 21 Feb 2023	Experts (JMA, JMBSC, Tohoku University)	6
Final seminar on activity summary of output 1 and output 4 (Section 5.4)	Hanoi	14 Apr 2023	Ryohei Kobayashi, Hiroyuki Ichijo, Nguyen Viet Huy, Kenji Akaeda, and Tsutomu Jomura	40

5.1. Training course on QPE and QPF, and short term weather forecast

From 16 to 24 November 2022, two comprehensive training courses, “Training course on QPE quality improvement and quantitative precipitation forecast (QPF) by using weather radar data and ARGs data” and “Training course on short term weather forecast” were held at VNMHA Headquarters in Hanoi. The first seminar was mainly held in the first week (16 to 18), but the lecture by M. Ttonouchi was held in the afternoon on 22 November (Table 6). The seminar was attended by 40 participants from VNMHA's Observation Division (AMO), NCHMF, and 9 regional forecast centers.

Table 6. Time tablet of training courses in Novemebr 2022.

Date	Items	Personal in charge
16 (Wed)	AM: 8:30 - 9:00: Registration	
	9:00 - 9:10: Opening time	AMO
	- Introduction of training course	Vice director - Tran
	- Opening speech of AMO leader	Xuan Tuan
	- Opening speech of Project Chief Advisor.	
	AM: From 9:10	
	- Lecture: Utilization of Radar data for Monitoring/Nowcasting Various Severe Phenomena	Kenji Akaeda
	PM: From 14:00	Chiho Kimpara
	- Lecture: Introduction of radar products and usage notes	(Online)
	AM: From 9:00	Chiho Kimpara
	- Lecture: Application of dual-polarization and future prospects	(Online)

Date	Items	Personal in charge
17 (Thu)	PM: From 14:00 - Lecture: Test of very short range forecast of precipitation in Vietnam	Kazuo Saito
18 (Fri)	AM: From 9:00 - Lecture: Some research results on the utilization of radar data in AMO	Bui Thi Khanh Hoa
21 (Mon)	AM: From 9:00 - Lecture: Mesoscale numerical weather prediction	Kazuo Saito
	PM: From 14:00 - Lecture: Mesoscale meteorology on local circulation and convection initiation	Kazuo Saito
22 (Tue)	AM: From 9:00 - Lecture: Mesoscale ensemble prediction	Kazuo Saito
	PM: From 14:00 - Lecture: Quality check of ARG and QPE	Michihiko Tonouchi
23 (Wed)	AM: From 9:00 - Lecture: Kalman filter T_{max}/T_{min} Temperature Guidance	Kiichi Sasaki
	PM: From 14:00 - Lecture: Precipitation Guidance (POP, regional mean/max 24h-rain)	Kiichi Sasaki
24 (Thu)	AM: From 9:00 - Exercise: Case study of heavy rainfall in Vietnam	Kiichi Sasaki

5.1.1. Training course on QPE and QPF

"Training course on QPE quality improvement and quantitative precipitation forecast (QPF) by using weather radar data and ARGs data" was held from 16 to 22 November 2022 (Table 5) at VNMHA. The lectures are K. Akaeda of JICA (am on Wednesday 16), C. Kimpara of JWA (online, pm on Wednesday 16 and am on Thursday 17), K. Saito of JMBSC (pm on Thursday 17), Hoa Bui of AMO, VNMHA (am on Friday 18), and M. Tonouchi of JMBSC (pm on Tuesday 22). Akaeda summarized the radar echo characteristics in Vietnam and explained some techniques to detect severe phenomena by radar. Kimpara explained the algorithm of QPE and the results of the evaluation of QPE. She also explained how to utilize dual-polarized data for precipitation observation. Tonouchi explained the result of the rain gauge evaluation and the effective utilization of rain gauge data for QPE calculation. Kazuo Saito introduced the development of a very short range forecast of precipitation system in Vietnam [2].

5.1.2. Training course on short term weather forecast

"Training course on short term weather forecast" was held from 21 to 24 November 2022 (Table 5) at VNMHA (Figure 9). The lectures are K. Saito of JMBSC (Monday 21 and pm on Thursday 22), and K. Sasaki of JMBSC (Wednesday 23 and am on Thursday 24). K. Saito gave lectures on mesoscale-numerical weather prediction on the morning of November 21, meteorology of local circulation and convective initiations in the afternoon, and mesoscale-ensemble forecasting on the morning of November 22. These lectures were prepared based on the materials at the forecasting technology training at the Meteorological College of Japan and the Japan Society of Certified Meteorological Forecasters, while original materials were added (Figure 10).

The training on temperature guidance by K. Sasaki included presentations on the development of MOS and Kalman filter guidance [3], verification results of GSM and IFS temperature guidance, statistical analysis using observation and GPV data sets, and simple hands-on training on MOS and Kalman filter temperature guidance calculations. On the last

day of this training course, comprehensive heavy rainfall case studies [4] were presented and practiced using surface observation data, radar QPE, satellite data, numerical prediction data, and precipitation guidance. The cases were the case of 24-hour rainfall exceeding 300 mm due to Typhoon NORU, which made landfall in central Vietnam from the night of September 27 to the early morning of September 28, 2022, and the case of 24-hour rainfall exceeding 500 mm due to Typhoon SONCA, which made landfall in central Vietnam on October 15, 2022.

Figure 9. Training course on short-term weather forecast.

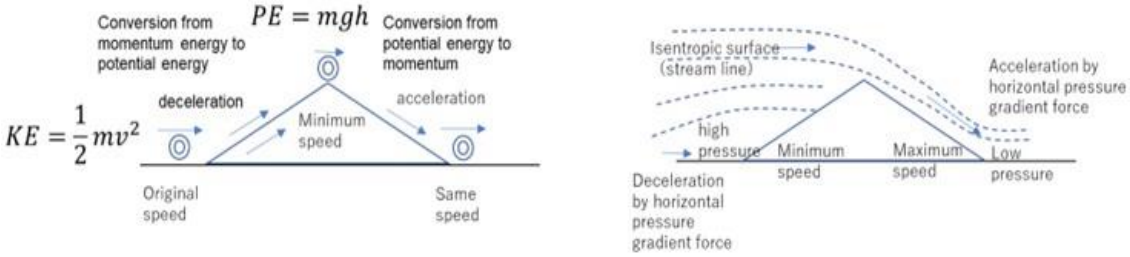

Figure 10. Difference between mass point past over a mountain (left) and downslope wind (right) in the lecture on mesoscale meteorology on local circulation and convection initiation.

5.2. Training course on inspection and quality control of AWS/ARG

This project invited two experts of calibration, maintenance, and data quality control from JMA to Hanoi for the training, besides, one quality control expert from JMA provided training remotely. This training provided organizing the traceability system as a foundation of the data quality and method of quality control in operation in JMA, especially rain gauge check. This seminar reached not only staff working in Hanoi but also from the whole country.

Figure 11. Data quality control training by JMA experts in Hanoi on 13-15 Dec 2022.

5.3. Training course on weather forecasting (output 3) in Japan

This training program was held from February 7 to 21, 2012, for trainees of VNMHA to acquire skills and knowledge related to precipitation nowcasting, short-time precipitation forecasting, numerical weather prediction and guidance, and use of meteorological observation data, through lectures and visits to Japanese meteorological agencies, research institutions, universities, and other institutions. Six VNMHA staff members and two project assistant staff members participated in the training according to the schedule shown in Table 7.

Table 7. Training details.

Date	Contents of Training	Location
7 (Tue)	Visiting Japan, Check-in JICA Tokyo	JICA Tokyo
8 (Wed)	Briefing on the training	JICA Tokyo
	Presentation "JMA technical meeting on forecasting (country report, sharing and discussing experiences on forecasting operations)"	JMA Headquarters
	Lecture "JMA Operations (general lecture on operations, discussion on meteorological operations)"	
9 (Thu)	Courtesy visit	JMA Headquarters
	Discussion "JMA forecast technical meeting (guidance, precipitation nowcasting, short-time precipitation forecast, satellite analysis)"	Weather Science Museum
	Observation tour "JMA Operation Room"	
	Site visit "Weather Science Museum"	
10 (Fri)	Lecture "Meteorological Disaster Prevention Information Released by JMA and Responses by Local Governments" (Figure 12)	JMBSC
	Observation tour "Life Safety Learning Center"	Life Safety Learning Center
12 (Sun)	Travel (Tokyo to Sendai)	
13 (Mon)	Observation tour "Sendai District Headquarters (District Meteorological Observatory Forecasting Service)"	Sendai District Meteorological Headquarters
	Visit the areas affected by the Great East Japan Earthquake and Tsunami and related facilities (Arahama Elementary School, Sendai City, Ishinomaki City Okawa Earthquake Lore Museum)	Arahama Elementary School Okawa Earthquake Lore Museum
14 (Tue)	Lecture "Numerical simulations of extreme weather phenomena with fine resolution" (Figure 13)	International Research Institute of Disaster Science, Tohoku University
	Travel (Sendai to Tokyo)	
15 (Wed)	Lecture "Operational Use of Numerical Weather Prediction" at JMA Forecasting Technical Meeting	JMA Headquarters
	Tour "Minato Science Museum (including Planetarium)"	Minato Science Museum
16 (Thu)	Transfer (Tokyo to Tsukuba)	Meteorological Research Institute
	Observation tour "Meteorological Research Institute (Phased Array Radar, Dual Polarized Radar, GPS, Wind Profiler, Lidar)"	
17 (Fri)	Observation tour "JMA Numerical Prediction Development Center, Aerological Observatory and Meteorological Instrument Testing Center (Spectrometer, Wind Tunnel)"	Numerical Prediction Development Center Aerological Observatory and Meteorological Instrument Testing Center
	Observation tour "Tsukuba Space Center"	Tsukuba Space Center
	Transfer (Tsukuba→Tokyo)	
20 (Mon)	Evaluation meeting Certificate Awarding	JICA Tokyo
21 (Tue)	Trainees return to Japan	

Figure 12. Lecture "Meteorological Disaster Prevention Information Released by JMA and Responses by Local Governments" at JMBSC.

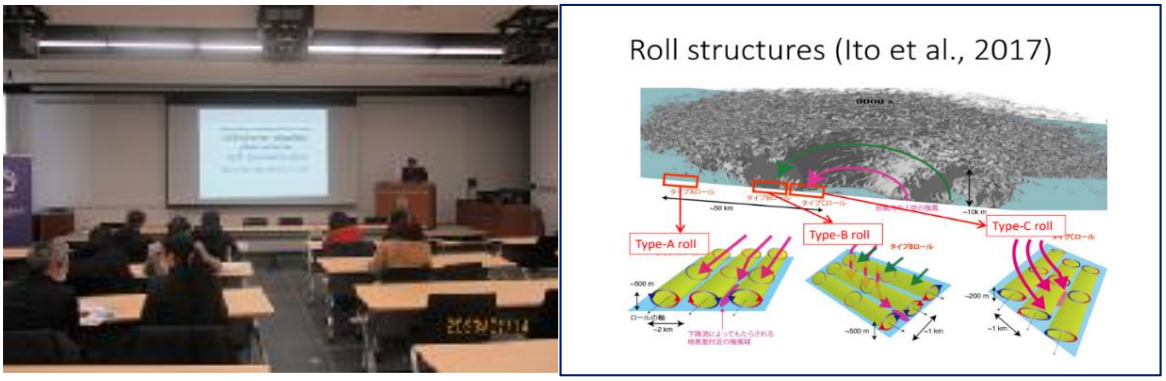

Figure 13. Lecture "Numerical simulations of extreme weather phenomena with fine resolution" at the International Research Institute of Disaster Science, Tohoku University.

At the evaluation meeting held on the last day of the training course, all six trainees gave presentations on what they learned from this training and how they will use the research results in the future. The participants gained a better understanding of the JMA's weather forecasting services, guidance, nowcasting, satellite analysis operations, numerical forecasting, and observation equipment. Participants also commented that the importance of early warning and impact-based forecasting (IBF), the JMA's use of disaster mitigation information, and its services for supporting regional disaster management were very helpful. Regarding the future application of the training outcomes, participants expressed their opinions on both short-term applications and long-term perspectives.

5.4. Final seminar on activity summary of output 1 and output 4

A series of seminars were planned to summarize the activities of each output. The first seminar for this purpose was held on 14 April 2023. This seminar summarized the activities of output 1 by R. Kobayashi, K. Akaeda and T. Jomura, and output 4 by H. Ichijo and N.V. Huy. Kobayashi recommended detailed plan for quality control of surface observation. He also introduced a quality monitoring system that can be easily accessed via Internet from every office. Akaeda and Jomura focused on how to improve the quality of radar observation. Their target is to improve scan strategies and improve some settings for PCAPPI calculation. Ichijo and Huy explained their activities to install a new ARG system and a new operational mobile web/app system. They also suggested their plan to improve information service.

6. Conclusion

During five-year period of this technical cooperation project, 29 training courses and 17 seminars have been conducted so far. As this project continues until the end of December 2023, a few more courses or seminars will be added. In these training courses and seminars,

we provided topics depending on each output as (1) surface observation methods, surface instrument maintenance and calibration, quality control, and radar maintenance, (2) radar observation basics, radar data quality control, radar data analysis methods, and QPE product algorithm and evaluation, (3) temperature and rainfall forecasting by using guidance methods, analyzing method for heavy rainfall cases, and QPF algorithm, (4) installation and maintenance of automatic rain gauge(ARG) system, data acquisition system for ARG and constructing mobile web/application information sharing systems.

We believe that these materials used in the training courses and seminars will be useful for future staff in charge of this field. If you would like to refer to these materials, please contact to the project office or the person involved in this technical project.

Author contribution statement: The section related to output 1 is written by R.K. The section related to output 3 is written by K.S., K.S. The section related to output 4 is written by H.I. The section related to output 2 and other parts is written by K.A.

Acknowledgments: This JICA technical cooperation project was supported by the people of Japan as JICA projects and technical assistance by JMA as DRR technical cooperation of WMO international cooperation frame for Southeast Asian countries. The training courses and seminars were given by Michihiko Tonouchi, Chiho Kimpara, Koji Matsubara, Masao Mikami, Tsutomu Jomura, Masaru Wakabayashi, Shuji Nishimura, Marika Ono, Yasutaka Makihara, Nguyen Vinh Thu, Bui Thi Khanh Hoa, Hiroumi Shigeoka, Masaki Kuroiwa, Hirokatsu Onoda and Nguyen Viet Huy. We express our thanks to Nguyen Thi Thuy Linh to summarize the list of training courses and seminars. We also express our special thanks to Phan Vu Thanh Nhan, Nguyen Thi Thuy Linh and Tran Hoang Lan Phuong to translate those training/seminar materials into Vietnamese and interpret lectures/ seminars into Vietnamese.

Competing interest statement: The authors declare no conflict of interest.

References

1. Akaeda, K.; Tonouchi, M; Thu, N.V. Achievement of JICA Technical Cooperation Project in Period 2. *J. Hydro-Meteorol.* **2023**, *15*, 1–9.
2. Saito, K.; Hung, M.K.; Tien, D.D. Development of a prototype system of the very short-range forecast of precipitation in Vietnam. *J. Hydro-Meteorol.* **2023**, *15*, 59–79.
3. Sasaki, K.; Anh, V.T.; Hang, N.T.; Trang D.T. Development of maximum and minimum temperature guidance with Kalman filter for 63 cities in Vietnam up to 10 days ahead. *VN J. Hydrometeorol.* **2020**, *5*, 51–64. Doi: 10.36335/VNJHM.2020(5).51-64.
4. Sasaki, K.; Anh, V.T. Development of precipitation guidance for 36 regions in Vietnam up to 5 days ahead. *J. Hydro-Meteorol.* **2023**, *15*, 40–58.

Table of content